Abstract

THE UNIQUE ROLES OF IFE-1, A GERMLINE-SPECIFIC ISOFORM OF EUKARYOTIC TRANSLATION FACTOR 4E, DURING GAMETOGENESIS

by MELISSA ANNE HENDERSON
JUNE, 2009
Director: BRETT D. KEIPER
DEPARTMENT OF BIOCHEMISTRY AND MOLECULAR BIOLOGY

Fertility and embryonic viability are measures of efficient germ cell growth and differentiation. During oogenesis, spermatogenesis and embryogenesis cells initially proliferate then differentiate into specific tissues. New proteins are required for both cell growth and differentiation, requiring qualitative and quantitative changes in protein synthesis. During late gametogenesis and early embryogenesis the expression of the appropriate proteins is a primarily due to translational control. Translational control of mRNAs is mediated in part by eukaryotic initiation factor 4E (eIF4E). eIF4E binds the methylated 5’ cap of mRNA and recruits it to the ribosome. The nematode worm *C.elegans* expresses five isoforms of eIF4E (termed IFE-1 through 5). IFE-1 is expressed primarily in the germline and is the only isoform that associates with P granules by binding directly to PGL-1. P granules are ribonucleoprotein particles (RNPs) that contain stored mRNAs and proteins needed for oogenesis and early embryogenesis. Using a strain that lacks IFE-1, I assessed the translational efficiency of maternal mRNAs bound and not bound to P granules by polysome fractionation. Translation of *pos-1, pal-1, mex-1, oma-1, ced-4* and *glp-1* mRNAs was inefficient in the *ife-1* strain relative to wild type worms. GAPDH (*gpd-3*) mRNA translation was not affected. We also observed differences in the pattern of expression of the MEX-1 protein during oogenesis. In males, secondary spermatocytes failed to complete cytokinesis at 25°C in absence of IFE-1. Males deficient of IFE-1 therefore lacked mature sperm. In addition, *ife-1* spermatocytes prematurely accumulated pro-apoptotic CED-4, homolog to mammalian Apaf-1, during spermatogenesis. In *ife-1* worms fertility was decreased by 80% due to decreased viability of both oocytes and spermatocytes. Our data indicate two unique roles for eIF4E (IFE-1 isoform) in late oogenesis and spermatogenesis. We suggest that IFE-1 preferentially recruits regulated mRNAs at critical times during germ cell development.

THE UNIQUE ROLES OF IFE-1, A GERMLINE-SPECIFIC ISOFORM OF EUKARYOTIC TRANSLATION FACTOR 4E, DURING GAMETOGENESIS

A Dissertation

Presented To

The Faculty of the Department of Biochemistry and Molecular Biology

East Carolina University

In Partial Fulfillment

of the Requirements for the Degree

DOCTOR OF PHILOSOPHY

by

MELISSA ANNE HENDERSON

JUNE, 2009

THE UNIQUE ROLES OF IFE-1, A GERMLINE-SPECIFIC ISOFORM OF EUKARYOTIC TRANSLATION FACTOR 4E, DURING GAMETOGENESIS

by

MELISSA ANNE HENDERSON

APPROVED BY:

DIRECTOR OF DISSERTATION:______ BRETT D. KEIPER, PHD_______________
BRETT D. KEIPER, PHD

COMMITTEE MEMBER:____ PHILLIP H. PEKALA, PHD______________________
PHILLIP H. PEKALA, PHD

COMMITTEE MEMBER:_____ BRIAN A. SHEWCHUK, PHD___________________
BRIAN A. SHEWCHUK, PHD

COMMITTEE MEMBER:_____ ANN O. SPERRY, PHD_________________________
ANN O. SPERRY, PHD

CHAIR OF THE DEPARTMENT OF BIOCHEMISTRY AND MOLECULAR BIOLOGY:

_____ PHILLIP H. PEKALA, PHD___________________
PHILLIP H. PEKALA, PHD

DEAN OF THE GRADUATE SCHOOL:

______ PAUL GEMPERLINE, PHD_________________

PAUL GEMPERLINE, PHD

Dedication:

To my husband Jesse for the countless support and love you supplied during the completion of this dissertation.

Acknowledgement

I would like to thank my family for their love and support during my studies at East Carolina University. I would especially like to thank my wonderful husband for his encouragement especially during the tough times. His love and support allowed me to focus on the completion of this dissertation. I am thankful for the love and support of my parents and their efforts moving me 3,000 miles to follow my dream even if they did not understand why it had to be on the other side of the country. My siblings added much needed laughter and support during my time in graduate school and for this I am thankful.

I would also like to show my appreciation to all those in the Department of Biochemistry at ECU. The faculty established an atmosphere that was like a family and truly nurtured my education. I would especially like to thank Dr. Brett Keiper for countless support and guidance on this project. His laboratory allowed me to develop into the scientist I am today with the perfect balance of guidance and freedom for me to truly "own" my project. I would also like to thank Enhui Hao for her help in support in the lab. Vince Contreras has been a wonderful colleague and I am truly thankful for all of your advice on science and life.

I would also like to thank all of the graduate students at Brody School of Medicine. The friends I have made during graduate school made up my North Carolina family which supported me though the countless hours of courses and experiments.

TABLE OF CONTENTS

LIST OF TABLES ix

LIST OF FIGURES x

LIST OF ABBREVIATIONS xi

CHAPTER 1: INTRODUCTION OF LITERATURE REVIEW 1

- Cell fate: growth, differentiation, and death involve protein synthesis 1
  - Newly synthesized protein during the cell cycle 1
  - Differentiation: gametogenesis 4
  - Apoptosis – the selective loss of cells during development 6
- Mechanisms of Translational Control 8
  - mRNA Recruitment During Translation Initiation 8
  - Stress Response: eIF2a phosphorylation 9
  - mRNA recruitment by eIF4E 13
  - Utilization of Internal Ribosome Entry Sites (IRESes) 16
  - MicroRNAs 18
- Ceanoraditis elegans as a model system 20
  - C.elegans Spermatogenesis 20
  - C.elegans Oogenesis 22
  - Fertilization and meiotic maturation in C.elegans 25
  - C.elegans Embryogenesis 25
  - P granules 26

CHAPTER 2: EXPERIMENTAL PROCEDURES 28

- Growth and Maintenance of C.elegans 28
- Genomic PCR 29

Calculating Fertility and Extent of Development by Observation 30
Determining the Temperature Sensitive Period (TSP) for Fertility 31
Microscopy and Imaging 31
Immunostaining 33
Creation of ced-1::gfp, ife-1 homozygous strain 34
Analysis of polysomes by sucrose gradient fractionation 34
qRT-PCR 35
Construction of pSKflgife-1let and pie-1flgife-1 36
Injection of DNA into the hermaphrodite gonad for transformation 39
Detecting protein levels by western blot 40

CHAPTER 3: THE ROLE OF IFE-1 IN OOGENESIS IN *C.ELEGANS* 41

Introduction 41
Results 43
Conclusion 66

CHAPTER 4: THE ROLE OF IFE-1 IN SPERMATOGENESIS IN *C.ELEGANS* 69

Introduction 69
Results 72
Conclusion 92

CHAPTER 5: IFE-1 IS REQUIRED FOR EFFICIENT TRANSLATION OF SPECIFIC GERMLINE mRNAs 95

Introduction 95
Results 96
Conclusion 117

CHAPTER 6: EXPRESSION OF FLAG:IFE-1 TRANSGENE 121

Introduction 121
Results 122
Conclusion 130

CHAPTER 7: CONCLUSION 135

REFERENCES 150

APPENDIX A: ATTEMPTS TO ASSAY PGL-1 AND IFE-1 BINDING *IN VITRO* 160

  Introduction 160
  Results 160
  Conclusion 171

APPENDIX B: DISRUPTION OF IFG-1 GENE EXPRESSION USING A TRANSPOSABLE ELEMENT INSERTION 175

  Introduction 175
  Results 176
  Conclusion 189

LIST OF TABLES

2.1 Real-time PCR primers for *C.elegans* mRNAs 38
A.1 Buffers for washes of GST-PGL-1 and GST resins 170

LIST OF FIGURES

1.1 Formation of the pre-initiation complex 11
1.2 *C.elegans* hermaphrodite gonad 24
3.1 The bn127 allele is a deletion in the *ife-1* gene 46
3.2 Brood size and development of *ife-1* hermaphrodites 49
3.3 Capacity of *ife-1* oocytes to be fertilized by wild type sperm 51
3.4 Morphology of *ife-1* hermaphrodite gonad 56
3.5 Oocyte development in *ife-1* hermaphrodite gonads 60
3.6 Expression of pro-apoptotic protein, CED-1:GFP in hermaphrodite gonads 63
3.7 Expression of the pro-apoptotic protein, CED-4 in hermaphrodite gonads 65
4.1 Accumulation of sperm in the spermatheca of hermaphrodites at 25°C 74
4.2 Outline of mating experiments 77
4.3 Brood size as an indication of sperm and oocyte viability from mating experiments 79
4.4 Determination of the *ife-1* temperature-sensitive period by temperature-shift experiments 82
4.5 Schematic of the *C.elegans* male gonad and spermatogenesis 85
4.6 Morphology of spermatocytes in dissected male gonads 88
4.7 Expression of CED-4 in the male gonad 91
5.1 Isolation and analysis of mRNA resolved on sucrose gradients 99
5.2 Polysome profiles from wild type and *ife-1* worms 101
5.3 Translation efficiency of housekeeping mRNA *gpd-3* 103
5.4 Distribution of *oma-1* and *mex-1* mRNAs 107
5.5 Accumulation of MEX-1 in hermaphrodite gonad 109
5.6 Translation of mRNAs involved in embryonic development 113
5.7 Translational efficiency of *glp-1* and *ced-4* 116
6.1 DNA transformations of IFEs into *C.elegans.* 125
6.2 Expression of FLG:IFE-1 from the endogenous promoter 128
6.3 Expression of FLG:IFE-1 from the *pie-1* promoter 132
7.1 Repression of mRNAs by PGL-1 and IFE-1 139
7.2 Interpreting the rate of ribosome initiation on mRNAs 141
7.3 Proposed mechanism for repression of *ced-4* mRNA in spermatocytes 146
A.1 Site-directed mutations introduced into the dorsal face helix of IFE-1 163
A.2 Binding of PGL-1 to His-IFE-1 165
A.3 Binding of ^{35}S-IFE-1 to GST-PGL-1 168
A.4 Co-immunoprecepitations using anti-FLAG antibodies 172
B.1 The insertion of the Mos transposon in *ifg-1* 178
B.2 Isolation of homozygous *ifg-1:mos* strain 181
B.3 Brood size and developmental progression of *ifg-1:mos* worms at various temperatures 183
B.4 Gonad morphology of F1 offspring 186
B.5 Reduction of IFG-1 p170 levels in KX34 worms 188

LIST OF ABBREVIATIONS

eIF	eukaryotic translation factor
4E-BP	eIF4E binding protein
BSA	Bovine serum albumin
Cdk	cyclin-dependent kinase
cDNA	complementary DNA
CPE	cytoplasmic polyadenylation element
CPEB	cytoplasmic polyadenylation element binding protein
CPSF	cleavage and polyadenylation specificity factor
DAPI	4',6-diamidino-2-phenylindole
DEPC	Diethyl pyrocarbonate
DIC	differential interference contrast
dsRBM	double stranded RNA binding motif
DTC	distal tip cell
ER	endoplasmic reticulum
FADD	Fas-associated death domain protein
FB-MO	fibrous body-membranous organelles
FITC	Fluorescein isothiocyanate
FMRP	Fragile X mental retardation protein
GAPDH	glyceraldehyde 3-phosphate dehydrogenase
GCN2	general control non-derepressible -2
GFP	green fluorescence protein
GST	glutathione-S-transferase
HRI	haem-regulated inhibitor
IRES	internal ribosome entry site
ITAF	IRES trans-acting factor
miRNA	micro RNA
mRNA	messenger RNA
MSP	major sperm protein
mTor	mammalian target of rapamycin
NGM	nematode growth medium
PABP	poly(A) binding protein
PCR	polymerase chain reaction
PERK	pancreatic endoplasmic reticulum eIF2 kinase
PI3K	phosphatidylinositol 3-kinase
PKR	protein kinase activated by double-stranded RNA
PVDF	polyvinylidene fluoride membrane
RB	residual body
RISC	RNA interference silencing complex

RNAi	RNA interference
RNP	ribonucleoprotein
SDS	sodium dodecyl sulfate
TCE	translation control element
tRNA	transfer RNA
TSP	temperature-sensitive period
TST	Tris buffered saline with tween
uORF	upstream open reading frame
UPR	unfolded protein response
UTR	untranslated region

CHAPTER 1: INTRODUCTION OF LITERATURE REVIEW

The identity and function of cells differ in large part because of the proteins they make. These proteins allow a neuronal cell to transport signals across the synapse, a muscle cell to contract, and gametes (sperm and oocyte) to give rise to an embryo. When proteins are expressed at the wrong time or place, the fate of the cell can be in danger. In some situations this triggers programmed cell death (apoptosis) or leads to rapid cell replication (proliferation), and ultimately tumor formation and cancer. Mutations in proteins can also lead to other congenital diseases such as metabolic disorders, heart conditions, and neurological disorders. When errors in protein synthesis occur in gametes or embryos, they may ultimately result in birth defects or infertility. Understanding the expression of proteins and the mechanisms by which synthesis is controlled may lead to new means of treatment and detection of inherited disease and cancer.

Gene regulation occurs by multiple mechanisms at several levels. One mode that is often overlooked is at the level of protein synthesis. This translational control allows a rapid response to cellular signals triggering the production of new proteins from available mRNAs. Cells store specific mRNAs in ribonucleoprotein (RNP) complexes until times when the new synthesis of these proteins is required. The proteins bound to mRNAs often repress their translation. The sudden appearance of new proteins is frequently needed for a cell to regulate cell growth, differentiation, or even programmed cell death.

Cell fate: growth, differentiation, and death involve protein synthesis

Newly synthesized protein during the cell cycle

In all organisms cells must grow, duplicate their DNA, and undergo mitosis producing two daughter cells in order to transfer their genetic material to the next generation. The proliferation of cells is especially important during embryogenesis, when a reservoir of progenitor cells is needed prior to differentiation and development into specific cell types. This process allows the organism to maintain a supply of healthy undifferentiated cells with identical DNA content. Growth, chromosomal replication, and cell division occur through a highly regulated process termed the cell cycle. Cells progress through various cell cycle stages in which certain processes are completed. Between individual stages, the cell must enter a checkpoint which ensures the completion of one process before the next is started. These checkpoints are controlled by two classes of proteins, cyclins and cyclin-dependent kinases (Cdks). When cyclins bind the Cdks, they activate a kinase activity that regulates major events in the cell cycle. The concentrations of cyclins vary greatly during the cell cycle, controlled by protein synthesis and degradation (Puri, 1999; Murray, 2004). When the cell cycle process becomes deregulated, uncontrolled cell growth can result producing tumors and leading to cancer.

The cell cycle is divided into four major phases. The two most active periods are S phase (DNA replication) and M phase (nuclear and cellular division). The gap phases (G1 and G2) separate the M and S phases during the cycle. During G1 phase the synthesis of new proteins facilitates an increase in cell mass prior to S phase and the replication of the chromosomes (Puri, 1999). There are checkpoints in the G1 phase that require the binding of cyclin D1 to Cdk4 or Cdk6. Binding of cyclins activates the kinase activity and the Cdks can phosphorylate proteins necessary for the entry into S phase (Puri, 1999). After the entry into the S phase the cyclin-Cdk complex is inhibited and degraded. Similar Cdk activation occurs at the transition into M phase and completion of cell division (cytokinesis) (Puri, 1999; Murray, 2004). As mentioned, the cell cycle process itself is regulated by translational control. For example, Rosenwald et al have shown that the overexpression of eukaryotic initiation factor 4E (eIF4E) in NIH 3T3 cells induces the translation of cyclin D1 mRNA (Rosenwald et al., 1993). These results suggest that the translational control of cyclin D1 expression is responsive to the activity of translation initiation factor in the protein synthetic machinery.

In addition to the cell cycle, other pathways and regulatory signaling events that control cell growth and proliferation are linked to translational control. One pathway tightly associated with protein synthetic activity is the phosphatidylinositol 3-kinases (PI3K) /mammalian target of rapamycin (mTor) pathway. PI3K is activated by mitogens, hormones or growth factors such as insulin (Gingras et al., 2001; Proud, 2006). These substrates bind their respective receptors and induce intermolecular autophosphorylation at tyrosine residues (Schmelzle et al., 2000). The p85 and p110 subunits of PI3K bind these phosphorylated tyrosine residues and lead to the conversion of PIP_2 to PIP_3. The signaling cascade eventually activates the mTOR complex, which is responsible for phosphorylating 4E-binding proteins (4E-BPs) and S6K (Mamane et al., 2004). The phosphorylation of these proteins leads to an increase in cap-dependent protein synthesis of growth related proteins, which will be discussed in detail below.

Cell growth and proliferation respond to both cell cycle cues and signaling pathways such as PI3K/mTor. The involvement of translational control during these processes allow for the sudden onset of new protein synthesis. Cell growth-related signaling pathways also trigger the phosphorylation of translation initiation factors (Mamane et al., 2004). Translational control therefore allows the cell an additional mechanism of gene regulation that is able to respond more rapidly than transcription during growth and proliferation.

Differentiation: gametogenesis

The formation of gametes (oocytes and sperm) from stem cells involves many of the same mechanisms involved in somatic growth and proliferation, as described above. During late gametogenesis, however, chromosomes condense, silencing transcription and the control of gene expression at this level. This makes translational control of gene expression even more important. During oogenesis the oocyte in most species arrests with condensed chromosomes (Wolgemuth et al., 2002; Bettegowda et al., 2007). Translational control thus mediates the synthesis of all new proteins that are required for oocyte maturation and fertilization. It is equally important that these proteins are not made before the appropriate stage. There are many examples of mRNA translational repression during oogenesis that occurs by the binding of inhibitory proteins, which will be discussed later.

During mammalian oogenesis there are two periods in development in which the oocyte arrests and awaits signals to resume development. The first arrest occurs during late embryonic development and stalls at the diplotene stage in meiosis I. The second arrest occurs after ovulation in metaphase II, and is only released upon fertilization (Wolgemuth et al., 2002). As in cell proliferation, these pauses in development are subject to checkpoints for the meiotic process. The control of these checkpoints utilizes similar protein kinases to those used in cell proliferation (cyclins and Cdks) (Wolgemuth et al., 2002). Like cell cycle regulation, the control of these regulatory proteins is also directed by translational control. The prolonged (hours to months) arrests reinforce the importance of stably regulated RNPs in storing maternal mRNAs, and preventing both mRNA degradation and premature recruitment to the translational machinery.

Spermatogenesis also utilizes translational control to mediate gene expression. In order to become small, motile spermatozoa that can survive hostile environments, spermatocytes must condense in size by removing most of their cytoplasmic contents, including ribosomes. It has been suggested that a few nuclear-encoded mRNAs may utilize mitochondrial associated ribosomes for translation in mature sperm, but the overall contribution of translation would be minute (Gur et al., 2008). During spermatogenesis, primordial germ cells undergo multiple rounds of mitotic divisions resulting in a supply of stem cells. These stem cells (spermatogonia) give rise to the primary spermatocytes through an initial differentiation step. These cells enter into meiosis producing secondary spermatocytes and ultimately haploid spermatids (Sutovsky, 2006). Early haploid spermatids are round with full cytoplasmic content and decondensed chromosomes. This allows transcriptional machinery to remain active, producing mRNAs required for the remaining processes of spermiogenesis and fertilization. During mouse spermiogenesis the *Prm1* and *Prm2* mRNAs are made in round spermatids and repressed (stored) by the binding of the Y-box protein, MSY4 (Giorgini et al., 2002;

Kleene, 2003; Gupta, 2005). Progression through spermiogenesis leads to the elongation of the nucleus with condensation of the chromosomes. Transcription becomes silenced by the replacement of histones on the DNA with proteins TP1 and TP2, and no further mRNAs are made by Polymerase II (Gupta, 2005; Sutovsky, 2006). Coincidentally, this stage in spermatogenesis requires the protamine 1 and 2 proteins encoded by *Prm1* and *Prm2* mRNAs to further condense the DNA by replacing TP1 and TP2. Repression of translation of the mRNAs by MSY4 is released and the required synthesis of protamine ensues. As was noted for oogenesis, the regulated use of mRNPs is vital to proper differentiation of sperm.

Translational control therefore facilitates the *de novo* synthesis of specific proteins during delicate times in development. Translational regulation of specific mRNAs allows the introduction of new activities in the gametes, fostering their developmental progression and the completion of differentiation under circumstances in which transcription is silenced and new mRNAs are not synthesized. The repression of these mRNAs by associated inhibitory proteins allows the gamete to selectively recruit the mRNAs for proper temporal expression.

Apoptosis – the selective loss of cells during development

In order for an organism to complete development and maintain homeostasis, select cells undergo programmed cell death (apoptosis). Like cell proliferation and differentiation, apoptosis is also mediated in part by translational control (Holcik et al., 2005). Apoptosis is utilized during development to complete limb formation and tissue/organ morphology in addition to the maintenance of gamete cell number. During gametogenesis in *C.elegans,* for example, apoptosis reduces the number of germ cells that will develop into mature oocytes in the hermaphrodite gonad. Cells destined to die allow for the normal development of remaining oocytes, presumably by acting as nurse cells supplying cytoplasmic contents to the sibling oocytes that survive.

Apoptosis can utilize two separate pathways to trigger the death and degradation of the cell (Hengartner, 2000). In the extrinsic pathway, death receptors such as CD95 or tumor necrosis factor receptor bind their appropriate ligands and become activated. This leads to the binding of Fas-associated death domain protein (FADD) and multiple procaspase-8 molecules. The close proximity of the procaspase-8 subunits leads to their autoactivation through cleavage and the release of active caspase-8. Released protease can then cleave procaspase-3, which is the major executioner protease of the programmed cell death pathway. In addition to the extrinsic pathway, the intrinsic/mitochondrial pathway is induced by cellular stress such as DNA damage, hypoxia, and growth factor depletion (Hengartner, 2000). The intrinsic pathway utilizes members of the Bcl family of proteins for both positive and negative control. When pro-apoptotic Bcl proteins localize to the mitochondria, they penetrate the outer membrane allowing the release of mitochondrial proteins including cytochrome c. Cytochrome c is a key component of apoptosomes, which are composed of Apaf-1 and procaspase-9. Formation of the apoptosome leads to further cleavage and activation of procaspase-9, which in turn also cleaves procaspase-3. Thus both pathways lead to the activation of caspase-3, the protease responsible for cleaving several factors involved in protein synthesis initiation (Hengartner, 2000; Spriggs et al., 2005). This insult to the translational machinery leads to an alteration of the initiation mechanism and the selective translation of specific programmed cell death mRNAs as will be discussed later.

Mechanisms of Translational Control

mRNA Recruitment During Translation Initiation

The rate of protein synthesis for any protein is nearly always determined by the rate of initiation (recruitment) of its mRNA to the ribosome. Since this step limits the rate of translation, it is a common target for translational control. Eukaryotic initiation factors (eIFs) are responsible for the assembly of the ribosome mRNA complex in preparation for translation, including separating the 40S and 60S subunits, recruiting the initiator Met-tRNA, recruiting the mRNA, and scanning the mRNA for the start codon (Gebauer et al., 2004; Sonenberg et al., 2009). The following sections will focus on the pivotal roles of two initiation factors, eIF4 and eIF2, and their involvement in the regulation of protein synthesis in cells.

Before mRNA can be recruited, the ternary complex must join the small ribosomal subunit to form the 43S complex. The ternary complex is comprised of eIF2, Met-tRNA$_i^{Met}$, and GTP (Gebauer et al., 2004; Sonenberg et al., 2009). eIF2 is a heterotrimer comprised of γ, α, and β subunits. The α subunit has a demonstrated regulatory role in the activity of the complex. The recruitment of the Met-tRNA$_i^{Met}$ to the ribosome is essential for translation initiation. In the absence of ternary complex recruitment to the ribosomal complex, all translation is inhibited. By controlling the availability of the ternary complex, cells slow the rate of protein synthesis during times of stress or starvation. eIF2 availability to join the pre-initiation complex is facilitated by the exchange of GDP for GTP by the guanine exchange factor eIF2B. When a cell undergoes stress or starvation, eIF2α kinases phosphorylate the α-subunit of eIF2 and prevent the exchange of GDP for GTP (Merrick, 1992). This prevents eIF2 from binding Met-tRNA$_i^{Met}$ in preparation for another initiation complex. Specific examples of eIF2 regulation during stress and starvation are discussed below.

To complete pre-initiation complex formation, mRNA is recruited to the ribosome. During cap-dependent translation, eIF4E binds the methylated cap of the mRNA and associates with eIF4G, a scaffolding protein that subsequently associates with eIF3 and the 40S subunit (Gingras et al., 1999; Sonenberg et al., 2009). eIF4G also binds the poly(A) binding protein (PABP) bringing the 3' poly(A) tail in close proximity to the methylated cap in a circularized structure (Figure 1.1). In addition to enhancing the recruitment of the mRNA to the ribosome, it is believed that the circularized structure also increases the rate of translation on mRNAs in polysomes, since ribosomes that have terminated translation at the 3' end are in close proximity to the 5' cap. This ordered set of interactions leading to the formation of the pre-initiation complex regulates the rate of translation for most cellular mRNAs.

Stress Response: eIF2α phosphorylation

Translational regulation can be exerted on all mRNAs by global repression or on specific mRNAs by preventing the formation of individual pre-initiation complexes. Global repression of translation initiation is mediated by the phosphorylation of eIF2. As mentioned above, eIF2 is part of the ternary complex responsible for bringing the Met-tRNA$_i^{Met}$ to the 40S ribosomal subunit in translation initiation. The α subunit of

Figure 1.1 Diagram of the 48S pre-initiation complex. The pre-initiation complex is responsible for the recruitment of mRNA to the ribosome for translation. This step is the rate-determining step in translation and therefore a common point for translational control. Essential to cap-dependent translation is eIF4E, which binds the methylated cap of mRNA as well as eIF4G, the scaffolding protein for the complex. Also depicted is eIF2 (2) and Met-tRNA$_i^{Met}$. eIF3 (3) binds the 40S ribosomal subunit as well as eIF4G. eIF4A (4A) is an RNA helicase responsible for removing secondary structure of the 5’ UTR. Poly(A) binding protein (PABP) binds the poly(A) tail of the mRNA and eIF4G.

Figure 1.1

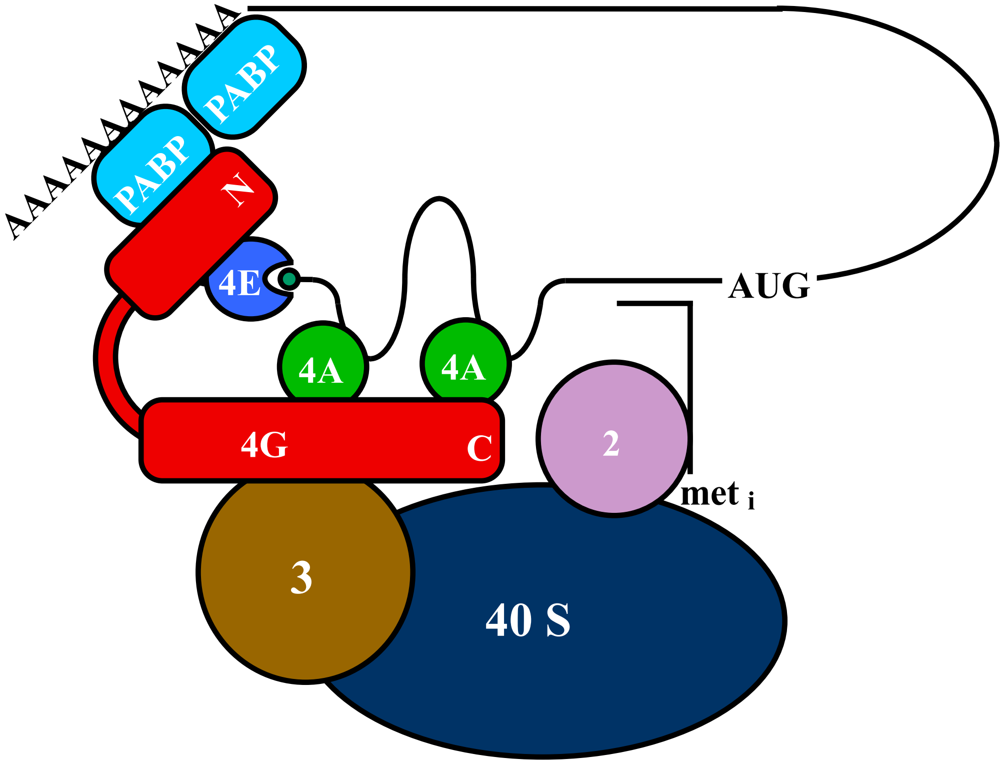
AAAAAAAAAAAAA
PABP
PABP
N
4E
4A
4A
AUG
4G
C
2
met i
3
40 S

from Keiper, *et al.*, (1999) *Intl. J. Biochem. Cell Biol.* **31**: 37-41 eIF2 can be phosphorylated at Serine 51, which leads to a higher affinity for eIF2B, the guanine exchange factor responsible for exchanging the GDP to GTP (Gebauer et al., 2004; Wek et al., 2006). Since all translation initiation requires Met-tRNA$_i^{Met}$ to start the polypeptide, all protein synthesis is inhibited by eIF2 phosphorylation. In some unique instances the mechanism of global repression can pardoxically activate specific mRNAs, usually transcription factors, that subsequently activate genes needed to change the cell's response to stress.

There are four known kinases that phosphorylate Ser51 on eIF2α (Gebauer et al., 2004). Haem-regulated inhibitor (HRI) is utilized during low levels of heme to coordinate hemoglobin biosynthesis. When heme levels are low in mature red blood cells the reduction in protein synthesis prevents the cell from synthesizing globins and the misfolding of apo-hemoglobin (Chen et al., 1995), (Chen, 2007). General control non-derepressible-2 (GCN2) was originally discovered in yeast and phosphorylates eIF2 under low amino acid levels. The resulting low levels of charged tRNAs regulate the scanning mechanism in translation initiation such that the 40S ribosome passes upstream open reading frames (uORFs) in favor of later uORFs, one in particular favors the translation of GCN4 mRNA. The resulting protein activates the transcription of genes involved in amino acid synthesis. Protein kinase activated by double-stranded RNA (PKR) is activated as a cellular response to viral infection and can phosphorylate eIF2 inhibiting translation machinery so that viral proteins cannot be made. PKR is induced by the interferon response and the binding of dsRNA to two separate double strand RNA binding motifs (dsRBM) (Garcia et al., 2007). Pancreatic endoplasmic reticulum eIF2 kinase (PERK) phosphorylates eIF2 in response to unfolded proteins accumulating in the endoplasmic reticulum (ER). In mammals the unfolded protein response (UPR) activates three protein cascades that jointly lead to the induction of specific transcription factors, and the reduction in protein synthesis through the PERK protein (Wek et al., 2007). By reducing the rate of translation, the number of proteins being supplied to the ER lumen is reduced and proper folding can resume. Each of these kinases phosphorylates eIF2 and inhibits global translation during times when the cell needs to conserve or redirect energy, focus on the production of a specific protein, and determine if apoptosis is an appropriate means of action.

mRNA recruitment by eIF4E

Cap-dependent translation involves the recruitment of mRNA to the pre-initiation complex by eIF4E binding to the 7-methylguanosine cap. Another mechanism exists in which the mRNA becomes recruited to the ribosome without the association of eIF4E. These mRNAs contain an internal ribosome entry site (IRES) that is utilized for the recruitment to the pre-initiation complex. Translation that does not utilize eIF4E is termed cap-independent translation and is discussed in a later section. The following paragraphs introduce several mechanisms of translational control that involve eIF4E and cap-dependent translation.

As mentioned above, eIF4E binds the 7-methylguanosine cap of mRNA and recruits it to the pre-initiation complex. The cell’s supply of active eIF4E is tightly regulated and results in a rate-limiting step in translation. A control mechanism to inhibit eIF4E’s association with the pre-initiation complex involves its sequestration by 4E-binding proteins (4E-BPs) (Gingras et al., 1999). In mammalian systems there are at least two canonical 4E-BPs that can be found in most cell types. 4E-BPs are regulated by phosphorylation at multiple residues by various kinases and pathways, including mTor. 4E-BPs bind the dorsal face of eIF4E on the opposite side of the protein from the cap-binding pocket. 4E-BPs bind the same face bound by eIF4G, preventing eIF4E association with the initiation complex, and therefore recruitment of mRNA to the ribosome (Ptushkina et al., 1999). Phosphorylation of 4E-BPs reduces their affinity for eIF4E. Once free eIF4E becomes available, it can recruit the mRNAs to the ribosome for translation. This mechanism of translational repression allows cells to induce translation of mRNAs quickly, particularly in response to growth, cell cycle, and developmental stimuli.

In addition to the canonical 4E-BPs, there are also tissue-specific forms of 4E-BP-like proteins that regulate translation during differentiation processes. An example of this regulation has been well described in *Xenopus* oocytes for the translation of mRNAs required during oocyte maturation. In the quiescent oocyte prior to maturation, mRNAs encoding cell growth proteins such as *c-mos*, cdk2, and cyclins A and B are repressed by the inhibitory 4E-BP like protein, Maskin (Stebbins-Boaz et al., 1999; Richter, 2007). Maskin also binds cytoplasmic polyadenylation element binding protein (CPEB) which interacts directly with the CPE on the 3'UTR. Maternal mRNAs in oocytes tend to contain short poly(A) tails which are unfavorable for translation. Upon induction of meiotic maturation by progesterone, the Aurora kinase phosphorylates CPEB (Barnard et al., 2005; Richter, 2007). Phosphorylated CPEB associates with the cleavage and polyadenylation specificity factor (CPSF) and recruits poly(A) polymerase to elongate the poly(A) tail, favoring translation through binding of poly(A) binding protein (PABP) and eIF4G. Coincident with the 3'end modification, Maskin becomes phosphorylated and releases eIF4E allowing for recruitment to eIF4G and the pre-initiation complex. This example demonstrates that specific 4E-BPs regulate the selective translation of maternal mRNA containing a CPE in the 3'UTR. With the onset of translation of these mRNAs the oocyte begins to synthesize proteins that now allow it to undergo oocyte maturation. Translational control of growth related mRNAs by the association of Maskin and eIF4E demonstrates how regulation of cap-dependent translation can affect development.

A very similar process of regulation occurs in *Drosophila* oocytes and embryos. Translation of the *nanos* mRNA is repressed during oogenesis. During embryogenesis the translation of *nanos* is limited to the posterior pole of the embryo (Johnstone et al., 2001). The mRNA maintains its repression throughout the rest of the embryo by its association with Smaug protein, which binds the translation control element (TCE) on the 3'UTR. Smaug also binds the 4E-BP called Cup. Cup prevents the binding of eIF4G to eIF4E on the *nanos* mRNA and prevents its translation (Nelson et al., 2004). At the posterior pole of the embryo the Oskar protein associates with Smaug allowing the Cup/Smaug repression to be released. The 4E-BP Cup therefore represses translation of *nanos* in an anterior portion of the embryo. This distinct mechanism of cap-dependent translational control allows the establishment of the anterior-posterior axis of the *Drosophila* embryo.

In addition to examples in oogenesis and embryogenesis, specific 4E-BPs are also observed in distinct adult tissues. Nerve cells have two very distinct functional ends (the dendrites and axons) that require separate subsets of proteins in order to relay the response to stimuli. Translational control allows the expression of specific proteins at each end of the neuron. A form of mental retardation arises from the mutation or deletion in the Fragile X mental retardation protein (FMRP) (Napoli et al., 2008). The absence of this protein results in the loss of synapse maturation. FMRP has been shown to exert translational control by directly binding many neuronal mRNAs, but little was know about the mechanism until recently. In association with a 4E-BP, CYFIP1, FMRP represses translation of specific neuronal mRNAs (Napoli et al., 2008). Like Cup and Maskin, CYFIP1 has similarities to many 4E-BPs, including a structural configuration that resembles a reverse L-shape. CYFIP1 and FMRP bind mRNAs near synapses, repressing translation. When the action potential reaches the synapse, CYFIP1 releases eIF4E and bound mRNA. This mechanism used in neurons to control mRNA translation is very similar to the development examples discussed earlier. This suggests that a multitude of cell types may utilize similar modes of cap-dependent translational control that have not yet been discovered.

Utilization of Internal Ribosome Entry Sites (IRESes)

In addition to translational control that affects cap-dependent translation, a less well studied mode called cap-independent translation is used to regulate specific mRNA translation, particularly during times of stress. During apoptosis and some viral infections, proteases are activated that cleave eIF4G to remove the N-terminal region that binds eIF4E and the poly(A) binding protein (PABP) (Coldwell et al., 2004). The removal of the eIF4E binding motif inhibits the recruitment of mRNAs based on the

5’-methylated cap and binding to eIF4E. This new mode of translation is termed cap-independent translation. Without the association with eIF4E, mRNAs must utilize another mechanism to join the pre-initiation complex. Internal ribosome entry sites (IRESes) allow certain mRNAs to bind the translation machinery directly through binding eIF4G, eIF3, and the 40S ribosomal subunit. IRESes contain a high degree of secondary structure (Spriggs et al., 2005). In addition to the structure of the 5’UTR, proteins termed IRES trans-acting factors (ITAFs) act as chaperone proteins, setting up the IRES to join the ribosome.

IRESes are found in a number of cellular and viral mRNAs. Positive-strand RNA viruses contain genomic RNA that doubles as mRNA, encoding proteins necessary for virulence. They must utilize the host cell’s translational machinery to make the necessary proteins (Sarnow et al., 2005). By cleaving eIF4G and shifting the cell to cap-independent translation, the virus reduces translation of cellular mRNA to 3-5%, favoring the translation of uncapped viral mRNAs (Prevot et al., 2003). Cells also utilize the cap-independent translation mechanism during times when a select few mRNAs need to be well translated, such as during apoptosis. Caspase-3 is a very important protease involved in apoptosis, and its activation leads to the majority of cleavage and breakdown of proteins in the dying cell. Early in apoptosis, caspase-3 cleaves eIF4G and shifts translation to the cap-independent mode. This potentiates the induction of apoptosis by the selective translation of pro-apoptotic mRNAs. One pro-apoptotic mRNA translated via an IRES is Apaf-1, which is an important member of the intrinsic pathway for the induction of apoptosis (Coldwell et al., 2000; Holcik et al., 2005). Apaf-1 self-assembles to form apoptosomes with procaspase-9. The formation of apoptosomes allows for the activation of caspase-9, which subsequently activates caspase-3. Up-regulation of caspase-3 and Apaf-1 drives apoptosis until the cell is able to be phagocytized by surrounding cells.

MicroRNAs

A new mode of translation control has been discovered recently. This novel mechanism in translational control by small non-coding RNAs was originally discovered in *C.elegans*. It was found that the production of the LIN-14 protein was repressed by a small RNA, *lin-4*. LIN-14 is necessary for proper larval development. The 22 nucleotide *lin-4* RNA was termed a microRNA (miRNA) and found to bind a site in the 3'UTR of the *lin-14* mRNA with imprecise complementarity (Ambros, 2004; He et al., 2004). Seven separate *lin-4* miRNAs binding sites are found in the 3'UTR of *lin-14* mRNA that prevented translation, but the mRNA still associates with polyribosomes. The mechanism of translational repression is still not completely understood, but appears to affect translation at a point beyond the initiation steps (He et al., 2004). Since the discovery of *lin-4*, hundreds of miRNAs have been discovered in all forms of metazoan animals (He et al., 2004).

Genes encoding miRNAs are generally found in clusters on the chromosomes or in introns of related genes (He et al., 2004). Many of the miRNA genes share transcriptional promoters, which may be involved in their temporal and spatial expression. After transcription, the miRNAs exist in a pri-miRNA form comprised of polycistronic miRNAs in multiple hairpin formations. Individual hairpins are cleaved from one another by the RNase-III enzyme, Drosha (He et al., 2004). Each hairpin fragment (pre-miRNA) is approximately 70 nucleotides and is then transported out of the nucleus by Exportin 5. Once in the cytoplasm the pre-miRNA is cleaved to a 21-25 nucleotide dsRNA fragment by the enzyme Dicer. One of the miRNA strands joins the RNA-induced silencing complex (RISC) and binds the 3'UTR of a target mRNA, repressing translation (He et al., 2004).

Translational control by miRNAs is believed to affect the translation of nearly 30% of all human mRNAs (Erson et al., 2008). miRNAs have been found to regulate the translation of mRNAs in various cell types, including neurons and embryos. Recent studies have also linked miRNAs to tumorigenesis and cancer. Since *lin-4* miRNA does not interfere with the translation initiation process on *lin-14* mRNA, it is suggested that miRNAs repress translation after the recruitment of the mRNA to the ribosome (He et al., 2004). This mode of translational control may regulate both cap-dependent and cap-independent translation.

The descriptions above demonstrate that translational control facilitates the growth, differentiation, function and even death of a cell. Furthermore, translational control can also be mediated by several different mechanisms, many of which involve translation initiation factors. The role of regulated cap-dependent translation through eIF4E is especially important for the development of gametes. The synthesis of proteins encoded by stored maternal/paternal mRNAs in both oocytes and spermatocytes is facilitated through translational control. In order to efficiently study the role of a tissue-specific isoform of eIF4E, I have utilized the model organism, *Ceanoraditis elegans*. The use of this nematode facilitated studies in which use of a higher organism would be difficult. In addition, many of the developmental pathways for gametogenesis, and the involvement of translational control, have been well established in this organism.

Ceanoraditis elegans as a model system

The small nematode *C.elegans* is commonly used as a model system to study an array of cellular and molecular processes. As one of the first eukaryotic genomes completely sequenced, *C.elegans* is well studied, such that many gene expression and development pathways such as neural and muscle development as well as reproductive pathways are well documented (Schafer, ; Kimble et al., 2007). This worm exists as either male or hermaphrodite. The hermaphrodites produce both sperm and oocytes and are capable of self-fertilization. When exposed to males, hermaphrodites mate with males to produce cross progeny. The availability to produce cross progeny in addition to self-fertilized clones makes this nematode very useful for a myriad of genetic experiments. *C.elegans* also has a relatively short life cycle, reaching sexual maturity 72 hours after hatching. The transparency of the organism allows for easy microscopy and live imaging of organs and tissue (Riddle et al., 1997). A number of useful techniques have been established in the worm including RNA interference (RNAi) by the injection of dsRNA or by inclusion of dsRNA in the bacterial food source (Fire et al., 1998). Such techniques allow for the selective reduction of specific gene products. Overall, the well characterized development and versatile molecular transgenics and imaging techniques using this organism make it a desirable choice to study translational control and associated regulation.

C.elegans Spermatogenesis

The reproductive tract in *C.elegans* has many advantages for studying translational control. The hermaphrodite gonad makes up approximately half the mass of the worm. In the hermaphrodite, spermatocytes are made during the L4 larval stage and stored in the spermatheca. Following larval stages, oocytes are only made during adulthood (Hubbard et al.). All gametes are derived from the distal tip cell (DTC) in the gonad and undergo mitosis in a shared cytoplasm (syncytium). Upon entering meiosis I the primary spermatocytes are released from the rachis (the central core of the syncytial gonad) and divide into two diploid secondary spermatocytes. At times the cytokinetic events are not complete and the two nuclei remain in the same cell (L'Hernault, 2009). Meiosis II leads to the production of four haploid nuclei (two from each diploid nucleus). Each haploid nucleus buds off as a spermatid, carrying with it mitochondria and fibrous body-membranous organelles (FB-MOs). The remaining cytoplasmic contents remain sequestered to the residual body (RB), which becomes resorbed into the somatic gonad. Spermatids are no longer capable of protein synthesis since ribosomes are also lost to the residual bodies. In hermaphrodites, the spermatids activate and become motile spermatozoa when pushed into the spermatheca by the first mature oocyte. For spermatids made in males, activation is triggered by seminal fluid during ejaculation. Spermatids develop a pseudopod, develop into spermatozoa and crawl to the spermatheca (L'Hernault). Many mutations have been found for genes associated with spermatogenesis (L'Hernault, 2009). One mutation of particular interest removes the cytoplasmic polyadenylation element binding protein, CPB-1. This CPEB-like protein is required for completion of meiosis during spermatogenesis, but the mechanism of its action is not known (Luitjens et al., 2000). Since CPB-1 is likely involved in translational control, as it is in *D.melanogaster* and *X.laevis*, it may regulate the translation of mRNAs necessary for spermatogenesis. This and other observations suggest that translational control plays an essential role in *C.elegans* spermatogenesis.

C.elegans Oogenesis

Like spermatocytes, oocytes arise from the DTC by mitosis. Multiple cycles of mitotic divisions in the hermaphrodite gonad lead to the accumulation of cells that will continue through oogenesis (Figure 1.2). The DTC produces the protein LAG-2 that binds the GLP-1/Notch receptor on the nearby cells to signal mitotic divisions. This signaling produces a stem cell niche in which cells directly proximal to the DTC receive the highest levels of LAG-2, and the signal dissipates in a gradient from the DTC (Figure 1.2). Cells that are pushed further away from the DTC receive little or no LAG-2 and can transition to meiosis. Thus entry to meiotic divisions is also controlled by the loss of expression of the GLP-1 receptor. The *glp-1* mRNA is translationally repressed by the binding of GLD-1 on the 3'UTR (Kimble et al., 2007). This is just another example of translational control in the development of gametes.

During mitosis and meiosis the developing oocytes share a common cytoplasm (Kimble et al., 2007). As the nuclei transition into the pachytene stage nearly half will undergo programmed cell death (Gumienny et al., 1999). The large degree of apoptosis allows for the additional supply of cytoplasmic contents for the cells that survive and continue through oogenesis. The cells destined to die may act as nurse cells, supplying the additional cytoplasmic contents for the rapidly growing, surviving oocytes (Wolke et al., 2007). Cells that survive become enclosed by a plasma membrane and increase in

Figure 1.2 Diagram of *C.elegans* hermaphrodite gonad. Depicted is one lobe of the hermaphrodite bi-lobed reproductive tract. During the L4 larval stage, sperm are made and stored in the spermatheca. During adulthood the gonad switches to produce oocytes. All germ cells arise from the Distal Tip Cell (DTC) and undergo several rounds of mitotic proliferation in the distal portion of the gonad until the transition to meiotic prophase I. As oocytes progress toward the bend in the gonad arm, nearly half of the developing oocytes will be selected for apoptosis. Those who progress exit pachytene and enter diakinesis where meiosis will arrest as the cell grows and is pushed toward the spermatheca. Once fertilization occurs, meiotic maturation commences and meiosis is completed as the fertilized oocyte becomes an embryo in the uterus.

Figure 1.2

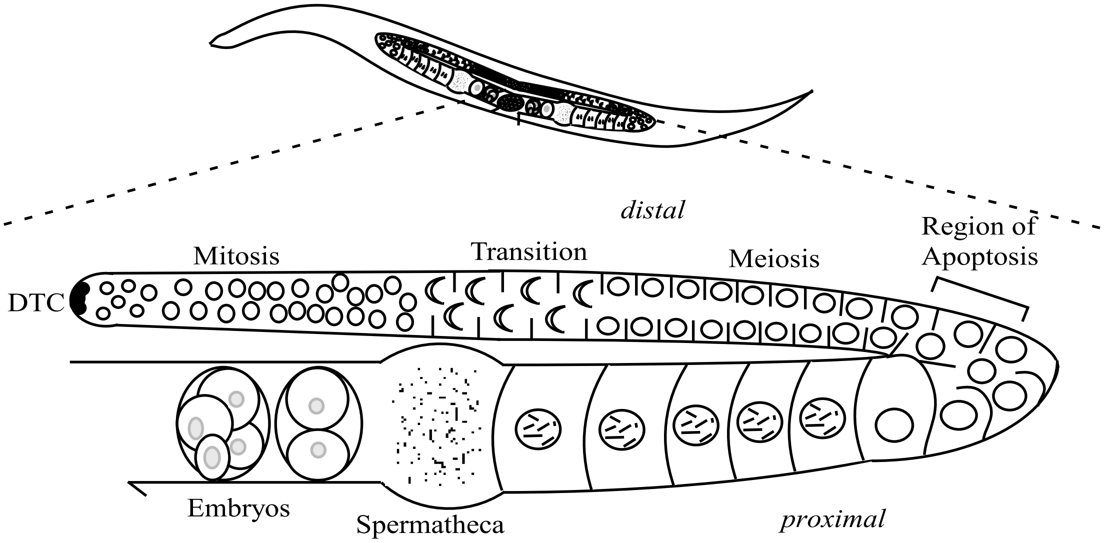
distal
Mitosis
Transition
Meiosis
Region of Apoptosis
DTC
Embryos
Spermatheca
proximal

cell mass. These late stage oocytes arrest in diakinesis of prophase I and await fertilization to trigger oocyte maturation.

Fertilization and meiotic maturation in C.elegans

Fully grown *C.elegans* oocytes arrest in diakinesis prior to metaphase I and accumulate in the proximal arm of the gonad in a linear array. Ovulation through the spermatheca into the uterus is regulated by the somatic sheath cells and triggered by the presence of sperm and involves pushing the oocyte through the constriction of the spermatheca (Miller et al., 2001). Upon fertilization oocytes complete meiotic maturation prior to embryogenesis. The onset of maturation and gonadal constriction is triggered by major sperm protein (MSP) supplied by the sperm (Yamamoto et al., 2006). MSP binds the VAB-1 receptor inhibiting the endocytic recycling of the receptor (Hang et al., 2008). This leads to the activation of mitogen-activated protein kinase (MAPK), which regulates oocyte maturation. The VAB-1 receptor is also found on the surface of somatic sheath cell, and may play a role in MSP induction of sheath cell contractions. Other proteins involved in the completion of meiosis, nuclear envelope breakdown, cortical rearrangement and prevention of fertilization by additional sperm are OMA-1 and OMA-2, which will be discussed further in chapter 5 (Greenstein, ; Govindan et al., 2007). Maturation and fertilization therefore requires the proper expression and localization of various proteins, both maternally and paternally supplied. This temporal and regional expression is likely accomplished by specific translational control of mRNAs.

C.elegans Embryogenesis

The first critical decision made during embryogenesis is the establishment of the anterior-posterior (AP) axis (Gonczy et al., 2005). Sperm enters the oocyte at fertilization at the end opposite the oocyte nucleus and thereby establishes the posterior end. Additionally, the sperm deposits centrioles that become centrosomes required for the development of axial asymmetry. After fertilization, the acto-myosin network induces surface contractions that distribute the PAR proteins throughout the embryo. These proteins are some of the first synthesized proteins in the embryo and are responsible for the early establishment of cell polarity. Some PAR proteins localize to the posterior end while others are found throughout or at the anterior pole (Bowerman, 1998). Cortical contractions end when the centrosomes are localized to the posterior cortex. Polar mediators (MEX-1, MEX-5/6, MEX-3, POS-1, SPN-4) are RNA-binding proteins that appear to mediate the translational expression of the PAR proteins regionally in the embryo and aid in the establishment of polarity (Gonczy et al., 2005). All of these mediator proteins are proposed to bind specific 3’ UTR sequences and inhibit mRNA translation by interfering with the recruitment of the mRNA to the ribosome.

P granules

The maintenance of the germ cell lineage is essential for propagation of a species. The establishment of the germ cell line (germline) occurs soon after fertilization to ensure protection and isolation from the differentiated somatic cells. Germ granules (P granules in *C.*elegans) aid in the recruitment and isolation of the germline in the developing embryo. P granules are RNPs that contain maternally supplied proteins and mRNAs (Kawasaki et al., 1998; Strome). They exist in developing oocytes and the germline of the developing embryo. These specific RNPs are localized around the nuclear envelope and are dynamic, containing many different proteins and mRNAs associated with the complex at various times. P granules play a unique role sequestering maternally supplied mRNAs and proteins during oogenesis and embryogenesis until these proteins or mRNAs are needed (Schisa et al., 2001). P granules segregate exclusively to the germline blastomeres during cell division by cytoplasmic flow or attaching to the nuclear membrane. P granules that remain in somatic blastomeres become rapidly degraded. P granules have also been found in early spermatocytes as they are derived from the germ line, but they do not persist in mature sperm (Seydoux et al., 1999; Strome); (Amiri et al., 2001).

Translational control mediates the development of gametes and embryos in *C.elegans* in a similar fashion as in other organisms. Using this nematode we have discovered that a germline specific isoform of eIF4E plays at least two unique roles in translation of selected mRNAs involved in development of both oocytes and sperm (Henderson et al., 2009). This unique translation factor isoform is required for successful spermatogenesis at elevated temperatures as well as for oocyte production at all temperatures. The work described in this dissertation supports a role for specific isoforms of translation factors in the expression of specific genes involved in development through selective mRNA recruitment to the ribosome.

CHAPTER 2: EXPERIMENTAL PROCEDURES

Growth and Maintenance of C.elegans

The wild type strain used was N2 var. Bristol and was maintained on NGM plates with *E.coli* strain OP50 (Brenner, 1974). Additionally strains utilized were SS712 {*ife-1(bn127)}* II and the heterozygous strain *{ife-1(bn127)*/mT1}, where the *ife-1* deletion is balanced over the lethal mT1 (II/III) translocation, which were graciously supplied by Susan Strome (UC Santa Cruz). MD701 {bcIs39V[P_{lim-7}ced-1::gfp]} was supplied by Barbara Condrandt and used to observe apoptotic events in the hermaphrodite gonad (Zhou et al.). The strain DH245 {*fem-2(b245)* III} was utilized as a control strain with a fully feminized gonad. This strain does not produce sperm at 25°C(Kimble et al.). The homozygous *ifg-1:mos* strain, KX34 was created by outcrossing the plate 9.75 (Laurent Segalat, CNRS) five times and allowing the hermaphrodites to produce self-progeny. All strains were maintained on NGM plates seeded with a lawn of *E.coli* OP50 as a food source. Maintenance of the strains also included washing and transferring large quantities of worms in 2-15 ml of M9 solution followed by centrifugation and subsequent freezing or placement to new plates (Portman, 2006). In addition individual worms can be transferred to new plates, microscope slides, or PCR reaction tubes using formed and polished 32 gauge platinum wire welded to a glass pasture pipette.

To grow large quantities of worms, strains were seeded to 5X peptone NGM plates with chicken egg yolk and OP50 *E.coli* (Portman, 2006). Prior to the consumption of all bacteria and egg mixture worms were washed off the plate in 0.1 M NaCl and pelleted using low-speed centrifugation. The worms were isolated from the top of the tube after centrifugation in a 35% sucrose solution at 4°C. Worms were then purged of bacteria from the intestines by incubation and rotation in Petri dishes in 1X M9 solution. The worms were rinsed several times in M9 and sedimented by centrifugation, then frozen with 4 mM vanadyl ribonucleotide complex in liquid N_2.

In order to synchronize worm to the same developmental stage, egg-laying hermaphrodites were exposed to 1.5% hypochlorite and 1 M NaOH. This solution kills and dissolves adult and larval stage worms, leaving embryos intact due to the protection of the chitin shell. The remaining embryos were washed in M9 solution and allowed to hatch to L1 larval stage. While in the M9 solution the worms will arrest at the L1 stage due to the lack of food supply.

Genomic PCR

To detect the *ife-1(bn127)* deletion in worms we utilized whole worm genomic PCR to amplify the *ife-1* gene. Whole worms were frozen then lysed in Single Worm Lysis Buffer (1X Amplitaq Gold PCR Buffer, 1 mM $MgCl_2$, 0.45% NP-40, 0.45% Tween-20) with 200 µg/µl Proteinase K in the thermocycler at 60°C for 60 minutes and 95°C for 10 minutes followed by storage at 4°C. Genomic PCR to detect wild type and mutant *ife-1* genes was performed in 1X Amplitaq Gold PCR buffer with 1.5 mM $MgCl_2$, 0.5 µM of each of the following primers (5’-CCAACCGACGATGACTACG-3’) and (5’-TTGGGXXTGGAAACCACAAG-3’), 0.2 mM of deoxynucliotide triphosphate (dNTP) mix, 0.2 µl of Amplitaq Gold. The following thermocycling conditions were used to amplify the target sequences: 95°C for 9 minutes, {95°C for 30 seconds, 55°C for 30 seconds, 72°C for 2 minutes} repeated 43 times, 72°C for 10minutes and stored at 4°C or on ice. Products of the PCR reaction were run on a 1% agarose/TBE gel in 0.5X TBE running buffer and stained with ethidium bromide. Bands at 1,359 base pairs (wild type) and 769 base pair (*ife-1* deletion) were detected by UV light.

Calculating Fertility and Extent of Development by Observation

To calculate the offspring produced by one hermaphrodite worm (brood size) by *ife-1* and wild type hermaphrodites, three plates of each strain containing three larval (L4 stage) hermaphrodites were placed at each temperature (15°C, 20°C, 25°C). Following a 24 hour incubation at that temperature the worms were transferred to new plates at the same temperature. This process was repeated for a total of 72 hours. At the end of 72 hours the hermaphrodites were removed and discarded. All offspring were observed, counted and staged every 24 hour for a total of 96 hours. Their progression through development was recorded and final developmental stage graphed. To analyze and display the data collected for brood sizes, the sum of all offspring produced for that strain was normalized to the number of hermaphrodite "mothers". These calculations allowed graphing of the average brood size per hermaphrodite with the calculated standard deviation shown in error bars. The brood sizes were graphed relative to time and temperature.

In order to determine the individual contributions of oocytes and sperm to fertility, *ife-1* worms were mated with wild type and *fem-2* worms. One hermaphrodite worm was placed on a plate with three male worms of the same or different phenotype. The hermaphrodite to male ratio ensures successful mating. All four worms were transferred to new plates at 48, 72, and 96 hours. Male worms were replenished when needed to guarantee an adequate supply of male sperm was available. Brood size was recorded as described previously. In addition, the proportion of male and hermaphrodite offspring were individually assessed and recorded.

Determining the Temperature Sensitive Period (TSP) for Fertility

The temperature-sensitive period (TSP) of gamete formation is the period in development that is critical for fertility at the sensitive temperature. Results from experiments in chapter 3 show that the *ife-1* mutant is sterile at 25°C. The TSP will show which stage in development is responsible for the sensitivity to the increased temperature for fertility. In order to determine the TSP, wild type and *ife-1* worms were synchronized by hypochlorite treatment and incubation in M9. After approximately 12 hours in M9, L1 larval worms were transferred to NGM plates seeded with OP50 *E.coli*. Four to ten worms were placed on seeded plates at either 20°C or 25°C. Every 12 hours a single plate for each strain was moved to the other temperature (e.g. 20°C to 25°C and 25°C to 20°C). At 120 hours the brood size of the shifted worms was recorded.

Microscopy and Imaging

All images were acquired using an Axiovert 200M inverted microscope (Carl Zeiss) using differential interference contrast (DIC) microscopy and fluorescence microscopy equipped with FITC, and DAPI filter cubes and analyzers. Images were analyzed using the Axiovision 4.3 software (Carl Zeiss). In preparation of whole worm samples in order to examine the accumulation of late stage oocytes in the hermaphrodite gonad, young adult (approximately 24 hours post L4 stage) hermaphrodites were placed in 1X M9 with 30 mM Sodium Azide on a microscope slide. The sample was covered with a glass cover slip and sealed with clear fingernail polish. Images were visualized and captured using the 40X objective.

Whole worms were fixed for DAPI staining in order to visualize nuclear material in the intact animal. Worms were picked into 20 µl of M9, 2 µl of 36% formaldehyde, and 22 µl of Modified Ruvkun's witches brew, MRWB (160 mM KCl, 40 mM NaCl, 20 mM Na_2EGTA, 10 mM spermidine, 30 mM Pipes pH 7.4, and 50% methanol). Fixed samples were stored at -80°C. Upon thawing, the sample was diluted in M9, spun down, and supernatant removed, leaving fixed worms. Next, 200 µl of M9 containing 1 µg/ml of DAPI was added. The worms were incubated in this solution for 30 minutes to 2 hours. The worms were transferred to a clean microscope slide, covered, and sealed.

The dissection and microscopy of male and hermaphrodite gonads utilized two different buffer solutions. Hermaphrodite gonads were dissected from worms in 1X egg buffer (60 mM NaCl, 32 mM KCl, 3 mM Na_2HPO_4, 2 mM $CaCl_2$, 5 mM Hepes pH 7.2, 0.2% glucose, 4 mM levamisole) by cutting worms just below the pharynx with a 31.5 gauge needle (Edgar et al., 1994). Gonads spontaneously extrude from the worm and were separated from other body fragments, covered with a glass coverslip and sealed. Male gonads were dissected in sperm buffer (45 mM NaCl, 25 mM KCl, 1 mM $MgCl_2$, 0.5 mM $CaCl_2$, 50 mM Hepes ph 7.8, 10 mM dextrose)(Zannoni et al., 2003). Male worms were decapitated with 31.5 gauge needles between the pharynx and the bend of the gonad. Carcasses were not teased away from gonad due to the delicate nature of the male gonads. A coverslip was applied to the sample with small amounts of silicon gel and pressed until spermatids were released from the gonad. Both male and hermaphrodite gonads were dissected in the presence of 0.5-1.0 µg/ml Hoechst dye. Prepared slides were mounted on the inverted microscope and visualized using DIC and fluorescence microscopy.

Immunostaining

All immunohistochemistry utilized a protocol obtained from Dr. Jennifer Schisa (Central Michigan University). Ten to fifteen worms were picked into 7-15 µl of 0.75X M9 and 10 mM levamisole on a 22 mm X 40 mm coverslip. Worms were decapitated by cutting below the pharynx with a 31.5 gauge syringe needle. After the gonad was extruded, gut and other body tissue is dismantled and removed using a mouth pipette. Additional buffer solution was added as needed. The coverslip was inverted onto a poly-L-lysine treated brown 3-well slide (Fisher). The slide was quickly placed on a 0.25 inch thick metal plate exposed to dry ice, and pressure was applied for the first 10 seconds. After the minimum 10 minute incubation, the coverslip was quickly popped off and the slide immersed in a Coplin jar of methanol at -20°C for 10 minutes. Slides were then transferred to a Coplin jar of -20°C acetone for 10 minutes. Next the slides were placed in a Coplin jar containing Tris-buffered saline with tween (TST). Incubation in fresh TST was repeated. The sides and back of the slides were dried and 10 µl of diluted primary antibody was added [(goat anti-CED-4 or goat anti-MEX-1 (Santa Cruz), each 1:50 in TST)]. Slides were incubated with antibody dilutions at 4°C overnight. Slides were then rinsed twice in TST for five minutes and dried. Next, 10 µl of diluted donkey anti-goat Alexa 488 (Molecular Probes, 1:1000 in TST) was applied to the slide and incubated in the dark for one hour at room temperature. The slides were rinsed in a Coplin jar with TST for five minutes and placed in TST containing DAPI for five minutes. The slide was dried and covered with a 18 mm X 18 mm coverslip with 5 µl of mounting media (20 mM DABCO, 90% w/v glycerol) and sealed with fingernail polish (Contreras et al., 2008).

Creation of ced-1::gfp, ife-1 homozygous strain

The *ced-1::gfp, ife-1* homozygous strain was created by mating *ced-1::gfp/+* males with *ife-1* hermaphrodites. The F1 hermaphrodites that expressed GFP were allowed to self propagate to produce F2 populations. Sixteen individual GFP expressing F2 hermaphrodites were selected to individual plates. After the laying of the F3 population, the F2 hermaphrodites were assessed for the *ife-1* gene by PCR, while *ced-1::gfp* was analyzed by the expression of GFP in the F3 population.

Analysis of polysomes by sucrose gradient fractionation

Large quantities of worms were grown on chicken egg/ OP50 *E.coli* plates. Worms were washed off and frozen in liquid N_2 as mentioned above. Seven to ten frozen pellets of concentrated worms in 4 mM Vanadyl Ribonucleotide Complex were ground under liquid N_2 with mortar and pestle. Prior to grinding 750 µl of 2X lysis buffer (50 mM Tris HCl pH 8, 300 mM NaCl, 10 mM $MgCl_2$, 1 mM EGTA, 0.4 mg/ml heparin, 800 U/ml RNasin, 4 mM Vanadyl Ribonucleotide Complex, 5 mM PMSF, 0.4 mg/ml cycloheximide, 2 mM DTT, 1% Triton X-100) was added to the sample(Dinkova et al.). The ground sample was thawed and centrifuged at 10,000 rpm at 4°C for 15 minutes. The supernatant was divided and layered on two 10-45% sucrose gradients (300 mM KCl, 50 mM Hepes, 2 mM $MgCl_2$, 1 mM DTT, sucrose). Gradients (11 ml) were prepared using the Seton gradient maker. The gradients were centrifuged in the SW-41 rotor at 38,000 rpm for 1 hour and 45 minutes at 4°C. The break was not applied after centrifugation. The gradients were fractionated using the ISCO pump and fractionator with the A260 recorded by the ISCO UA-6 UV-VIS detector. Each gradient was separated into twelve 1 ml fractions.

RNA was isolated by extraction with TRIzol (Invitrogen). Each fraction was divided into three tubes, vortexed with 1 ml of TRIzol solution, and incubated at room temperature for five minutes. 200 μl of chloroform was added and shaken vigorously for 15 seconds followed by a two-minute incubation at room temperature. Samples were centrifuged at 4°C, 12,000 xg for 15 minutes. The top (aqueous) layer was removed, combined with 1 ml of isopropyl alcohol, vortexed, and incubated at room temperature for ten minutes to precipitate the RNA. Samples were then centrifuged for ten minutes at 12,000 xg at 4°C. The supernatant was removed and the pellet was washed with 70% ethanol. Centrifugation at 7,500 xg for five minutes followed. The supernatant was removed and the pellet was dried in a speedvac for two minutes. Pellets were resuspended in 10 μl of RNase/DNase-free water or DEPC-treated water. Each fraction's three samples were re-combined to yeild 30 μl of RNA. The concentration of RNA from each fraction was determined by absorbance at 260 nm using the Nanodrop.

qRT-PCR

cDNA was synthesized from the RNA isolated for each fraction, using the iScript cDNA synthesis kit (BioRad) as directed by manufacturer's instructions. 1 μg of RNA was combined with 1 µl of iScript reverse transcriptase and 4 µl of iScript reaction mix. The reaction volume was brought to 20 µl with RNase/DNase-free water and incubated at 25°C for five minutes, 42°C for 30 minutes and 85°C for five minutes. The cDNA was used for Real-time PCR using the Sybr Green Supermix (BioRad) in the iCycler iQ Real-time PCR machine (BioRad) according to manufacturer's instructions and an annealing temperature of 55°C. Table 2.1 shows the primers used in the Real-time PCR reaction. All cDNAs were diluted to 1:100 in each reaction mix.

The Ct values for each fraction were normalized using the linear equation determined by a set of wild type cDNA dilution samples. The equations allowed for the calculation of an arbitrary mass to be determined for each sample (3 samples/fraction) for each mRNA. The following linear equations were used: *gpd-3*, y=-4.118x+20.430; *glp-1*, y=-3.772x+29.443; *pal-1*, y=-4.167x+27.240; *pos-1*, y=-3.799x+23.335; *mex-1*; y=-4.172x+3.204; *oma-1*, y=-4.111x+30.433; and *ced-4,* y=-3.123x+31.563 (y= log starting quantity (ng), x= Ct value). The average arbitrary mass of each fraction was calculated and used to determine the % mRNA found in each fraction.

Construction of pSKflgife-1let and pie-1flgife-1

The ife-1 endogenous promoter was amplified by PCR from the pPD-ife-1 construct. The forward primer (5' – GACATAATCTAGATTTTTCGAGAAAA – 3') annealed approximately 1.5 kb upstream from the start codon, while the reverse primer annealed to the *ife-1* cDNA with adjacent sequence encoding the FLAG tag (DYKDDDDK) sequence (5' – GGCGCCAGAT CTGCAGCTTA TCGTCGTCAT CCTTGTAATC CATGGATCCT TTCTGAAATT TAAATATATT AA – 3'). The PCR product was

Table 2.1 Real-time PCR primers for *C.elegans* mRNAs. Primer sequences for the real-time PCR primers used for analysis of translation efficiency from polysome isolation. All primers are designed with an ideal annealing temperature of 55°C.

Table 2.1

mRNA	forward primer	reverse primer
oma-1	5’-CAAACTGCTAACTTGATTGCT-3’	5’-GGATCAAACTGTTGAAATGG-3’
mex-1	5’-AACAAACGTTTCTAGGCTTC-3’	5’-CCAACATTAGGCTTATCCATTT-3’
pos-1	5’-AAATTGTCGATGGGAATG-3’	5’-ACGAAGAGTGAATGATTGTG-3’
pal-1	5’-AAGGATCGAAGATCAAGCA-3’	5’-AATTCTTTTTCCAGTTCAAGG-3’
glp-1	5’-TGGACTTGTGAAGTCTGATG-3’	5’-ATCGATTTCGTTTCTCTTTG-3’
ced-4	5' -CAGCAACGCTTATGATGTTT-3'	5' -ACCGACTAATCCTCGACTTT-3'
gpd-3	5’-GATCTCAGCTGGGTCTCTT-3’	5’-TCCAGTACGATTCCACTCAC-3’

digested with PstI and XbaI and ligated into the pSKife-1 plasmid cut with the same enzymes. The resulting pSKflgife-1 construct was used to make pSKflgife-1let by similar methods. The let858 3'UTR was amplified using the let858Xhos primer (5'-GCCGGCTCGAGTGATCGACGCCAACGTCGTT – 3') and let858Kpna primer (5' – CGGCCGGTACCGGGCCCAAGCGAGGACAATT – 3'). The PCR product was digested with XhoI and KpnI along with pSKflgife-1. Products were isolated and ligated to pSKflgife-1let. Through collaborative efforts in the lab, the endogenous *ife-1* promoter was removed from the pSKflgife-1let construct and replaced with the *pie-1* promoter. These final constructs were linearized using the blunt end restriction enzyme, NaeI, for digestion.

Injection of DNA into the hermaphrodite gonad for transformation

By injecting linearized DNA into the distal hermaphrodite gonad, the DNA is dispersed throughout the early meiotically dividing oocytes. The DNA is incorporated into the nuclei of the oocytes for expression in the F1 generation. Transformations were made by "simple array" injection solution. This included 5- 200 ng/ul of each linearized pSKflgife-1 (or pie-1flgife-1) and pRF4, encoding the rol-6 selectable marker. Individual young hermaphrodite adults were picked onto a 1.8% agarose injection pad and submerged in mineral oil. The solution was injected into the gonad at 10-50 psi. The worms were allowed to recover in a drop of M9 for 10-30 minutes, and then transferred to NGM plates to recover and produce (transformed) offspring. Rolling F1 progeny were picked to individual clone plates and allowed to self-fertilize and produce progeny. Populations from F1 progeny that continued to produce rolling progeny where considered an expressing strain and frozen down for future experiments.

Detecting protein levels by western blot

Worms were prepared by lysis in 4X SDS Load Buffer by boiling or ground by mortar and pestle under liquid N_2. Protein concentrations were assayed by PVDF membrane with BSA standards and commasie staining. Adjustments are made to load approximately equal amounts of protein lysate on a SDS acrylamide gel. The gels were run at 50-100 volts in western running buffer and transferred to a PVDF membrane at 100 mAmp overnight in western transfer buffer. The membranes were blocked in 5% non-fat dry milk in TST for 1 hour at room temperature. Primary antibodies were diluted 1:500 to 1:1000 in 5% milk/TST and applied to the membrane for 2 to 3 hours or overnight. The blots were washed in TST for five minutes, three times and exposed to anti-rabbit alkaline phosphatase (1:2000) or anti-rabbit horse radish peroxidase (1:4000) in 5% milk/TST for 1 hour. The blots were rinsed with TST three times for five minutes and developed using either the BCIP/NBT kit (Vector) or ECL+(Amershan) and exposed to the Typhoon Phosphoimager.

CHAPTER 3: THE ROLE OF IFE-1 IN OOGENESIS IN *C.ELEGANS*

Introduction

The process of generating viable oocytes capable of fertilization and development into an embryo is essential for sexual reproduction. Primordial germ cells undergo multiple rounds of mitosis, supplying the embryo with cells that will differentiate into gametes (sperm or oocytes). In this chapter I will focus on the production of oocytes through the process of oogenesis. Meiotic divisions ultimately lead to the production of a haploid oocyte competent for fertilization and embryonic development. In most species there are various check points or arrests in the meiotic cycle that regulate the development of the oocyte. When the oocyte arrests during prophase I, the cell prepares for upcoming events in oogenesis, fertilization, and embryogenesis by synthesizing mRNAs and proteins. These mRNAs will be "stored" (translationally repressed) in ribonucleoproteins (RNPs) in the oocyte (Alberts, 2002). The progression through these checkpoints is triggered by extracellular signals such has hormones or fertilization and differ from species to species. As the cell is arrested in diplotene of prophase I, the cell remains transcriptionally active. RNAs needed for protein synthesis during oocyte maturation and embryogenesis are made and stored. The chromosomes then condense into a transcriptionally inactive state until embryogenesis. The stored mRNAs account for all new proteins expressed during late oogenesis and early embryogenesis.

The regulation of gene expression during oogenesis has been well studied in the nematode, *C.elegans.* The process differs slightly from oogenesis in the mammalian systems, but has many similarities such as the storing of maternal mRNAs. Oogenesis occurs in a linear progression in the two lobes of the hermaphrodite gonad in *C.elegans.* All germ cells arise from the distal tip cells (DTCs) and undergo multiple rounds of mitotic divisions in the niche regulated by the DTC (Kimble et al., 2007). The developing oocytes transition into meiosis where, like other organisms, the cells arrest in prophase I. Early in this process cells make mRNAs, which will be translated during oocyte maturation, fertilization, and embryogenesis. Many of these mRNAs are stored in germ granules, termed P granules, in *C.elegans*. P granules are RNPs that contain maternal mRNAs and proteins (Schisa et al., 2001; Strome). Many components of P granules have important roles in germline maintenance, oogenesis, and early embryonic development.

Interestingly, one isoform of eIF4E, IFE-1, has been shown to associate with P granules through binding to the protein, PGL-1 (Amiri et al., 2001). The co-localization of this translation factor to P granules may facilitate the eventual translation of the stored mRNAs. There are five isoforms of eIF4E in *C.elegans*, termed IFE-1 through 5. IFE-2 and IFE-4 are expressed in somatic tissue and have been associated with ageing and muscle/nerve development, respectively (Dinkova et al., 2005; Syntichaki et al., 2007). The expression of IFE-1, IFE-3 and IFE-5 has been observed in the cells of the reproductive system (oocytes or spermatocytes). Amiri et al. demonstrated that the depletion of IFE-1 by RNAi leads to defects in spermatogenesis (Amiri et al., 2001). This was shown by a reduction in fertility at 25°C that was rescued by wild type sperm. Additionally, this study suggested that IFE-1 had no obvious effects on oogenesis. Depletion of IFE-1 by RNAi does not completely abolish available IFE-1 from the worm. Furthermore, the role of IFE-1 during oogenesis may have been masked in part by the severity of the spermatogenesis defects or the low levels of available IFE-1. These deficiencies in the RNAi study support the need for further investigation into the role of IFE-1 during oogenesis.

Like the production of gametes in other organisms, the supply of available germ cells in *C.elegans* is reduced by programmed cell death (apoptosis) during oogenesis. Nearly half of the developing oocytes undergo apoptosis during diplotene stage (Zhou et al., 2001). During early oogenesis the cells share a common cytoplasm. It is plausible that the oocytes destined to die may act in a role similar to nurse cells, supplying the developing oocytes with mRNAs, proteins and organelles (Wolke et al., 2007). The process of apoptosis in the *C.elegans* germline has been well studied and is important for the maintenance of homeostasis.

In the studies described in this chapter I have observed a defect in the production of viable oocytes in the absence of IFE-1 by utilizing a *C.elegans* strain that is homozygous for a deletion in the *ife-1* gene. By using a viable null mutant, the role of IFE-1 can be analyzed without the presence of maternally supplied IFE-1. The data presented here demonstrate that IFE-1 is required to produce oocytes competent for fertilization at a rate equivalent to that of wild type hermaphrodites. I have also examined the role of IFE-1 in germline apoptosis. Unlike the depletion of the eIF4G isoform p170 (IFG-1), the lack of IFE-1 did not induce apoptosis in developing oocytes. The results presented here further assess the role of IFE-1 in the production of viable oocytes competent for fertilization.

Results

In order to more closely analyze the role of IFE-1 in oogenesis, we utilized a strain of worms bearing a null mutation in *ife-1*. By analyzing the progression through oogenesis in this mutant, we were able to assess which cellular processes require IFE-1. Characterization of a stable homozygous mutation, which removes all functional IFE-1, is superior to the use of RNAi for many reasons. First, the use of a null mutant prevents the accumulation of any functional IFE-1 in the organism. In addition, the availability of a stable and viable strain that lacks IFE-1 allows for the collection of large quantities of material for biochemical experiments. This is not feasible with RNAi treated worms. The availability of a large, homogeneous mass of worms proved most advantageous in work characterizing the role of IFE-1 in translation, which will be discussed in chapter 5. The acquisition of this homozygous stain was an indispensable resource for obtaining the results discussed below.

The *C.elegans* strain SS712 is homozygous for the *ife-1(bn127)*II mutation and was obtained through collaboration with Dr. Susan Strome (UC Santa Cruz). The *bn127* allele is a deletion made by the use of trimethylpsorale and UV treatment of *C.elegans.* This deletion removes 590 bases in the coding region, intron and 3' UTR of the *ife-1* gene (Fig 3.1A). The mutation removes part of exon 1 and all of exon 2, including the sequences necessary for m7G-cap binding and association with eIF4G. Since the regions necessary for binding to both the mRNA and pre-initiation complex are removed, the mutation was assumed to be null. Additionally, the *bn127* deletion can be detected by whole worm genomic PCR and distinguished from wild type, full length *ife-1* by the length of the amplified product (Fig 3.1B).

Figure 3.1 The bn127 allele is a deletion in the *ife-1* gene. (A) Depiction of the wild type and *ife-1*(bn127) gene. The deletion removes part of exon 1 and all of exon 2. Included in the deleted coding region (149 of 212 codons) are the sequences required for m7-GTP cap binding and eIF4G binding. (B) Products of whole worm genomic PCR. Three individual hermaphrodites homozygous for *ife-1*(bn127) show a single product band at 769 base pairs (bp). Heterozygous hermaphrodites produce a 769 bp and a 1359 bp, wild type band. PCR of wild type hermaphrodites produce only the longer 1359 bp wild type product.

Figure 3.1

A

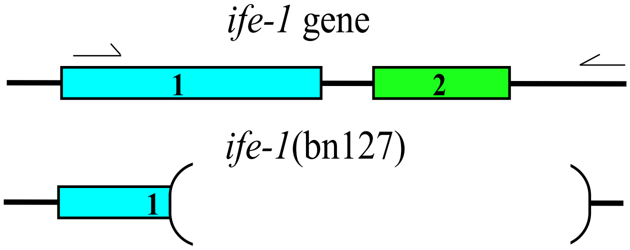
ife-1 gene
1
2
ife-1(bn127)
1

B

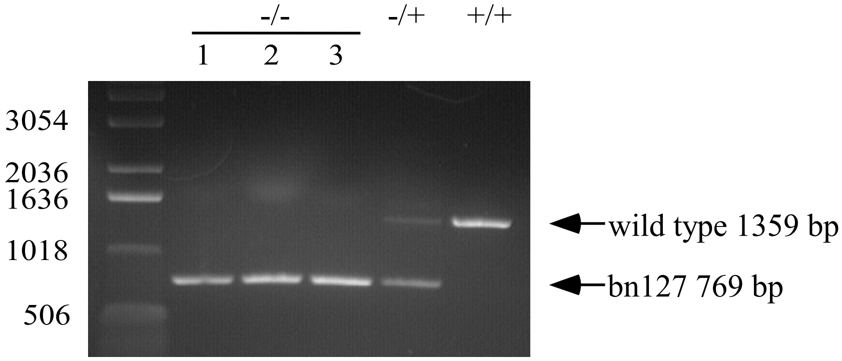
-/-
-/+
+/+
1
2
3
3054
2036
1636
1018
506
wild type 1359 bp
bn127 769 bp

Previous studies indicated that depletion of IFE-1 by RNAi caused a decrease in fertility as a function of temperature (Amiri et al., 2001). In order to investigate the fertility of the null mutant, we examined the offspring production (brood size) produced by wild type and *ife-1* hermaphrodites. We also observed the development of these offspring over 96 hours at their respective temperatures. At 15° and 20°C *ife-1* hermaphrodites produced some viable offspring. By comparison to wild type, the brood size of *ife-1* hermaphrodites was dramatically decreased (Fig 3.2A,B). The *ife-1* hermaphrodites produced 10-20-fold less viable offspring than wild type hermaphrodites at the same temperature. The development of these offspring was also significantly slower than that of wild type offspring. At 20°C all of the wild type hermaphrodites reached adulthood by 96 hours, whereas some *ife-1* offspring remained in larval stages. These observations made from hermaphrodite self-fertilization assays at 15° and 20°C demonstrated that the fertility of the IFE-1-deficient strain was reduced at least ten-fold. Therefore IFE-1 must play a role in the production of viable gametes competent for fertilization and embryonic development at 15°C or 20°C.

When the brood size was examined at 25°C, essentially no viable offspring were produced by *ife-1* hermaphrodites (Fig 3.2C). Wild type hermaphrodites were capable of producing significant broods at 25°C (approximately 150 worms). Some unfertilized oocytes were also produced by both strains. Other investigations have suggested that the unfertilized oocytes most likely result from the depletion of the hermaphrodites' sperm supply while oocyte production continues (Jud et al., 2008). Since *ife-1* hermaphrodites failed to produce any viable offspring, yet laid unfertilized oocytes, these

Figure 3.2 Brood size and development of *ife-1* hermaphrodites. The offspring production of *ife-1* and wild type hermaphrodites was observed, as was the development of those offspring over 96 hours. (A, B) At 15°C and 20°C the *ife-1* hermaphrodite produced less offspring (approximately 20-fold fewer at 20°C) than wild type hermaphrodites. At 96 hours the offspring produced from *ife-1* hermaphrodites did not reach the same developmental stage as wild type offspring. This suggests a delay in growth of *ife-1* mutant worms. (C) At 25°C the *ife-1* hermaphrodites failed to produce any viable offspring with only the accumulation of unfertilized oocytes. This indicates that the lack of IFE-1 results in temperature-sensitive sterility of the organism. Error bar represent standard deviation and n=9 per strain for each temperature. (oocytes "ooc", embryos "emb", larval stages L1 and L2 "L1/L2", larval stages L3 and L4 "L3/L4", and adult "Ad").

Figure 3.2

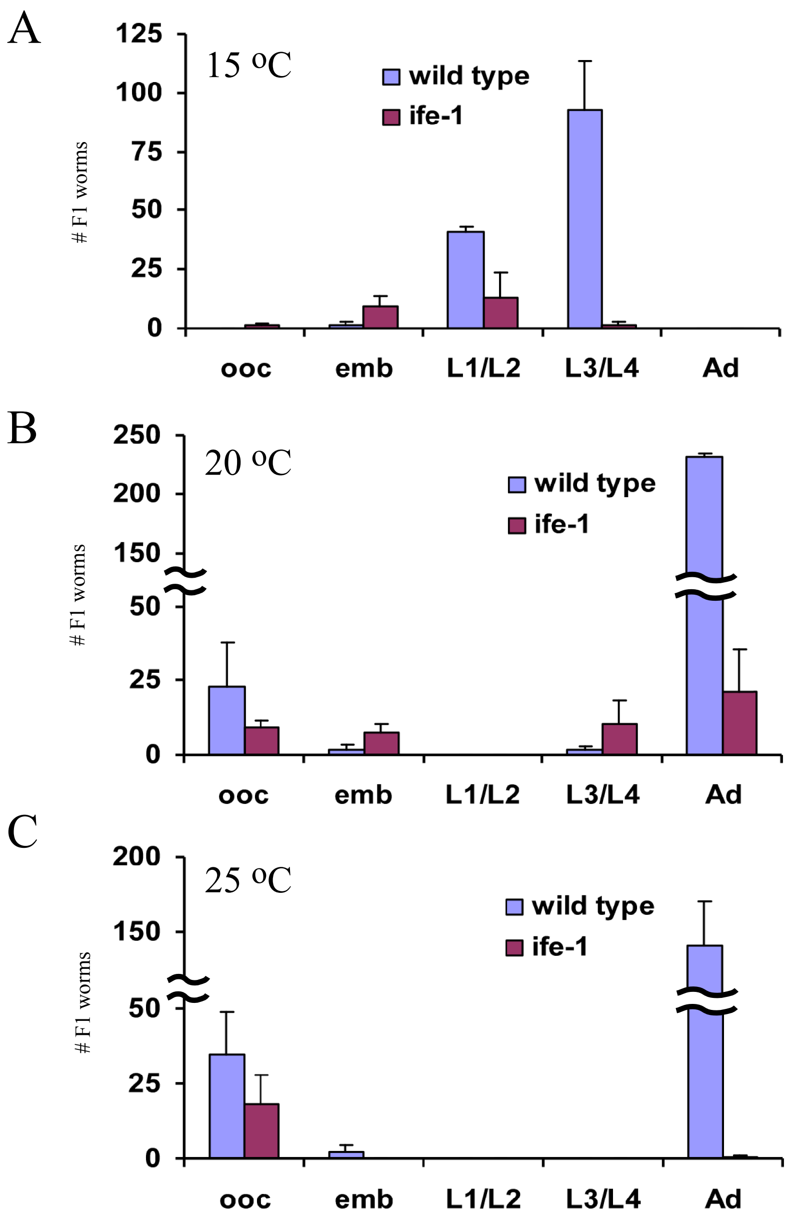
A
15 °C
wild type
ife-1
# F1 worms
125
100
75
50
25
0
ooc
emb
L1/L2
L3/L4
Ad
B
20 °C
wild type
ife-1
# F1 worms
250
200
150
50
25
0
ooc
emb
L1/L2
L3/L4
Ad
C
25 °C
wild type
ife-1
# F1 worms
200
150
50
25
0
ooc
emb
L1/L2
L3/L4
Ad

Figure 3.3 Capacity of *ife-1* oocytes to be fertilized by wild type sperm. Brood size from one hermaphrodite exposed to three male worms was recorded. (A) At 20°C, *ife-1* worms mated with wild type males produced approximately half as many offspring as wild type hermaphrodites with wild type males. (B) At 25°C a similar reduction in *ife-1* hermaphrodite brood size was observed in comparison to wild type hermaphrodites when mated with wild type males. This indicates that *ife-1* oocytes contribute to the reduced fertility of the *ife-1* strain, but oocyte viability is not temperature-sensitive. (C) Both *ife-1* and wild type hermaphrodites produced unfertilized embryos and arrested oocytes when mated with wild type males. The bars indicate overall number of observed cases, while the indicated percentages represent the outcome as a percent of total oocytes produced. *ife-1* oocytes are less capable of producing viable offspring when exposed to wild type sperm.

Figure 3.3

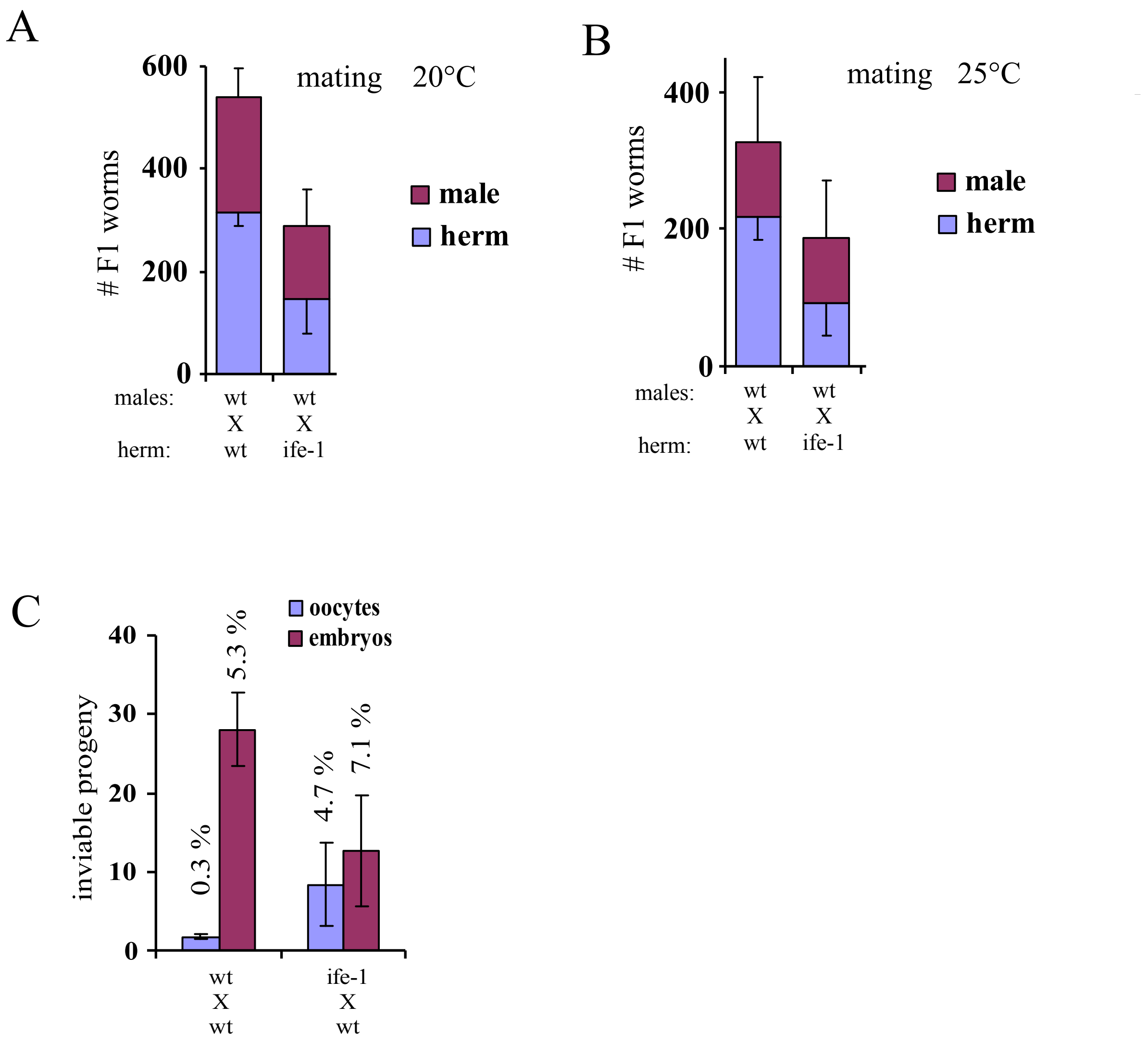
A
600
400
200
0
# F1 worms
mating 20°C
male
herm
males:
herm:
wt
X
wt
wt
X
ife-1
B
400
200
0
# F1 worms
mating 25°C
male
herm
males:
herm:
wt
X
wt
wt
X
ife-1
C
oocytes
embryos
40
30
20
10
0
inviable progeny
0.3 %
5.3 %
4.7 %
7.1 %
wt
X
wt
ife-1
X
wt

data suggest a defect in spermatogenesis at 25°C. The observed spermatogenesis defect in *ife-1* worms is consistent with previous observations using *ife-1*(RNAi) work and will be further addressed in chapter 4. At all three temperatures the overall production of oocytes from *ife-1* hermaphrodites, whether or not fertilization occurred, was dramatically reduced compared to wild type. These observations provided the first evidence that the production of viable oocytes competent for fertilization was dependent on the presence of IFE-1. In the following experiments I have sought to establish the nature of the oocyte defect.

In order to specifically address the effect of IFE-1 loss on oogenesis, we conducted mating experiments with wild type males. When a hermaphrodite worm is exposed to a male worm and mating occurs, the male sperm out-compete the hermaphrodite sperm that has been stored in the spermatheca for oocyte fertilization. Male sperm ejaculated into the hermaphrodite uterus crawls to the spermatheca to fertilize oocytes (L'Hernault). Male supplied sperm is also larger than hermaphrodite sperm. Therefore, by mating *ife-1* hermaphrodites to wild type males we were able to examine the competence of *ife-1* oocytes without the background of potentially defective *ife-1* sperm. At 20°C brood sizes of *ife-1* hermaphrodites were nearly half of the brood sizes of wild type hermaphrodites, when both were mated to wild type males (Fig 3.3A). Similar results were observed at 25°C. *ife-1* hermaphrodites mated with wild type males produce nearly half the number of offspring as wild type hermaphrodites (Fig 3.3B). Since the sperm fertilizing the oocytes in the *ife-1* and wild type hermaphrodites is the same, the *ife-1* hermaphrodite either does not make the equivalent number of oocytes as the wild type hermaphrodite, or the oocytes are not competent for fertilization.

IFE-1 may therefore play a role in the rate of oocyte production or in the competence of oocytes to complete oocyte maturation or fertilization.

In order to determine whether *ife-1* oocytes are as competent as wild type oocytes to be fertilized, we assessed the number of unfertilized oocytes and arrested embryos produced by each strain. Wild type and *ife-1* hermaphrodites were mated with wild type males and the number of oocytes and arrested embryos laid were counted (Fig 3.3C). Laid oocytes appear round and flaccid on the seeded OP50 *E.coli* lawn, while embryos are oval-shaped with a distinct outline from the chitin shell. Embryos that did not hatch within 24 hours were assumed to be stalled in development (arrested). The *ife-1* hermaphrodites produced more unfertilized oocytes than wild type hermaphrodites, indicating that either *ife-1* oocytes were deficient in accepting sperm for fertilization, or were unable to undergo meiotic maturation. *ife-1* hermaphrodites produced a larger number of unfertilized oocytes than wild type hermaphrodites. When compared to overall oocyte production, those left unfertilized from wild type worms accounted for only 0.3%, while the *ife-1* hermaphrodite had 4.7% unfertilized oocytes from total oocytes produced (i.e. total offspring). The *ife-1* oocytes are also less likely to produce viable offspring that completed embryogenesis. In wild type hermaphrodites, 5.3% of oocytes failed to successfully complete embryonic development when fertilized. This percentage is still significantly lower than the 7.1% of *ife-1* oocytes that arrested during embryogenesis. The implication of these results is that oocytes lacking IFE-1 may fail to synthesize the appropriately required proteins for the completion of both oocyte fertilization and embryo development.

The decrease in *ife-1* fertility that is due to defects in oogenesis may result from a reduction in oocyte production or in the competence for fertilization. To further investigate the rate of oocyte production, we examined the progression of late stage oocytes and their retention in the proximal gonad in hermaphrodite gonads by DIC microscopy. We have also discovered that *ife-1* hermaphrodites are unable to accumulate mature spermatozoa at 25°C (discussed in chapter 4). The absence of available sperm for fertilization decreases the rate of ovulation in *C.elegans,* such that late oocytes accumulate or "stack up" in the proximal arm of the gonad (Kimble et al., 1984). Miller et al. demonstrated that ovulation is triggered by the sperm-supplied protein MSP, which binds to oocyte receptors to induce oocyte maturation (Miller et al., 2001). MSP also binds to receptors on the sheath cells that line the gonad in order to trigger contractions by sheath cells to push fertilized oocytes through the spermatheca into the uterus. We examined hermaphrodite gonads by DIC microscopy to determine if the stacking phenotype was present in the *ife-1* hermaphrodites at 25°C (Fig 3.4) as an indication of normal oocyte production. Wild type hermaphrodite successfully make and store sperm in the spermatheca. The late-stage oocytes in the wild type gonad progress normally and are fertilized and ovulated to the uterus where the embryos (indicated by "e") develop (Fig 3.4A). Approximately ten late stage oocytes accumulated in the proximal region of the gonad (indicated by carets). In *ife-1* hermaphrodites, few if any sperm were present in the spermatheca at 25°C and the oocytes did not become fertilized. Ovulation occurred in the absence of sperm. Oocytes that are not fertilized but are ovulated undergo multiple rounds of chromosomal

Figure 3.4 Morphology of *ife-1* hermaphrodite gonad. The absence of sperm available for fertilization results in a back up or stacking of oocytes in the distal gonad. (A) At 25°C, wild type hermaphrodite gonads accumulate approximately 10 late oocytes prior to fertilization. (B) *ife-1* hermaphrodites show a similar number of accumulated oocytes but fail to produce embryos, indicating fertilization is not occurring. (C) The *fem-2* mutant fails to produce sperm at 25°C and accumulates many more late oocytes in the distal portion of the gonad (approximately 18 oocytes). Carets represent late oocytes, while stars indicate unfertilized oocytes that have been ovulated. The wild type hermaphrodite uterus contained embryos designated by the letter e.

Figure 3.4

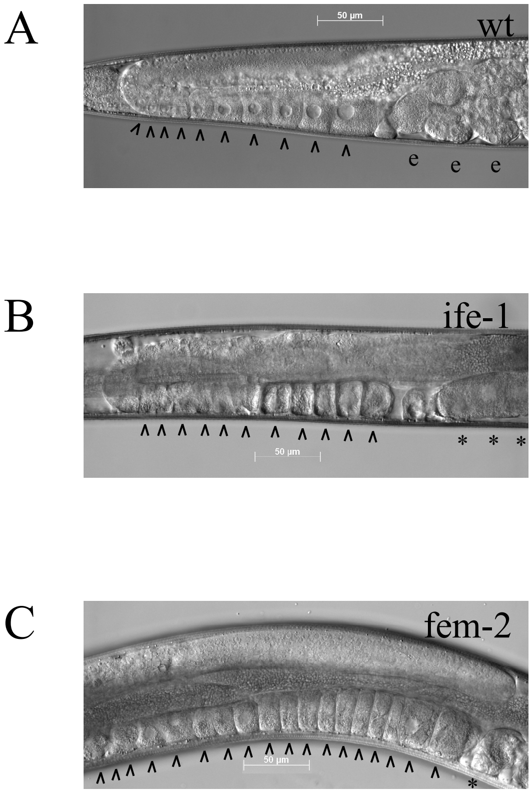
A
50 µm
wt
e
e
e
B
ife-1
50 µm
* * *
C
fem-2
50 µm
*

replication. These cells fail to undergo cytokinetic events resulting in endomitosis (Fig 3.4B,C indicated by *). The *ife-1* hermaphrodites had similar numbers of late stage oocytes in the distal gonad as wild type despite a decreased rate of fertilization (Fig 3.4B). As a control for oocyte development and ovulation, we examined *fem-2* hermaphrodites which do not produce any viable sperm at 25°C. This strain possesses normal properties of oocyte growth and production. Again we observed a lack of fertilization with endomitotic oocytes accumulating in the uterus (Fig 3.4C). However, there were twice as many late-stage oocytes in the proximal arm of the gonad as compared to either wild type or *ife-1*. Since both *fem-2* and *ife-1* lack sperm, and therefore have reduced rates of ovulation, both strains should have the same accumulation of late-stage oocytes if the rate of oocyte production is the same. The decreased number of late oocytes suggests the opposite, namely that the rate of oocyte production is substantially reduced in worms lacking IFE-1.

In order to examine the morphological properties of the *ife-1* oocytes, whole gonads were dissected from *ife-1* and wild type hermaphrodites. In order to visualize the cellular morphology, I conducted DIC and fluorescence microscopy in the presence of Hoechst to stain nuclear material. Wild type oocytes arrested in diakinesis of meiosis I awaiting fertilization as expected (Fig 3.5A, B, depicted with carets). Most *ife-1* oocytes (Fig 3.5C,D) also arrested in diakinesis, as seen by the configuration of condensed chromosomes, but a few (depicted in figure 3.5D, labeled “d”) fail to form condensed chromosome structure. Additionally, the morphology of nearly all *ife-1* oocytes is more elongated and flaccid compared to the cubical, tightly-packed wild type oocytes. At 25°C, wild type oocytes appear similar to those produced at 20°C. Again, some *ife-1* oocytes failed to maintain diakinesis and had decondensed chromosomes and flaccid abnormal cellular morphology. Like figure 3.4, the lack of fertilization in *ife-1* hermaphrodites at 25°C resulted in the accumulation of oocytes undergoing endomitosis in the uterus (*). To determine if the unusual nuclear morphology was a result of the lack of sperm in the *ife-1* oocytes, we compared *ife-1* oocytes to *fem-2* oocytes. As expected, there were also oocytes in endomitosis in the uterus of the feminized *fem-2* strain lacking sperm. The oocytes appeared to progress to the arrest in diakinesis successfully with no abnormal nuclear morphology in both wild type and *fem-2* strains. Atypical nuclear morphology of the maturing oocytes seems to be a sporadic result of the absence of IFE-1 during oogenesis, and is not dependent on the depletion of sperm and lack of fertilization.

The observed abnormalities in the rate and integrity of oocyte production in the *ife-1* hermaphrodite led me to examine other attributes of *C.elegans* oogenesis. The process of germline apoptosis has been well studied in the hermaphrodite gonad and has a unique role in regulating the supply of germ cells for oogenesis. Apoptosis occurs in nearly half of all developing germ cells during *C.elegans* oogenesis. It is believed that these dying cells may play a role similar to nurse cells supplying mRNAs and cytoplasmic contents to the germ cells that will further develop into mature oocytes. Recently our lab has shown that a reduction in the level of the p170 isoform of IFG-1 (eIF4G) results in an increase in germline apoptosis. Since p170 is the scaffolding protein required for recruitment of IFE-1 and the other IFE isoforms to the pre-initiation complex, we were curious whether IFE-1 had a direct role in suppressing germline

Figure 3.5 Oocyte development in *ife-1* hermaphrodite gonads. Whole gonads were dissected from worms grown at 20°C (A-D) and 25°C (E-J). At 20°C, in the wild-type gonad there is normal late oocyte progression in the proximal region (A, DIC image; B, Hoechst stained). There are ten sequential oocytes with condensed chromosomes (post-pachytene) arranged in linear array (arrowheads; ^). *ife-1* gonads grown at 20°C showed somewhat elongated, but otherwise normal oocytes in the proximal region (C,D). In contrast to wild type, only seven post-pachytene oocytes were aligned in the *ife-1* gonad. Nuclear staining indicated that most *ife-1* oocytes contained aligned bivalent chromosomes (^); a few failed to condense (d). Wild-type worms raised at 25°C (E,F) showed similar characteristics to those raised at 20°C with eight postpachytene oocytes aligned in the proximal region. The gonad from *ife-1* worms raised at 25°C (G,H) also showed similar characteristics to the *ife-1* gonad at 20°C, with five oocytes with condensed bivalents (^). Fertilization did not occur in *ife-1* worms at 25°C, and four unfertilized oocytes were observed in the uterus undergoing endomitosis (*). The feminized *fem-2* gonad (I,J), in which no fertilization occurs, showed normal oocyte progression in the proximal region and accumulated 14 post-pachytene oocytes.

Figure 3.5

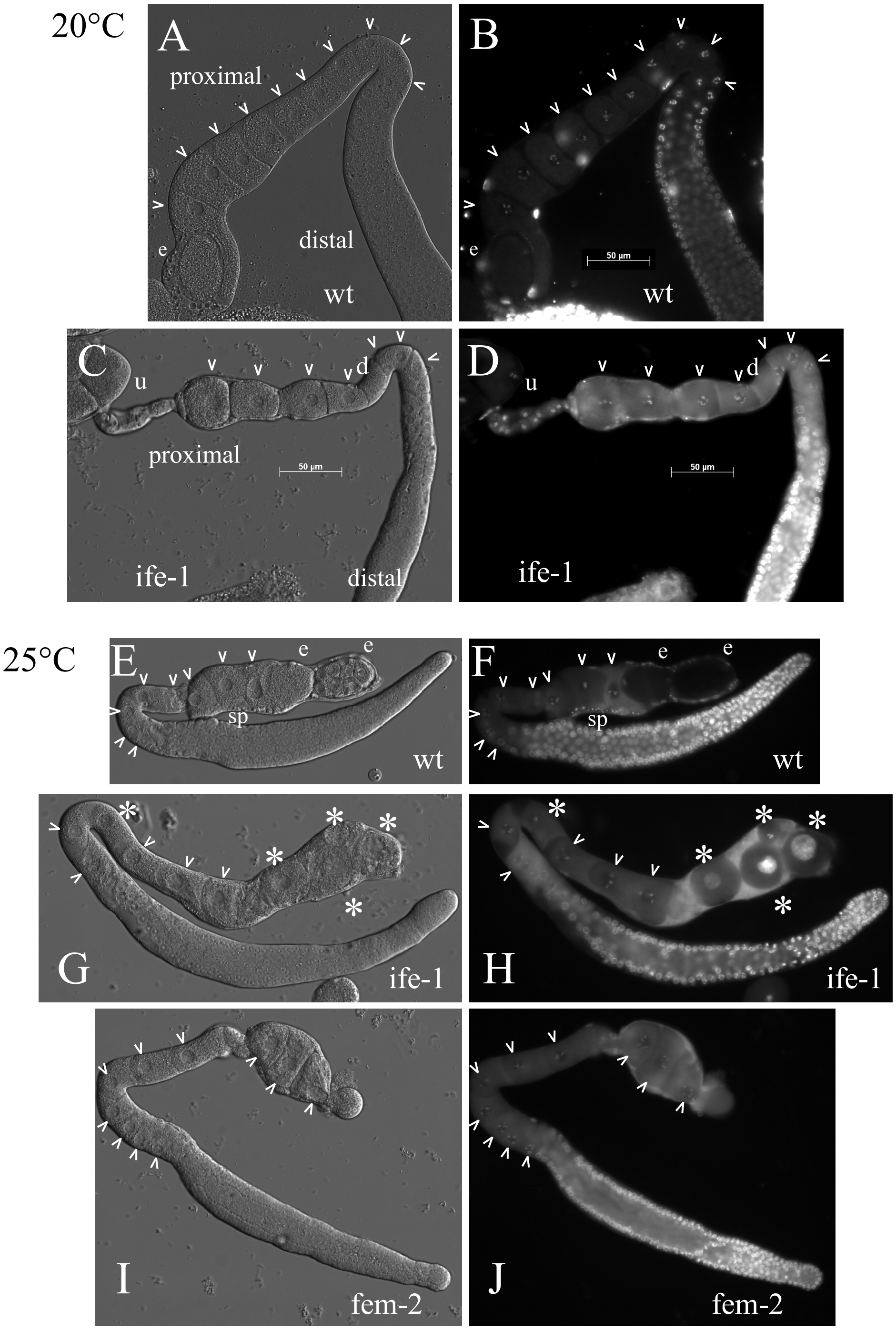
20°C
A
proximal
distal
e
wt
B
e
50 µm
wt
C
u
d
proximal
50 µm
ife-1
distal
D
u
d
50 µm
ife-1
25°C
E
e
e
sp
wt
F
e
e
sp
wt
G
ife-1
H
ife-1
I
fem-2
J
fem-2

apoptosis. In order to examine germline apoptosis in the gonad, we used the P_{lim-7}ced-1::gfp reporter strain (Barbara Conrandt) to label apoptotic cell corpses. The strain produces CED-1::GFP, which is a receptor expressed in the somatic sheath cells required for engulfment of apoptotic germ cell corpses. By examining these worms under fluorescence microscopy the apoptotic corpses are clearly outlined by GFP. Late apoptotic cells also have unique nuclear morphology with diffused, degraded DNA that lines the periphery of the nucleus. In a wild type background the CED-1::GFP reporter strain displays two to five apoptotic cell corpses with corresponding diffuse DNA, depicted by costaining with DAPI (Fig 3.6A,B). When the P_{lim-7}ced-1::gfp reporter strain was crossed into the *ife-1* homozygous strain, we were able to assess the role of IFE-1 in germline apoptosis. Surprisingly, the absence of IFE-1 did not induce any significant accumulation of apoptotic corpses over what was seen for wild type. The *ife-1* strain showed similar results as wild type with only two encapsulated cells (Fig 3.6C,D). Thus, IFE-1 does not show the same involvement in the apoptotic cascade as the p170 isoform. As a positive control for germ cell apoptosis, IFG-1(p170) was knocked down with RNAi and increased germline apoptosis 5-fold (Fig 3.6E). These results show that the defects in oogenesis (specifically the reduction in oocyte production) in *ife-1* hermaphrodites is not due to increased apoptosis.

To further investigate apoptosis in the wild type and *ife-1* gonads, immunostaining of dissected hermaphrodite gonads was performed using an anti-CED-4 antibody (Santa Cruz). CED-4 is the homolog of mammalian Apaf-1. CED-4 forms apoptosome structures with the caspase-3 homolog, CED-3. In previous work our lab observed CED-4 accumulation in apoptosome-like structures in the oocytes of p170

Figure 3.6 Expression of pro-apoptotic protein, CED-1:GFP in hermaphrodite gonads. (A,C,E) Germ cell apoptotic corpses were detected by expression of the CED-1::GFP engulfment reporter. Only two germ cell corpses (*) were evident in the wild-type hermaphrodite gonad (A). The *ife-1* gonad similarly showed two apoptotic corpses decorated with CED-1:GFP (C). (B,D) DAPI-staining verified the progression of oocyte nuclei through pachytene and diakinesis stages. As a positive control, depletion of IFG-1 p170 by *ifg-1*(RNAi) significantly increased germline apoptosis in the hermaphrodite gonad (E). Asterisks and brackets indicate the position of a cluster (six to eight) of cell corpses.

Figure 3.6

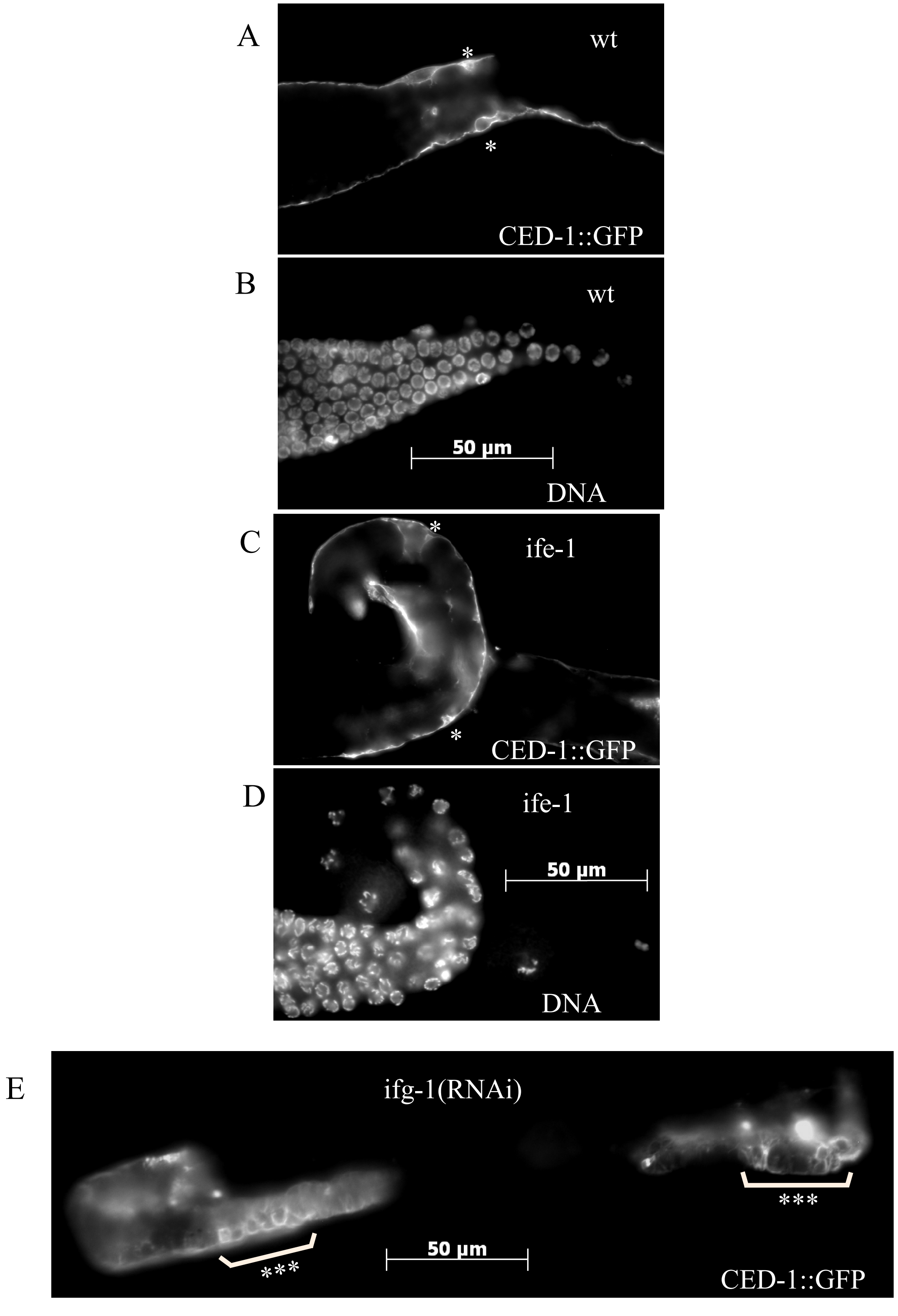
A
wt
*
*
CED-1::GFP
B
wt
50 µm
DNA
C
ife-1
*
*
CED-1::GFP
D
ife-1
50 µm
DNA
E
ifg-1(RNAi)
***
***
50 µm
CED-1::GFP

Figure 3.7 Expression of the pro-apoptotic protein, CED-4 in hermaphrodite gonads. (A,C) Immunostaining using the goat anti-CED-4 antibody (Santa Cruz) shows no apoptosome structures (indicated by green) surrounding nuclei (stained by DAPI, blue) in oocytes of wild type or *ife-1* hermaphrodites. (B) Examination at higher magnification (100X) indicated CED-4 expression in apoptosome-like structures surrounding sperm nuclei located in the spermatheca or uterus in wild type and *ife-1* hermaphrodites (arrows).

Figure 3.7

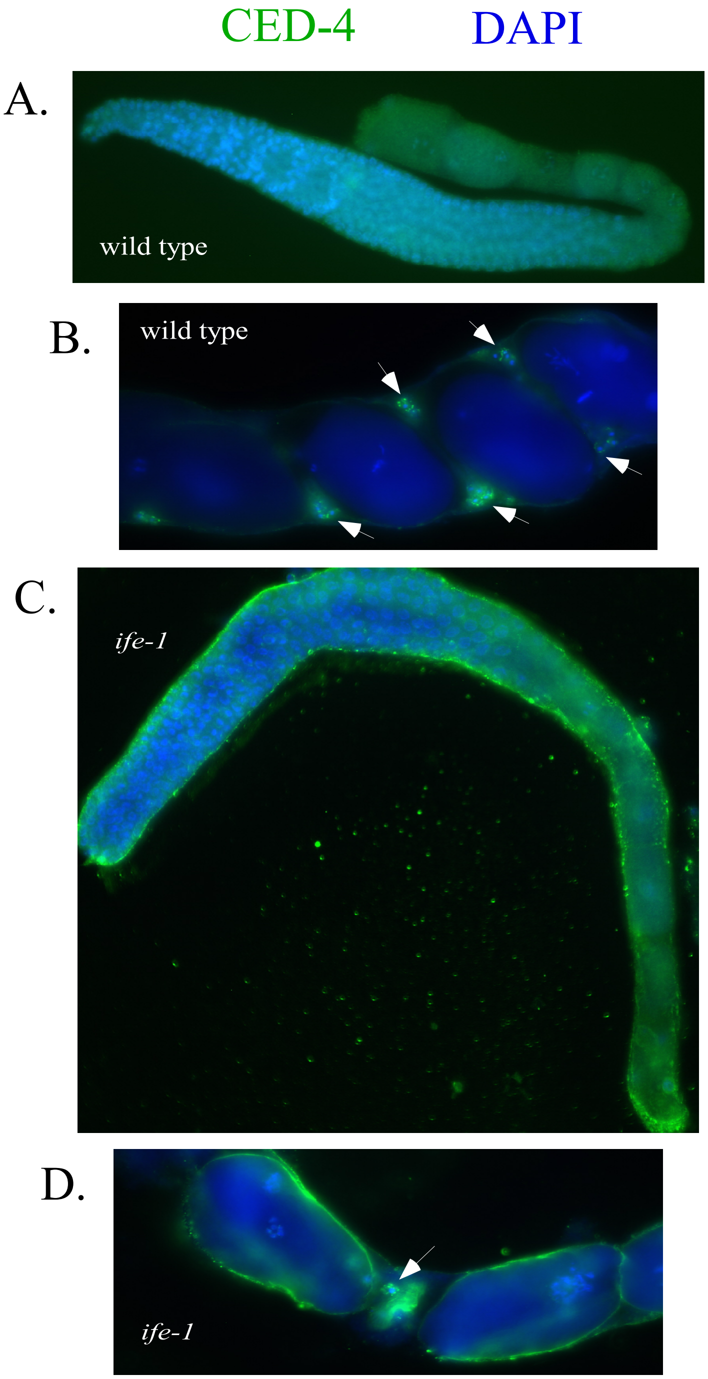
CED-4
DAPI
A.
wild type
B.
wild type
C.
ife-1
D.
ife-1

IFG-1 (RNAi) hermaphrodites by immunostaining (Contreras et al., 2008). When performed on *ife-1*dissected gonads, there was no observed accumulation of CED-4 in either *ife-1* or wild type oocytes (Figure 3.7). Detectable CED-4 is punctate apoptosome-like structures, was observed only in the spermatheca and uterus. DAPI co-staining showed that the CED-4 positive apoptosome structures surround sperm nuclei. These results suggest that CED-4 induction does not occur as a result of the lack of IFE-1. However, there may be some novel endogenous expression of CED-4 in sperm, which will be further addressed in chapter 4.

Conclusion

Utilization of a homozygous null *ife-1* strain allowed us to uncover new defects that result from more stringent loss of IFE-1 during oogenesis that were not previously uncovered using RNAi. The advantage of the homozygous null strain was that worms could be observed without the influence of maternally supplied IFE-1 protein. We were able to observe a dramatic decrease in fertility in the absence of IFE-1, which cannot be solely a result of sperm defects as suggested by Amiri et al (Amiri et al., 2001). As an example, the mating of *ife-1* hermaphrodites with wild type sperm demonstrated that a degree of the fertility defects caused by the lack of IFE-1 were a response to poor oocyte production. The *ife-1* mutant failed to supply a sufficient number of oocytes for wild type sperm to fertilize, resulting in a decrease in brood sizes compared to wild type worms. Interestingly, work examining the defects in *ife-4* mutant worms also observed decreased brood size, but attributed the effect to egg laying deficiencies (Dinkova et al., 2005). Dinkova et al showed that the lack of IFE-4 resulted in decrease translation of mRNAs involved in muscle and neuronal development, and results in an egg-laying deficient phenotype. Since IFE-4 is a somatic isoform of eIF4E, we do not expect a direct effect on oogenesis. Nevertheless, it is intriguing that the full loss of each isoform produces a similar, yet distinct phenotype leading to decreased brood size. We suggest that IFE-1 contributes to the translation of proteins required to efficiently produce oocytes for fertilization.

In addition to the rate of oocyte production, examination of the cellular and nuclear morphology of *ife-1* oocytes revealed abnormal chromosome condensation in late oogenesis. The occasional oocyte completely failed to establish or maintain condensed diakinetic chromosomes prior to fertilization. Such *ife-1* oocytes are most likely unable to undergo successful meiotic maturation and fail to be fertilized when mated with wild type males. This could explain the observation of a higher percentage of fertilized *ife-1* oocytes arrested in embryogenesis. Although we have not observed a direct correlation, it appears that oocytes which fail to maintain correct nuclear morphology are most likely the same cells that arrest as embryos and unfertilized oocytes.

Previously our lab demonstrated that the reduction of cap-dependent translation by RNAi of the larger IFG-1 isoform greatly enhances germline apoptosis (Contreras et al., 2008). Since IFE-1 is a mRNA-cap binding protein, its loss might also be expected to increase apoptotic events. This would have easily accounted for the decrease in oocyte production we observed. However, the lack of increased CED-4 or CED-1::GFP expression led us to conclude that the loss of IFE-1 does not induce germline apoptosis. The availability of other eIF4E isoforms (IFE-3 and IFE-5) in the germline may facilitate cap-dependent translation to sufficient levels in order to avoid inducing germline apoptosis.

The lack of IFE-1 in oogenesis does not prevent the formation of P granules (Amiri et al., 2001), nor does it suppress the production of oocytes, fertilization, or development to adulthood. The loss of IFE-1 does, however, dramatically reduce the rate of oocyte production by half. In addition, many of the oocytes that develop fail to maintain chromosome integrity during the growth phase that follows meiotic arrest. The distinct role that this translation factor plays in oogenesis is most likely related to the mRNAs with which it associates. The nature of mRNAs that specifically require IFE-1 for translation will be addressed in chapter five. The identities of these mRNAs and the proteins they encode suggest they may play important roles during oogenesis and the maintenance of the condensed chromosomes during meiosis.

CHAPTER 4: THE ROLE OF IFE-1 IN SPERMATOGENESIS IN *C.ELEGANS*

Introduction

Similar to oogenesis the process of making sperm begins with a supply of cells produced by primordial germ cells from multiple rounds of mitosis. Prior to sexual maturity, some of these stored cells enter meiosis in order to differentiate into fully mature haploid sperm (Sutovsky, 2006). In many organisms the spermatocytes share a syncytium with other developing spermatocytes. After the round haploid spermatid is formed after meiosis II, it enters the process known as spermiogenesis, where the round spermatid will elongate into motile, mature spermatozoa. This process varies between organisms but shares common attributes. In order to survive in an environment outside the male reproductive tract, the spermatid must make some structural changes. These changes include further condensation of the chromosomes by replacing histones with protamines. In many cases the mature spermatozoa utilizes a flagellum for movement, which must be made during this time. Finally the spermatid will remove unnecessary cytoplasmic contents such as organelles, ribosomes, and nonessential proteins and mRNAs. It is also at this final stage that the spermatid is released from the syncytium and gains a complete plasma membrane as a mature spermatozoon.

Spermatogenesis in *C.elegans* differs slightly from that in other higher organisms. *C.elegans* exists as hermaphrodites and males. In the hermaphrodite gonad, sperm is made during the L4 larval stage and stored in the spermatheca until fertilization of an oocyte (Hubbard et al.). The male worm contains a single lobed gonad, which, like the hermaphrodite, maintains gametogenesis in a linear progression. During mitotic and early meiotic divisions, the germ cells share a common cytoplasm as a syncytium. During prophase I, the spermatocytes bud off the rachis as primary spermatocytes. The completion of meiosis I leads to the production of secondary spermatocytes. Meiosis II differs in *C.elegans* relative to mammalian species, in that the removal of the cytoplasmic contents into residual bodies coincides with the formation of the haploid spermatids. In the worm, many processes that occur during mammalian spermiogenesis must occur earlier in spermatogenesis. *C.elegans* sperm is not flagellated and therefore does not need to elongate, but the haploid spermatid does need to maintain the same small dimensions to aid in the motility by its pseudopod (L'Hernault, 2006).

Like oocytes, spermatocytes must also synthesize mRNAs to be stored for later use during the spermatogenesis process. During early meiosis spermatocytes are transcriptionally active, but during spermiogenesis the DNA transitions into the further compact state of the mature spermatozoa. At this time transcription ceases and further regulation of gene expression must be through translational control. During spermiogenesis the spermatid must undergo various changes to facilitate motility and survival prior to fertilization. These changes require the synthesis of novel proteins. Like oocytes, the mRNAs for these proteins have been stored in RNPs until needed. An example of translational control in mouse spermatids occurs with the synthesis of protamines from the mRNAs, *Prm1* and *Prm2*. The synthesis of these proteins is not needed until after the elongation of the spermatid. The mRNAs are made in the transcriptionally active round spermatid and repressed by the binding of MSY1 and MSY2 to the 3’ UTR (Kleene, 2003). In mouse spermatids the repression lasts approximately one week before the synthesis of protamines is needed. Translational control of mRNAs in the spermatid facilitates the crucial timing of events during spermiogenesis.

Also crucial for the completion of spermiogenesis is the removal of unnecessary cytoplasmic contents. It has recently been shown that pro-apoptotic proteins facilitate the removal of cytoplasmic contents from *Drosophila* spermatids without inducing program cell death (Arama et al., 2003; Cagan, 2003). The homologs of Apaf-1 and caspase-3 are necessary to activate the removal of syncytial cytoplasm into the waste bag. Flies deficient in these proteins fail to produce mature spermatozoa and are sterile. The role of Apaf-1 in mouse spermatogenesis has also been studied. The absence of Apaf-1 results in the depletion of all spermatocytes in the adult mouse (Honarpour et al., 2000). Thus, there appears to be an essential role in spermatogenesis for pro-apoptotic proteins that may not involve the induction of programmed cell death. Endogenous apoptotic cell death events, like those seen in higher organisms, have not been observed in *C.elegans* spermatogenesis. By investigating the presence of pro-apoptotic proteins in worm spermatocytes, we may discover a role for these proteins in cytoplasmic clearance similar to that observed in flies and mice.

This chapter will further investigate the role of IFE-1 in spermatogenesis. Amiri et al. showed that the reduction of IFE-1 prevents progression of spermatocytes through meiosis (Amiri et al., 2001). The results presented here identify the exact cellular process in spermatogenesis that result in the temperature-sensitive sterility of the *ife-1* null mutant. The observation of pro-apoptotic protein, CED-4, in spermatocytes leads to a potential role in cytoplasmic clearance. The accumulation of CED-4 in the male gonad seems to be dependent on the translation factor IFE-1. This chapter will asses the role of IFE-1 during *C.elegans* spermatogenesis, leading to the potential role in spermatogenesis protein synthesis.

Results

Amiri et al demonstrated that the reduction in IFE-1 led to a temperature-sensitive deficiency in spermatogenesis (Amiri et al., 2001). The *ife-1*(RNAi) F1 hermaphrodites showed decreased fertility at 25°C due to an arrest during spermatogenesis. *ife-1*(RNAi) germ cells entered spermatogenesis but arrested in the primary and secondary spermatocyte stages. In order to further address the role of IFE-1 during spermatogenesis we utilized the *ife-1* mutant strain. As shown in the previous chapter, at 25°C *ife-1* hermaphrodites failed to produce any viable embryos, yielding instead only small number of unfertilized oocytes. To determine if *ife-1* hermaphrodites contained mature sperm in the spermatheca, we performed DAPI staining on fixed whole worms grown at 25°C (Fig 4.1). In wild type worms at least 20 small punctate sperm nuclei were observed in a single focal plane of the outlined spermatheca (Fig 4.1A). However, no condensed sperm nuclei were seen in the spermatheca of *ife-1* worms. The feminized *fem-2* strain was compared to *ife-1* worms as a relevant control. This temperature-sensitive strain undergoes normal somatic development and oogenesis, but does not produce sperm at 25°C (Fig 4.1B,C). The absence of mature sperm in *ife-1* hermaphrodite spermatheca appears to explain the lack of fertilization of oocytes at 25°C.

In order to determine the consequences of defects in spermatogenesis and oogenesis separately on fertility, the brood sizes were recorded for various wild type and

Figure 4.1 Accumulation of sperm in the spermatheca of hermaphrodites at 25°C. (A) DAPI staining of nuclei in the spermatheca (outlined in dashed line) of whole hermaphrodite worms. Sperm (sp) accumulation was evident as puncta in wild type spermatheca. (B) *ife-1* hermaphrodites grown at 25°C fail to accumulate mature sperm in the spermatheca. (C) The feminized *fem-2* strain also fails to make sperm at 25°C. Carets show the chromosomes of oocyte nuclei in adult gonad.

Figure 4.1

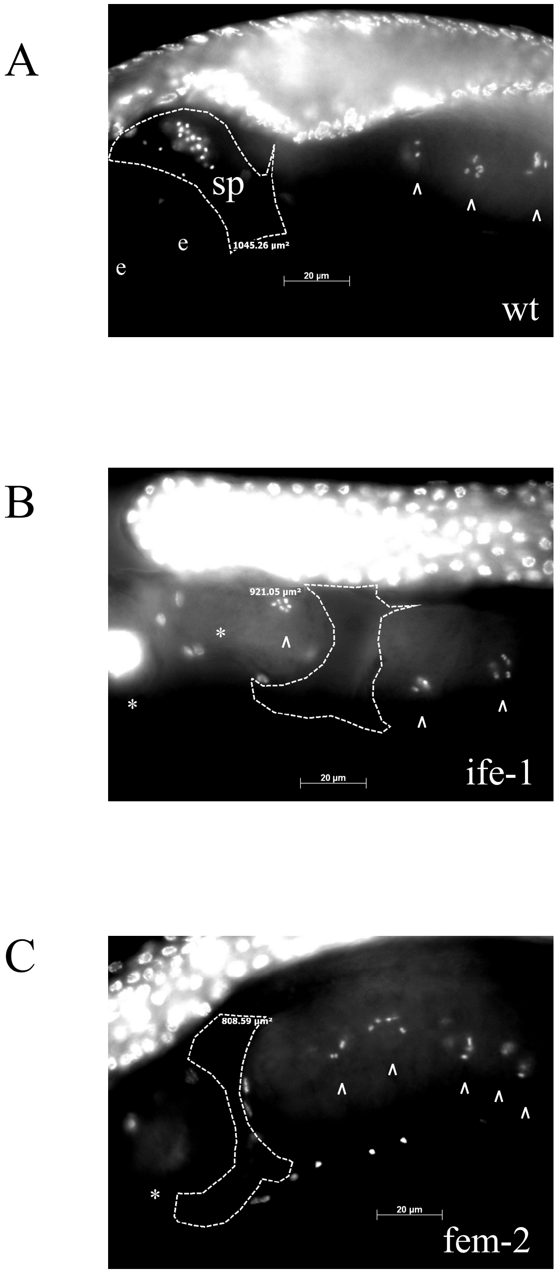
A
sp
e
e
1045.26 µm²
20 µm
wt
B
921.05 µm²
*
*
20 µm
ife-1
C
808.59 µm²
*
20 µm
fem-2

ife-1 matings. A hermaphrodite worm has two X chromosomes (XX) and is genetically equivalent to females in other species. Since all haploid gametes made in the hermaphrodite gonad contain one X chromosome, all "self" fertilized embryos produce hermaphrodite offspring. Occasionally, non-disjunction of the X chromosome occurs at a rate of one in one thousand meiotic events and leads to the production of an XO male (Figure 4.2). Consequently, sperm produced in the male are half "X" genotype and half "O" genotype. When males are exposed to hermaphrodites, mating will occur. Males supply the hermaphrodite with a population of larger sperm which out-compete hermaphrodite sperm for fertilization. This leads to a brood that is half males and half hermaphrodites. By evaluating the ratio of males to hermaphrodites in a given brood, the availability and potency of the sperm for fertilization can be estimated. The overall brood size of the hermaphrodite can be used to evaluate oocyte viability. The examination of both brood size and sex ratio of offspring were used to show the effect of IFE-1 depletion on spermatogenesis and oogenesis separately.

When *ife-1* males were mated with wild type hermaphrodites at 20°C, only six male offspring were produced per hermaphrodite (Figure 4.3A). The brood size was reduced by half compared to wild type males and wild type hermaphrodite matings. The offspring were likely produced from available wild type hermaphrodite sperm, suggesting that the supply or potency of *ife-1* sperm at 20°C is negligible. The *fem-2* strain is capable of producing viable sperm at 20°C, but not 25°C, and produces more male offspring than *ife-1* males. The *ife-1* males are capable of producing sperm and generating male offspring at 20°C, but the loss of IFE-1 may reduce the potency or number of sperm.

Figure 4.2 Outline of mating experiments. Hermaphrodites (XX) produce nearly 100% hermaphrodite offspring. When males (XO) are mated with hermaphrodites, males sperm (X or O) out-compete hermaphrodite sperm, leading to offspring population of 50% male and 50% hermaphrodite worms.

Figure 4.2

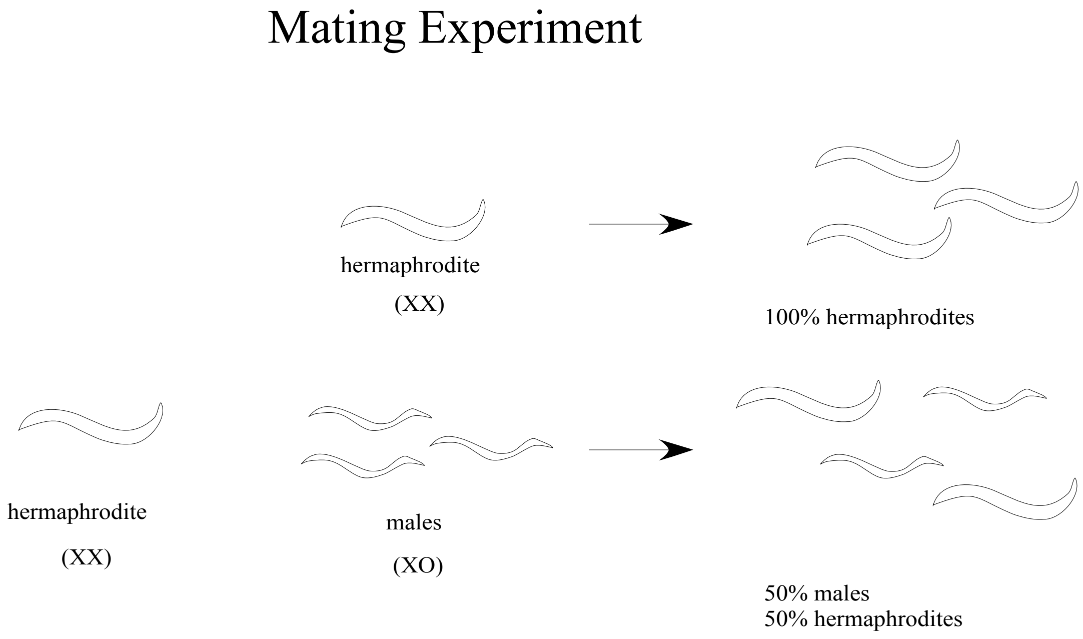
Mating Experiment
hermaphrodite
(XX)
100% hermaphrodites
hermaphrodite
(XX)
males
(XO)
50% males
50% hermaphrodites

Figure 4.3 Brood size as an indication of sperm and oocyte viability from mating experiments. (A) At 20°C, *ife-1* males fail to produce 50% male offspring when mated with wild type hermaphrodites, but do produce approximately 4% male offspring. The *fem-2* males are capable of producing sperm at 20°C, but produce brood sizes half that of wild type. (B) At 25°C, *ife-1* males are unable to produce any male offspring when mated with wild type hermaphrodites, and no offspring with *ife-1* hermaphrodites. The *fem-2* males also fail to produce any male offspring.

Figure 4.3

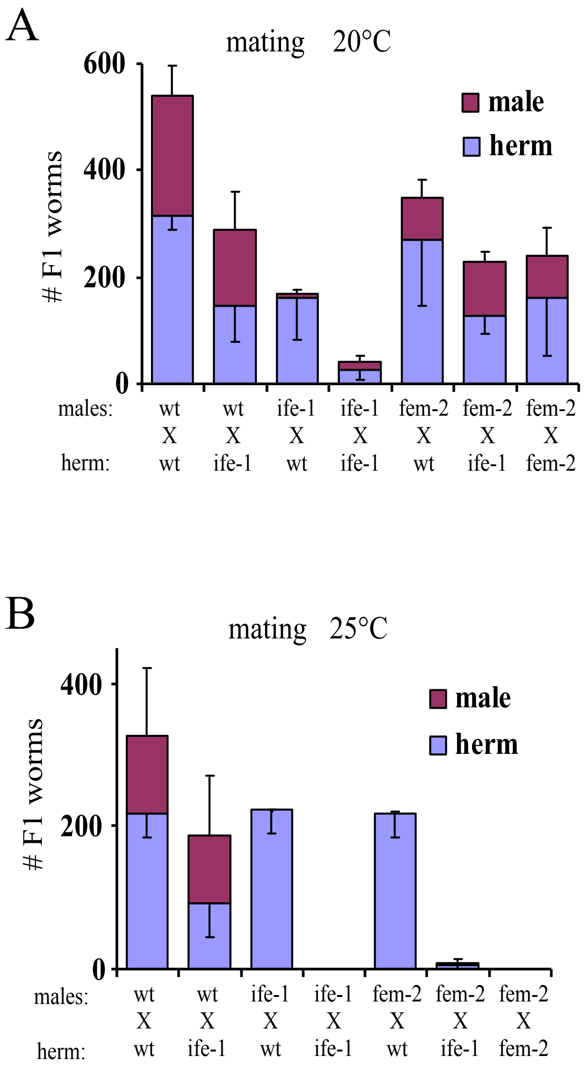
A
mating 20°C
600
400
200
0
# F1 worms
male
herm
males:
herm:
wt X wt
wt X ife-1
ife-1 X wt
ife-1 X ife-1
fem-2 X wt
fem-2 X ife-1
fem-2 X fem-2
B
mating 25°C
400
200
0
# F1 worms
male
herm
males:
herm:
wt X wt
wt X ife-1
ife-1 X wt
ife-1 X ife-1
fem-2 X wt
fem-2 X ife-1
fem-2 X fem-2

At 25°C, both the *ife-1* and *fem-2* males fail to produce any viable male offspring (Figure 4.3B). When these males were mated with wild type hermaphrodites, only hermaphrodite offspring were produced indicating that hermaphrodite supplied sperm was probably fertilizing the oocytes. There were also no viable offspring produced by *ife-1* males mated to *ife-1* hermaphrodites. This indicated that regardless of whether the sperm was produced by the hermaphrodite or male, the loss of IFE-1 prevented the production of viable, potent sperm. Since *ife-1* worms were able to produce some viable offspring at 20°C and were sterile at 25°C, the *ife-1* strain exhibits temperature-sensitive sterility. The temperature-sensitivity derives almost exclusively from sensitivity of spermatogenesis. Our data indicate that the *ife-1* oogenesis defect, though less dramatic than that for spermatogenesis, is largely unaffected by temperature.

The above findings indicated that the production of potent sperm is temperature-sensitive in the *ife-1* mutant. In *C.elegans,* spermatogenesis occurs during the larval L4 stage in the hermaphrodite. To further investigate the stage in development that correlates to the temperature-sensitive sterility of the *ife-1* strain, a temperature-shift experiment was performed. Synchronized populations of wild type and *ife-1* embryos were isolated and incubated in M9 solution to hatch and arrest as L1 larvae. Plates were placed at 20°C and at 25°C. Every 12 hours plates from one temperature were switched to the other and the developmental stage recorded. The shifted worms produced offspring and brood sizes were calculated 120 hours after the initial L1 stage. The change in temperature had little effect on the brood size from wild type hermaphrodites with each worm producing 120-250 offspring (Figure 4.4A). When *ife-1* hermaphrodites were shifted to the permissive temperature (25°C to 20°C) prior to

Figure 4.4 Determination of the *ife-1* temperature-sensitive period by temperature-shift experiments. Synchronized (A) wild type and (B) *ife-1* L1 larval worms were placed at either 20° or 25°C. Every 12 hours, one plate from each temperature was shifted to the other temperature. The brood size of the shifted worms were recorded and graphed (A,B). The temperature-sensitive period (TSP) for *ife-1* occurred at 60 hours post L1 stage. (C) Lack of IFE-1 also affected temporal progression through larval stages. The stage of development of the shifted worms was recorded and graphed. The *ife-1* hermaphrodites displayed a prolonged L4 stage, which corresponds to both the TSP and to the period of spermatogenesis.

Figure 4.4

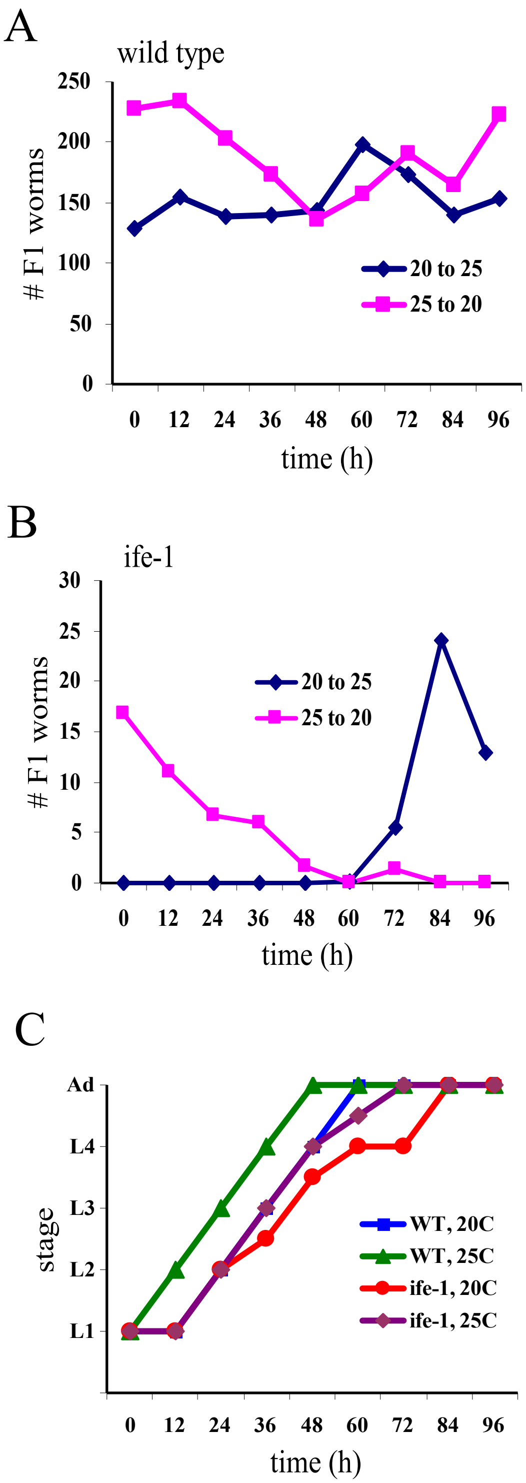
A
wild type
# F1 worms
250
200
150
100
50
0
0
12
24
36
48
60
72
84
96
time (h)
20 to 25
25 to 20
B
ife-1
# F1 worms
30
25
20
15
10
5
0
0
12
24
36
48
60
72
84
96
time (h)
20 to 25
25 to 20
C
stage
Ad
L4
L3
L2
L1
0
12
24
36
48
60
72
84
96
time (h)
WT, 20C
WT, 25C
ife-1, 20C
ife-1, 25C

60 hours post L1, they were able to produce viable offspring. Additionally any *ife-1* worms shifted from 20°C to 25°C after 60 hours were also fertile (figure 4.4B). This indicates that a limited developmental period at 60 hours post L1 is the temperature-sensitive period (TSP) for *ife-1* worms. The 60 hour time point corresponds to the L4 larval stage in development in *ife-1* hermaphrodites (figure 4.4C).

Given that a period of larval development defective in *ife-1* hermaphrodites was identified, it was decided to assess whether the overall progression of larval development had been altered by the defect or the lack of IFE-1. In figure 4.4C the developmental stages of worms grown at 20° and 25°C were graphed verses time post L1 larval stage. The L4 larval stage appeared to be prolonged in the *ife-1* hermaphrodites grown at 20° and 25°C by an additional 12 hours. This is also the stage in development that is responsible for spermatogenesis in hermaphrodites and was determined as the TSP in the *ife-1* worms. From these experiments we concluded that processes occurring during the L4 stage of development influence the fertility of the *ife-1* mutant and are sensitive to the elevated temperature.

To evaluate the cellular and morphological effects of IFE-1 deficiency on spermatogenesis, we examined germ cells at all stages of spermatogenesis in dissected *ife-1* male gonads. The male gonad is comprised of a single lobe with all germ cell derived from the distal tip cell (DTC) (Figure 4.5A). Stem cells undergo mitotic divisions followed by a transition to meiosis I. Like gametogenesis in hermaphrodites, early spermatocytes have a shared cytoplasm and do not form a complete plasma membrane until the pachytene stage. The completion of meiosis I leads to the formation

Figure 4.5 Schematic of the *C.elegans* male gonad and spermatogenesis. (A) Male germ cells are derived by mitosis from the distal tip cell (DTC) followed by a region of mitotically dividing cells. Germ cells transition to meiosis in a shared cytoplasm similar to the process in hermaphrodite gonads. At the pachytene stage the spermatocytes become enclosed in plasma membrane. (B) Primary spermatocytes undergo meiosis I to produce secondary spermatocytes. The cytokinetic divisions at this stage may or may not be complete. During meiosis II cytoplasmic clearing occurs partitioning the nucleus and proteins required for fertilization into the spermatid. The cleared cytoplasmic contents are sequestered into the residual body (RB). Once ejaculated into the uterus of the hermaphrodite, spermatids develop pseudopods and become spermatozoa.

Figure 4.5

A.

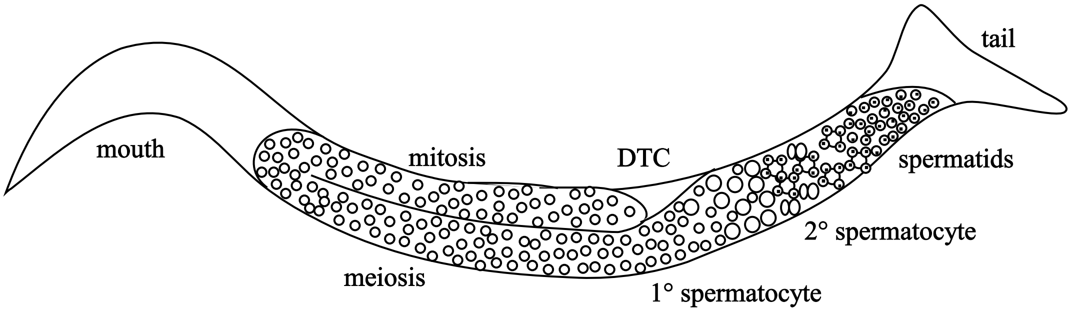
mouth
mitosis
DTC
tail
spermatids
2° spermatocyte
meiosis
1° spermatocyte

B.

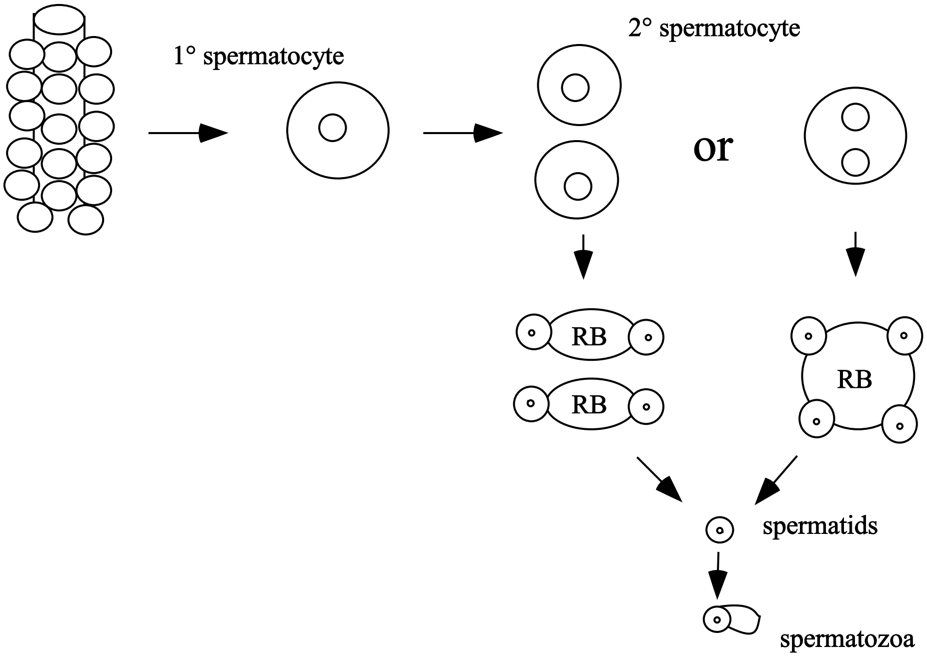
1° spermatocyte
2° spermatocyte
or
RB
RB
RB
spermatids
spermatozoa

of secondary spermatocytes (Figure 4.5B). Cytokinetic events at the end of meiosis I may or may not completely resolve separate daughter cells, but this appears to have little effect on further development of sperm (L'Hernault,2006). Meiosis II leads to the production of spermatids budding away from residual bodies (RB). The majority of the cytoplasmic contents, including translation machinery, are sequestered into the RB for degradation and phagocytosis. At this time the spermatids are morphologically characterized by a small dimple and show compact nuclei by nuclear staining. The spermatids develop a pseudopod and become spermatozoa when ejaculated into the hermaphrodite uterus. Successful progression through this process at 20°C was seen in wild type and *ife-1* dissected male gonads as observed by nuclear staining (Figure 4.6 A,C) and cellular morphology (Figure 4.6 B,D). The gonads of wild type males grown at 25°C, however, displayed normal spermatogenesis, with the production of dimple-like mature spermatids (Figure 4.6 E,F). Gonads dissected from *ife-1* males grown at 25°C showed multinucleated spermatocytes and the absence of mature spermatids (Figure 4.6 G,H). Hoechst staining identified two or four tightly condensed nuclei in secondary spermatocytes, suggesting the completion of meiosis II into haploid nuclei but failure in cytokinesis. These results demonstrated a single, precise cellular event in spermatogenesis that is aberrant in the absence of IFE-1.

The removal of cytoplasmic contents is required for the completion of spermatogenesis in all species. The specific mechanisms involved in the formation of the residual body and the budding of spermatids is not yet fully understood. By comparing the process of cytoplasmic clearing to that in other species, the process in

Figure 4.6 Morphology of spermatocytes in dissected male gonads. Wild type male gonads were stained with Hoechst and examined under (A) fluorescence and (B) DIC microscopy to show normal sperm morphology with the formation of spermatids (sp), shown in inset. (C,D) At 20°C, *ife-1* male gonads produced mature spermatids with tight condensed nuclei and dimple-like appearance. (E,F) At 25°C wild type gonads showed similar characteristics as those at 20°C of normal spermatogenesis with the formation of small, mature spermatids. (G,H) Spermatogenesis in the *ife-1* male at 25°C resulted in the arrest of spermatogenesis. Secondary spermatocytes failed to undergo cytokinesis, but did complete nuclear divisions of meiosis II resulting in large, multinucleated cells and no RBs. Multinucleated cells are indicated by carets. (g = gut, t = testes).

Figure 4.6

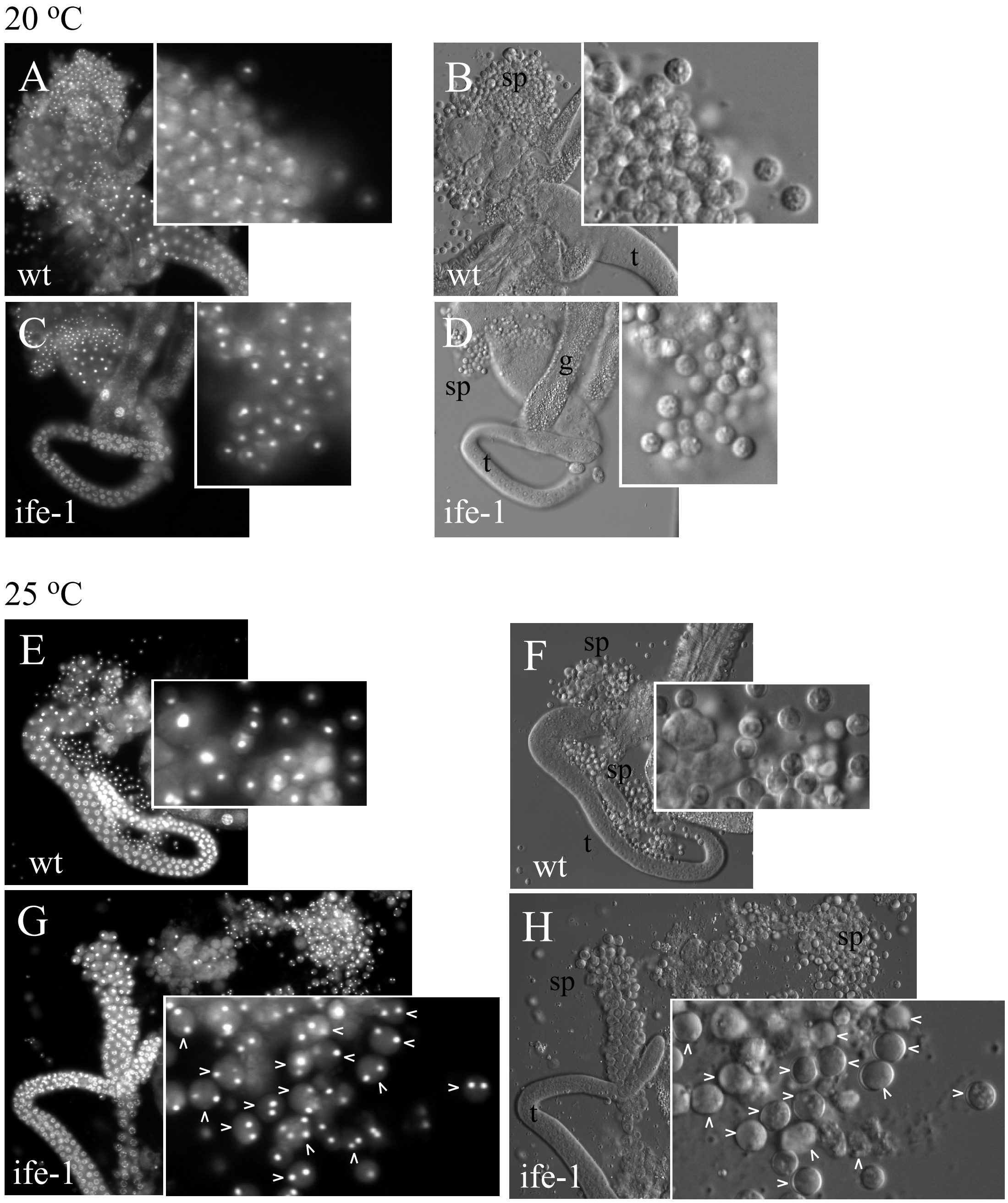
20 °C
A
wt
B
sp
t
wt
C
ife-1
D
g
sp
t
ife-1
25 °C
E
wt
F
sp
sp
t
wt
G
ife-1
H
sp
sp
t
ife-1

C.elegans may be determined. *Drosophila* and mouse spermatogenesis make use of apoptotic factors during cytoplasmic clearing (Arama et al., 2003; Cagan, 2003). Proteins such as Apaf-1 and caspase-3 are responsible for moving cytoplasmic contents during the elongation of the spermatid. Importantly, expression of these proteins does not induce apoptosis in the sperm. There is no documented evidence of naturally-occurring apoptosis in *C.elegans* spermatogenesis, in contrast to that which is documented during oogenesis (Dr. Steve L'Hernault, personal communication). To investigate this unique process in *C.elegans* and the possible involvement of apoptotic factors, dissected male gonads were immunostained with the anti-CED-4 antibody. CED-4 was detected in wild type male gonads and accumulated in apoptosome-like structures in primary and secondary spermatocytes as distinguished by DAPI staining (Figure 4.7A,B). This novel discovery of CED-4 expression in wild type spermatogenesis supports the utilization of pro-apoptotic factors in *C.elegans* spermatogenesis much like that observed in higher species. Since native expression of CED-4 coincided with the region of cytoplasmic clearing, it is plausible that CED-4 has similar functions as its homologs in *Drosophila* and mouse. In *ife-1* male gonads the expression of CED-4 extended throughout the male gonad including the early mitotic stage with similar apoptosomes structures appearing in primary and secondary spermatocytes (Figure 4.7C,D). The loss of IFE-1 may therefore promote the premature expression of CED-4 during spermatogenesis.

Figure 4.7 Expression of CED-4 in the male gonad. (A) Dissected wild type male gonads showed expression of CED-4 in primary and secondary spermatocytes. (B) Nuclear staining by DAPI shows the meiotic progression of spermatogenesis and that CED-4 staining is perinuclear with no overlap of signal. (C,D) The CED-4 and DAPI staining in the *ife-1* male gonad show premature expression of CED-4 throughout the gonad. CED-4 is localized perinuclear in apoptosome structures only in primary and secondary spermatocytes. (ps = primary spermatocyte, sp = spermatid).

Figure 4.7

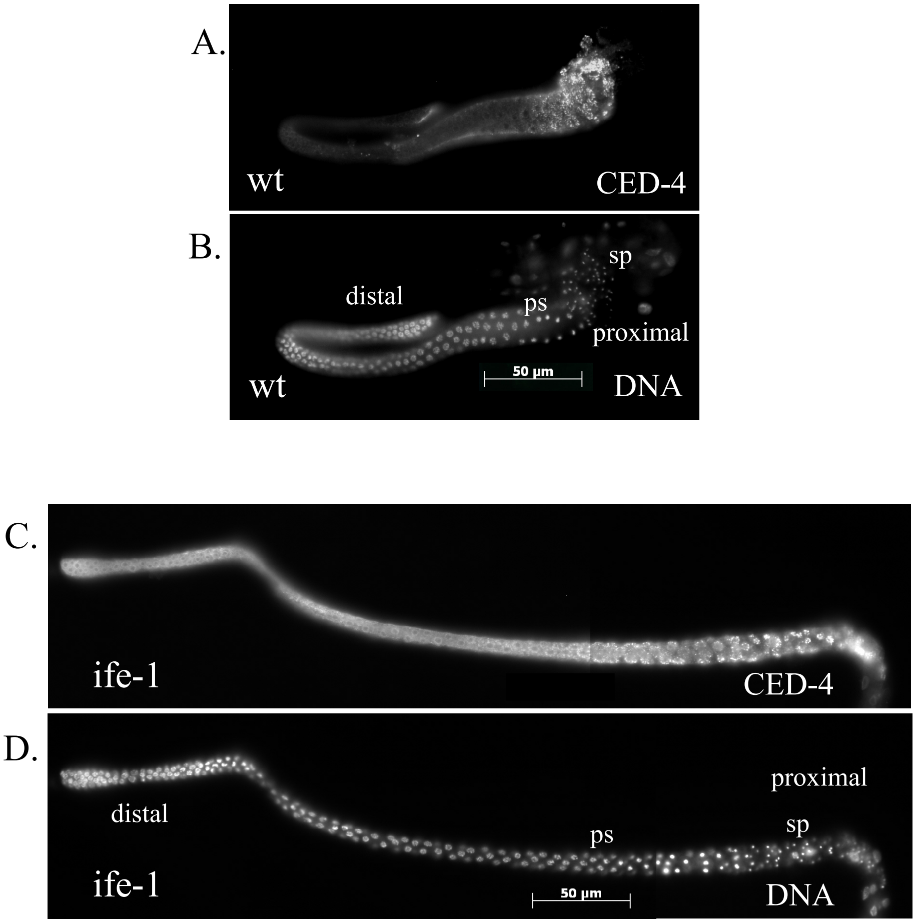
A.
wt
CED-4
B.
sp
distal
ps
proximal
50 µm
wt
DNA
C.
ife-1
CED-4
D.
proximal
distal
sp
ps
ife-1
50 µm
DNA

Conclusion

The production of viable gametes is required for successful fertilization and development of an organism. Here I have begun to described the role of a unique eIF4E isoform, IFE-1, in the development of sperm in *C.elegans*. Loss of this translation factor results in decreased fertility at 15°C and 20°C, as well as complete sterility at 25°C. The temperature-sensitive period affected by the lack of IFE-1 has been determined to be the L4 larval stage. During this late larval stage, germ cells in hermaphrodite worms undergo spermatogenesis to produce mature spermatozoa that are stored in the spermatheca. They are later called upon to fertilize oocytes moving through the spermatheca. Worms lacking IFE-1 produce fewer mature sperm at the permissive temperature, and are devoid of any mature spermatids at 25°C. At the elevated temperature the *ife-1* spermatocytes fail to complete cytokinesis to become individual spermatids. I suggest that IFE-1 is involved in the translation of mRNAs required for the completion of cell division during late spermatogenesis.

Expression of CED-4 in *C.elegans* germ cells and early embryos has been well documented, but expression in spermatocytes has not been investigated due to the absence of apoptosis in this process. Apoptotic events during *C.elegans* oogenesis have been well studied. There is evidence that half of all developing germ cells in the adult hermaphrodite undergo apoptosis rather than produce oocytes (Gumienny et al., 1999). The novel detection of pro-apoptotic factor supports the role for apoptotic-like acivities during spermatogenesis. Despite a role for apoptosis during oogenesis, there has been no documentation of apoptosis in *C.elegans* spermatogenesis. Evidence has recently been shown that apoptotic factors such as Apaf-1 and caspase-3 are utilized in *Drosophila* and mouse spermatocytes to complete the removal of cytoplasmic content prior to completion of spermatogenesis (Arama et al., 2003; Cagan, 2003). Given the large quantity of sperm produced by a male worm, apoptotic events to the degree seen in oogenesis are very unlikely.

Male worms lacking IFE-1 showed premature accumulation of CED-4 in spermatocytes. The presence of CED-4 was not limited to the meiotically dividing cells, but was observed in the distal mitotic region. Apoptosome structures, however, first appeared toward the region of primary and secondary spermatocytes, indicating similar timing as wild type cells. IFE-1 may be responsible for inhibiting the premature expression of CED-4 in spermatocytes, or for the degradation of CED-4 in early spermatogenesis. It is known that the mammalian CED-4 homolog, Apaf-1 is translated in a cap-independent manner. The lack of IFE-1 may lead to an increase in cap-independent translation of CED-4 resulting in uncontrolled, premature expression. The role of IFE-1 on the expression of CED-4 in spermatocytes still needs further investigation.

The studies in this chapter detail the involvement of IFE-1 in spermatogenesis, further clarifying an earlier study which first described the loss of sperm production with decreased IFE-1(Amiri et al., 2001). Here we have discovered the distinct cellular process obstructed by the loss of IFE-1. In addition, a unique role for the pro-apoptotic protein in spermatogenesis, and its misregulation in the absence of IFE-1 was uncovered.

This isoform of eIF4E clearly has unique roles in the proper formation of viable spermatozoa.

CHAPTER 5: IFE-1 IS REQUIRED FOR EFFICIENT TRANSLATION OF SPECIFIC GERMLINE mRNAS

Introduction

Translational control of gene expression is defined as the change in the rate (efficiency) of translation of a group or individual mRNAs. As has been discussed in chapter 1, translational control is an essential means of gene regulation during gametogenesis and embryogenesis, when control at the level of transcription is not feasible. By examining the changes in the rate or efficiency of translation of specific mRNAs in the germline we can gain insight into what genes are regulated by translational control. I will focus on the role of IFE-1 in efficient mRNA translation during *C.elegans* oogenesis and embryogenesis. Several of the regulated mRNAs encode proteins required for meiotic maturation or early embryogenesis. In addition, based on the over expression of CED-4 in the male *ife-1* gonad, I will examine the role of IFE-1 on the translation of the *ced-4* mRNA.

The number of ribosomes actively translating an mRNA is an accurate measure of the efficiency of its translation. An mRNA with multiple ribosomes bound and translating constitutes polysomes or polyribosomes. Ribosomes bind to mRNA cooperatively. The binding of one or two ribosomes favors the binding of more ribosomes (Nelson et al., 1987). This allows the cell to compartmentalize mRNAs in polysomes, and segregate them from mRNAs not bound to any ribosomes. When a cell lysate is resolved by sedimentation in a sucrose gradient, mRNAs bound to numerous ribosomes sediment to the bottom after centrifugation, free non-translated mRNAs remains near the top and intermediate sized polysomes in the middle. By analyzing the location of specific mRNAs in the sucrose gradient, the relative translation efficiency can be determined.

Early in its characterization, the eIF4E isoform, IFE-1, was shown to associate with P granules through the binding of the RNA binding protein PGL-1. P granules are RNPs present in germ cells that store both proteins and mRNAs subsequently utilized in oogenesis, spermatogenesis, and embryogenesis. In this complex, IFE-1 is in close proximity to the stored maternal mRNAs, and it is probable that IFE-1 facilitates mRNAs leaving these P granules for recruitment to ribosomes. The timing of this event likely involves regulating dissociation of IFE-1 from PGL-1. Low levels of IFE-1 are found in the cytoplasm of developing oocytes and may also initiate the translation of non-P granule mRNAs. By examining the translation efficiency of mRNAs found both in P granules (*mex-1*and *pos-1*) and outside of P granules (*glp-1, oma-1, pal-1*, and *ced-4*), we can determine if association with P granules dictates the function of IFE-1 as a translation factor.

Results

In order to determine if IFE-1 influences the translation of stored mRNAs, wild type and *ife-1* whole worm lysates were resolved on 10-45% sucrose gradients by centrifugation. This process separates mRNAs based on the number of ribosomes bound (figure 5.1A,B). The gradient is fractionated with continuous monitoring of the absorbance at 260nm and recorded as a polysome profile (figure 5.1C). The mRNAs free or resting in RNPs (not actively translated) are found in fractions 1-4. The mRNAs with one ribosome bound are found in fraction 5, distinguished by the large absorbance peak for 80S subunits. Each additional peak following the 80S represents the addition of one more ribosome, leading to the formation of polysomes. If an mRNA is being actively translated than it will be found in a later fraction (6-12).

The absorbance profiles generated from wild type and *ife-1* worms were very similar (figure 5.2). Both strains were able to maintain the high efficient levels of translation shown by the formation of polysomes. This shows that despite the absence of IFE-1, mutant worms can still efficiently translate mRNAs and support protein synthesis and strain viability. There is a slight decrease in amplitude of peaks in the polysome region, which may be a consequence of the decrease in the rate of development for the *ife-1* strain. Total RNA was isolated from each fraction and individual mRNAs quantified using real-time PCR to determine the distribution of mRNAs through the gradient. The translation efficiency of the housekeeping mRNA *gpd-3*, which encodes an isoform of glyceraldehyde 3-phosphate dehydrogenase (GAPDH), remained constant in both wild type and *ife-1* worms (figure 5.3). In fact the majority of the *gpd-3* mRNA was located towards the bottom of the gradient (fractions 8-12) in “heavy polysome” in both wild type and *ife-1* strains. This indicates that the *gpd-3* mRNA is very efficiently translated as might be expected based on the high demand for this metabolic protein. The implications of efficient GAPDH mRNA translation lead to the assumption that the absence of IFE-1 does not dramatically reduce total protein synthesis.

Figure 5.1 Isolation and analysis of mRNA resolved on sucrose gradients. (A) The experimental outline consists of applying whole worm, mixed stage lysate to a 10-45% sucrose gradient for sedimentation. (B) After centrifugation mRNAs in polysomes sediment to the bottom while mRNA not bound to ribosomes remain at the top. The gradient is fractionated with continuous absorbance readings at 254 nm. (C) The resulting polysome profile shows the position of the 80S monosome peak, followed by additional peaks each indicating the addition of another ribosome.

Figure 5.1

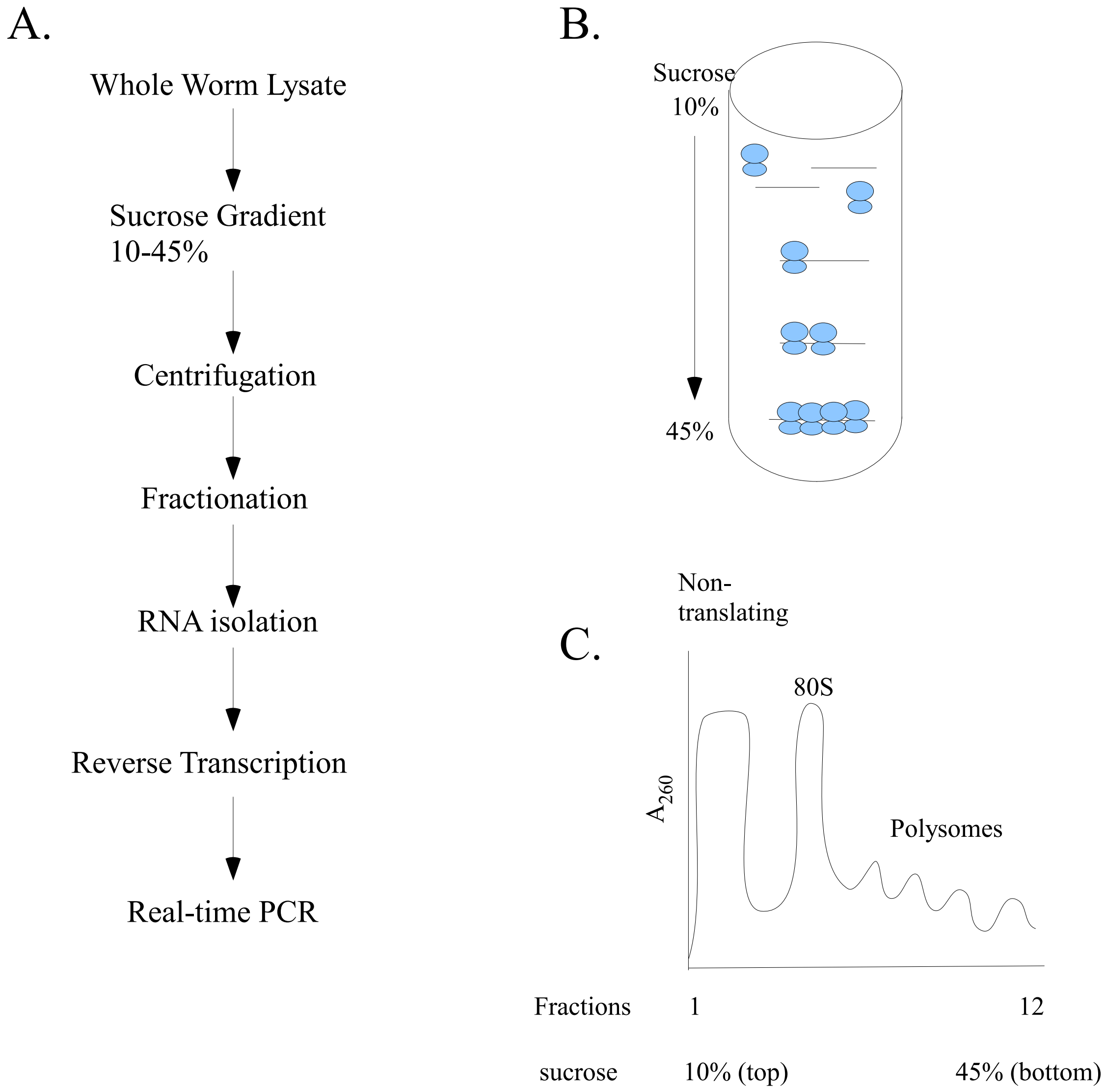
A.
Whole Worm Lysate
Sucrose Gradient 10-45%
Centrifugation
Fractionation
RNA isolation
Reverse Transcription
Real-time PCR
B.
Sucrose 10%
45%
C.
Non-translating
80S
Polysomes
A_{260}
Fractions
1
12
sucrose
10% (top)
45% (bottom)

Figure 5.2 Polysome profiles from wild type and *ife-1* worms. (A) The wild type profile recorded and material collected in 12 fractions with fraction 5 containing the monosome 80S peak. Fractions 6-12 contain polysomes and fractions 1-4 contain non-translating mRNAs. Distribution of P granule protein, PGL-1 in sucrose gradient is shown by western blot. (B) The profile produced from *ife-1* worms verifies loading of mRNAs to a similar distribution of polysomes. This indicates efficient translation of most mRNAs even in the absence of the IFE-1 translation factor. Distribution of the 80S monosome, polysome, and non-translating mRNAs are consistent with the wild type profile.

Figure 5.2

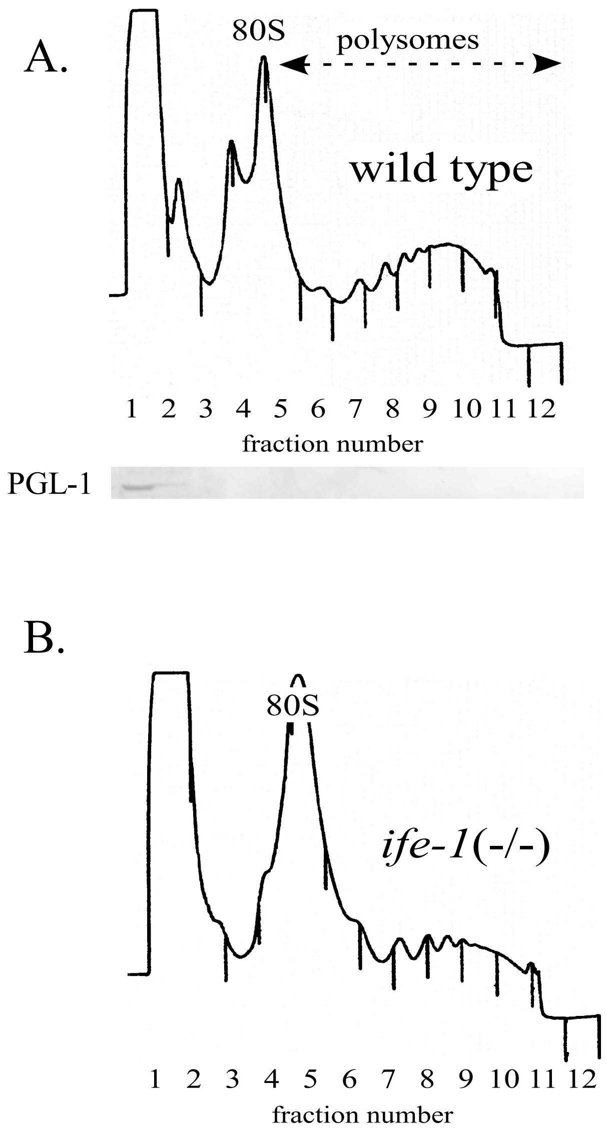
A.
80S
polysomes
wild type
1 2 3 4 5 6 7 8 9 10 11 12
fraction number
PGL-1
B.
80S
ife-1(-/-)
1 2 3 4 5 6 7 8 9 10 11 12
fraction number

Figure 5.3 Translation efficiency of housekeeping mRNA *gpd-3*. Real-time quantification of mRNA encoding the glyceraldehyde dehydrogenase (GAPDH) isoform GPD-3 shows that most of the *gpd-3* mRNA remains in the heavy polysome fractions of the sucrose gradient. Therefore, *gpd-3* mRNA is efficiently translated in both wild type (blue) and *ife-1* (pink) worms.

Figure 5.3

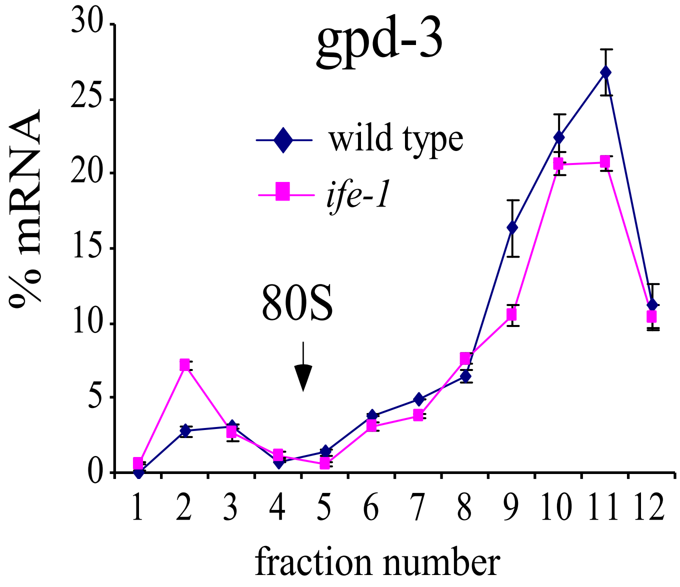
gpd-3
% mRNA
30
25
20
15
10
5
0
wild type
ife-1
80S
1
2
3
4
5
6
7
8
9
10
11
12
fraction number

Previous chapters discussed the role of IFE-1 in gametogenesis. I have further investigated the role of this translation factor by examining the translation efficiency for mRNAs involved in late oocyte maturation and embryogenesis. Prior to fertilization the oocyte must synthesize proteins that dispatch the sperm signal and induce oocyte maturation. One protein involved in this process is OMA-1, which is utilized in the maturation signaling of the oocyte from the binding of major sperm protein (MSP). The *oma-1* mRNA is found throughout the hermaphrodite gonad, but the protein accumulates in the proximal arm where oocytes prepare for and await fertilization. After fertilization the OMA-1 protein is quickly degraded. The distribution of *oma-1* mRNA was examined in sucrose gradients from wild type and *ife-1* worms. The *oma-1* mRNA was found efficiently loaded on polysomes in wild type worms (Figure 5.4A). In *ife-1* worms, the bulk of the mRNA shifts to early fractions indicating that *oma-1* was not as efficiently translated. *oma-1* mRNA was translated five-fold more efficiently in the presence of IFE-1. Roughly the same amount of *oma-1* mRNA “lost” from the heavy polysome is “found” in the non-translating region of the gradient. The amount of *oma-1* translation on intermediate polysomes (fractions 5-8) is roughly the same, indicating some population of the mRNA continues to translate but less efficiently. One possible explanation for remaining *oma-1* translation is that some *oma-1* is being recruited to the ribosome by IFE-3 or IFE-5. There remains a proportion of *oma-1* mRNA sedimented with heavy polysome in the gradient from *ife-1* worms. This may also be due to the other isoforms, IFE-3 and IFE-5 that are available to re-initiate translation of *oma-1* in the formation of polysomes. This suggests that IFE-1 facilitates both the initial recruitment of *oma-1* to the ribosome and the efficient re-initiation of this mRNA. A basal rate of *oma-1* initiation supported by IFE-3 and IFE-5 may give rise to the lack of change in the "weak" or light polysomes.

MEX-1 is a protein that helps mediate the establishment of polarity in the embryo by acting as a translational repressor for other stored mRNAs. MEX-1 is first expressed during oogenesis and accumulates to high levels in large oocytes prior to fertilization. The temporal and spatial expression of this protein plays an important roles in controlling the synthesis of other proteins involved in embryogenesis. We examined the role of IFE-1 on the translational efficiency of *mex-1* due to the importance of MEX-1 protein for the fate of the embryo. The distribution of *mex-1* in sucrose gradients from wild type and *ife-1* lysates is very similar to the distribution of *oma-1* (Figure 5.4B). In wild type worms *mex-1* is efficiently loaded to polysomes, while most of the mRNA in *ife-1* worms is remains in the non-translating region (Figure 5.2). This indicates that most *mex-1* mRNA remains in P granules and is not loaded on ribosome in the absence of IFE-1. Western blot of sucrose gradient fractions have indicated that PGL-1 and P granules remain in fractions 1-2 in the non-translating region. When the difference in *mex-1* distribution was calculated, wild type translation of *mex-1* is seven times higher than in *ife-1* worms. Like *oma-1, mex-1* requires IFE-1 for initial recruitment and maintenance in polysomes. The recruitment role of IFE-1 for *mex-1* mRNA may be facilitated by proximity to IFE-1 in the P granules.

To determine if the dramatic decrease in *mex-1* mRNA translational efficiency affected the accumulation of MEX-1 protein in oocytes, immunostaining of dissected gonads from wild type and IFE-1 deficient worms was performed using a MEX-1

Figure 5.4 Distribution of *oma-1* and *mex-1* mRNAs. (A) In the wild type sample most of the *oma-1* mRNA is found in the polysome regions of the gradient. In the *ife-1* mutant, the *oma-1* mRNA is shifted to the non- translating earlier fractions. Wild type worms translate *oma-1* mRNA 5-fold more efficiently than *ife-1* worms. (B) The *mex-1* mRNA was loading onto polysomes in the wild type worms. A low percentage of the mRNA is in the non-translating or monosome regions. In the *ife-1* sample the *mex-1* mRNA is mostly found in the top of the gradient, in the non-translating region.

Figure 5.4

A.

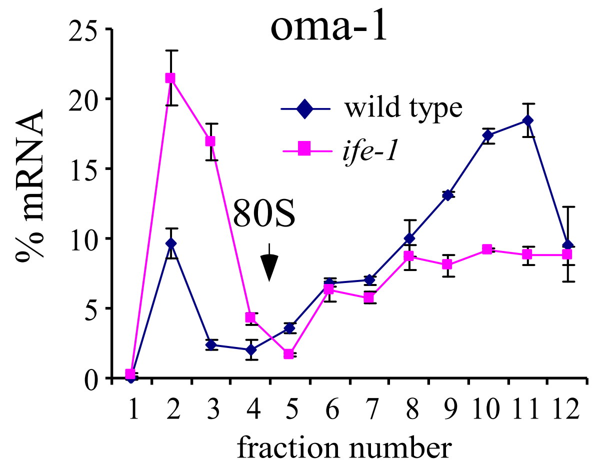
oma-1
% mRNA
25
20
15
10
5
0
1 2 3 4 5 6 7 8 9 10 11 12
fraction number
wild type
ife-1
80S

B.

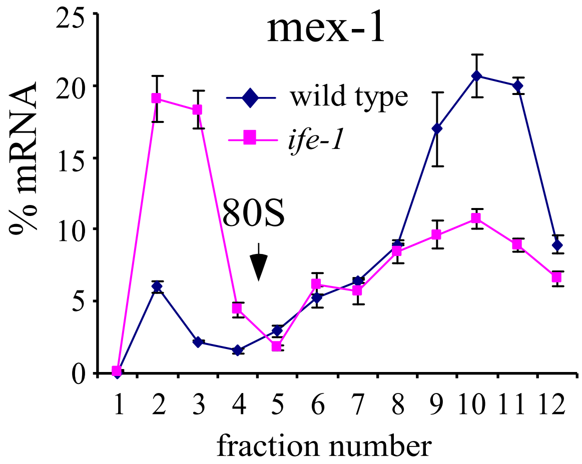
mex-1
% mRNA
25
20
15
10
5
0
1 2 3 4 5 6 7 8 9 10 11 12
fraction number
wild type
ife-1
80S

Figure 5.5 Accumulation of MEX-1 in the hermaphrodite gonad. Dissected hermaphrodite gonads were fixed and immunostained for MEX-1 protein and co-stained with DAPI to visualize oocyte nuclei. (A) In the wild type, MEX-1 was first detected in the late pachytene stage of meiosis and progressively accumulates to the –1 oocyte. (B,C) In *ife-1* gonads, the MEX-1 protein appeared in late pachytene, but then remained relatively constant (B) or decreased (C) in later oocytes. MEX-1 signal was normalized to exposure time using identical incident light and filter settings to allow direct comparisons.

Figure 5.5

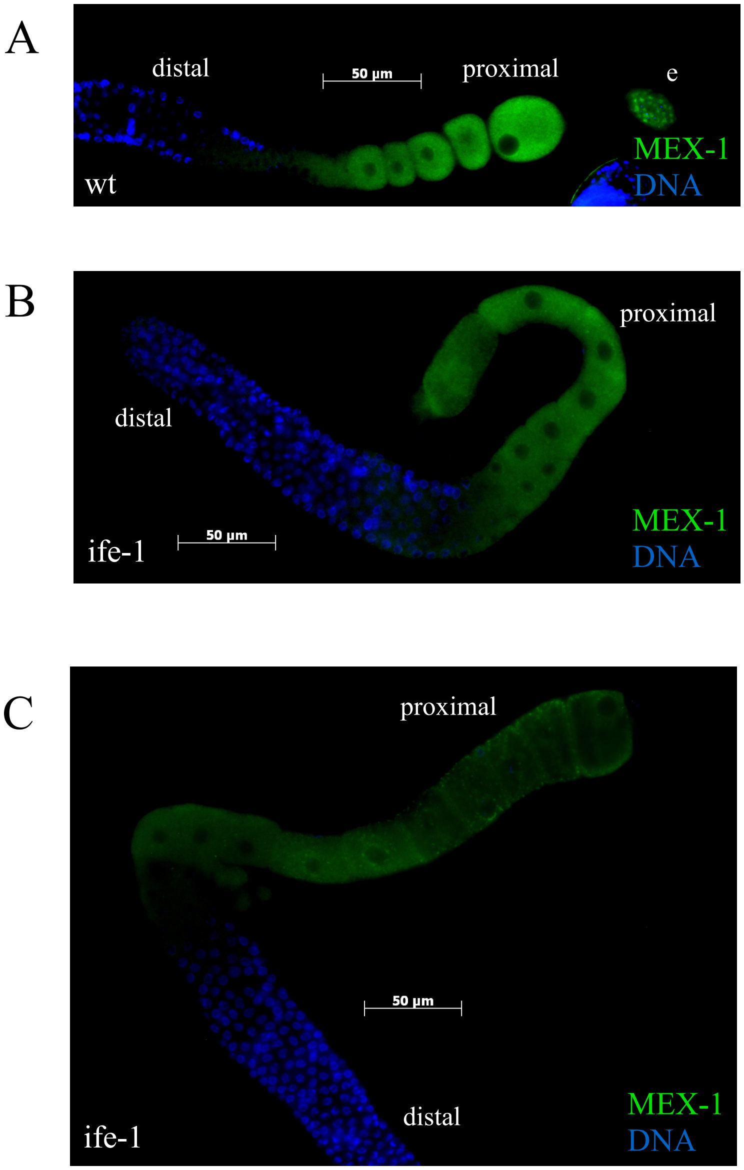
A
distal
50 µm
proximal
e
MEX-1
DNA
wt
B
proximal
distal
ife-1
50 µm
MEX-1
DNA
C
proximal
50 µm
distal
ife-1
MEX-1
DNA

antibody (Santa Cruz). Gonads were dissected from young adult hermaphrodites (<24 hour after larval L4 stage), fixed, stained and the level of MEX-1 protein was observed by immunofluorescence microscopy (Figure 5.5). In wild type gonads, MEX-1 expression is not detected in the small oocytes of the distal gonad, but gradually becomes visible in the large oocytes of the proximal gonad and continues to accumulate to the -1 oocyte next to the spermatheca. The intensity of staining suggests that the level of MEX-1 protein gradually increases in post-pachytene oocytes as cell growth progresses. In the *ife-1* gonad, the first visible detection of MEX-1 appears in the same location as in wild type gonads. However, the subsequent increase in intensity is not observed. Detected MEX-1 also appears more granular in the cytoplasm. It has been reported that as oocytes age, new RNPs develop to house the accumulating proteins required for fertilization and embryogenesis (Jud et al., 2008) but such granules are not as evident in the oocyte of young hermaphrodites. I suggest that the punctate granules appear in oocytes that have "aged" due to the low rate of oocyte production in *ife-1* hermaphrodites. Our earlier results suggest that the rate of ovulation may be reduced and oocytes remain in the distal gonad longer (chapter 3). The MEX-1 immunostaining is consistent with the decrease in translation efficiency of *mex-1* mRNA in the absence of IFE-1. This results in abnormal expression of MEX-1 as oocytes now lack the gradual increase in this protein prior to fertilization. The consequences of this abnormal MEX-1 expression for oocyte maturation and early embryogenesis are not known, but could play a role in the decreased competence of *ife-1* oocytes as embryos.

In addition to the mRNAs whose protein products accumulate in oocytes, we have examined the translation efficiency of two mRNAs important for early embryonic development, *pos-1* and *pal-1*. Both mRNAs are reported to undergo translation repression during early embryogenesis. POS-1 is required in establishing the polarity of the embryo and accumulates in the 1-cell stage at the posterior end. Both the POS-1 protein and the *pos-1* mRNA are associated with P granules. In addition, the *pos-1* mRNA is regulated by inhibitory proteins binding the 3'UTR and repressing translation (Tabara et al., 1999). In both wild type and *ife-1* worms, much of the *pos-1* mRNA was not actively translated and only a low percentage of the mRNA found in polysomes in these whole worm lysates (Figure 5.6A). Regardless, the loss of IFE-1 further decreased the *pos-1* localization to the polysome region of the gradient approximately four-fold. This suggests that, following its release from translational repression, *pos-1* mRNA becomes recruited to the ribosome by IFE-1. *pal-1* mRNA, which is not found in P granules, is also regulated by 3' UTR binding proteins. The translational behavior of *pal-1* showed similar effects in the absence of IFE-1 (Figure 5.6B). Like *pos-1, pal-1* mRNA is not well translated with the majority of the mRNA found in the top of the gradient. With the absence of IFE-1 the amount of *pal-1* mRNA loaded on polysomes drops 5-fold. Both *pos-1* and *pal-1* therefore appear to utilize IFE-1 for recruitment to the ribosome. Translational control of these mRNAs is mostly regulated by other repression mechanisms, but without IFE-1 these mRNAs show little capability to initiate translation at all.

The GLP-1 protein has two unique and separate roles in development of the gamete and embryo. During mitotic divisions of germline stem cells GLP-1 protein receives the pro-mitotic signal from the distal tip cell to undergo mitosis (Crittenden et al., 1994). During meiosis the *glp-1* mRNA is repressed by the binding of GLD-1. During

Figure 5.6 Translation of mRNAs involved in embryonic development. (A) In both wild type and *ife-1*, most of the *pos-1* mRNA is found in the non-translated region of the gradient. IFE-1 deficient worms show a further decrease in *pos-1* mRNA in the polysome region and an increase in non-translating *pos-1*. (B) The distribution of *pal-1* mRNA shows similar distribution as *pos-1*. The majority of *pal-1* mRNA was in the non-translating fractions in both wild type and *ife-1*. The lack of IFE-1 leads to a reduction in *pal-1* mRNA associated with polysomes.

Figure 5.6

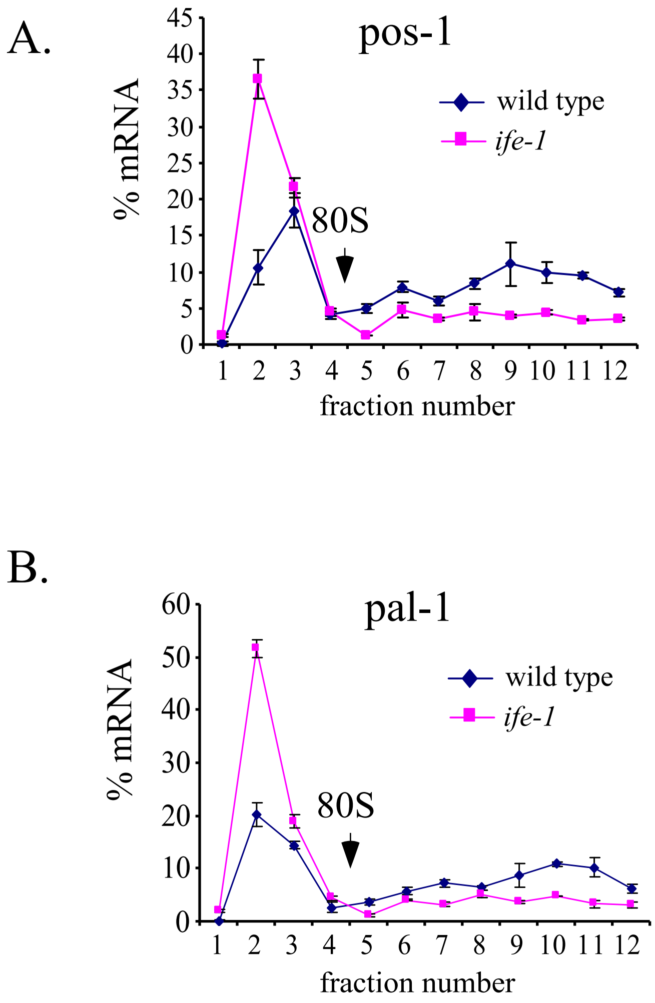
A.
pos-1
% mRNA
45
40
35
30
25
20
15
10
5
0
wild type
ife-1
80S
1
2
3
4
5
6
7
8
9
10
11
12
fraction number
B.
pal-1
% mRNA
60
50
40
30
20
10
0
wild type
ife-1
80S
1
2
3
4
5
6
7
8
9
10
11
12
fraction number

embryogenesis GLP-1 is again required for somatic tissue development in the embryo. The *glp-1* mRNA is regulated by various proteins (e.g. POS-1) binding the 3' UTR in addition to GLD-1 (Ogura et al., 2003); (Schubert et al., 2000; Evans et al.). This regulation resulted in a unique distribution of the mRNA in wild type and *ife-1* gradients (Figure 5.7A). Like *pos-1* and *pal-1*, most of the *glp-1* mRNA is found in the non-translating fractions. The absence of IFE-1 resulted in an increase of *glp-1* mRNA to the non-translating region (fractions1-4). Since GLP-1 is expressed at various points during development and repressed by several factors, and our analysis was conducted with populations of whole worms, the complicated control of this mRNA prevents us from drawing any significant conclusion on the role of IFE-1 in *glp-1* translation except that it does significantly promote *glp-1* translation.

Data presented in chapter 4 showed that a lack of IFE-1 leads to an increase in CED-4 expression in early spermatocytes. P granules are also present in early spermatocytes and may sequester IFE-1 in the male gametes also, though this has not been demonstrated. I addressed the translation of *ced-4* mRNA directly by polysome analysis. Despite the observed increase in CED-4 during spermatogenesis, the translation efficiency of *ced-4* decreases in hermaphrodite worms in the absence of IFE-1 (Figure 5.7B). In wild type worms most of the *ced-4* mRNA is recruited to polysome for efficient translation, while in *ife-1* worms the *ced-4* mRNA shifts to the non-translated fractions. The decrease in translation efficiency is inconsistent with what was expected for CED-4 abundance in *ife-1* spermatocytes. However, the lysates used with the sucrose gradients were unstaged hermaphrodites (mostly adults) that included few males. This extract would not be expected to represent the translation of early spermatocytes.

Figure 5.7 Translational efficiency of *glp-1* and *ced-4*. (A) Distribution of mRNA of *glp-1* shows nearly uniform levels of the mRNA throughout the gradient in wild type worms. The absence of IFE-1 shifts some *glp-1* mRNA to the non-translating fractions with a loss of the heavy polysome peak in fraction 11. (B) In wild type worms *ced-4* is distributed to primarily polysomal fractions indicating the mRNA translates well. The *ife-1* distribution of *ced-4* shifted substantially to the non-translating region demonstrating a significant role for IFE-1 in *ced-4* translation.

Figure 5.7

A.

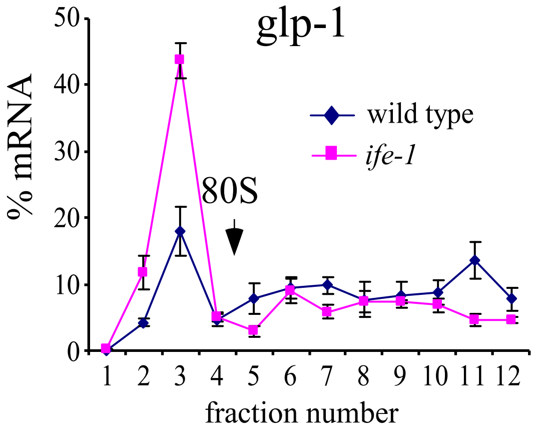
glp-1
% mRNA
0
10
20
30
40
50
wild type
ife-1
80S
1
2
3
4
5
6
7
8
9
10
11
12
fraction number

B.

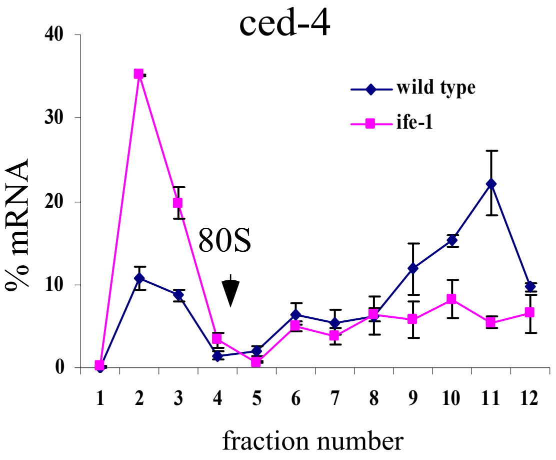
ced-4
% mRNA
0
10
20
30
40
wild type
ife-1
80S
1
2
3
4
5
6
7
8
9
10
11
12
fraction number

Furthermore, the increase in abundance of CED-4 may be a result of a decrease in the rate of protein degradation, specifically the clearing of cytoplasmic contents to the residual body. Figure 3.7 showed no detectable expression of CED-4 in oocytes by immunostaining in either wild type or *ife-1* hermaphrodite gonads. It is known that CED-4 is utilized during germline apoptosis in the hermaphrodite gonad as well as in somatic tissue (Gumienny et al., 1999). The polysome cosedimentation results suggest that the *ced-4* mRNA utilizes IFE-1 for recruitment to the ribosome in whole populations of hermaphrodites, but further investigation is needed to evaluate *ced-4* translation specifically in spermatocytes.

Conclusion

Earlier publications suggested that IFE-1 might not be an active translation initiation factor based on the lack of IFE-1 protein detection in polysome fractions isolated from a sucrose gradient (Dinkova et al., 2005). The results shown here refute that suggestion and demonstrate that IFE-1 is an active isoform of eIF4E that is responsible for the recruitment of at least some germline mRNAs to the ribosome. In worms lacking IFE-1 specific mRNAs (*pos-1, pal-1, oma-1, glp-1, mex-1* and *ced-4*) decrease in translation efficiency, suggesting that IFE-1 is required to maintain the normal rate of translation for these mRNAs. For proteins required in late oocytes prior to fertilization (OMA-1 and MEX-1), the mRNAs showed a strong dependence on IFE-1. The translation efficiency of *oma-1* and *mex-1* increased five- and seven-fold respectively when IFE-1 was present. Decreased translation efficiency altered the accumulation of the MEX-1 protein in oocytes. Compared to wild type, the *ife-1* hermaphrodites failed to demonstrate the gradual increase in MEX-1 prior to fertilization. Data in chapter 3 showed that *ife-1* hermaphrodites have a decrease in the rate of oocyte production. Decreased translation of mRNAs such as *mex-1* that are needed for late oogenesis could hinder the progression of the oocytes or may fail to trigger specific checkpoints which have not been discovered. Certainly the accumulation of other proteins in oogenesis are likely to be dependent of IFE-1, and any of these could affect oocyte growth rates. Further investigation into oogenesis is needed. Particularly intriguing will be elucidation of how the absence of IFE-1 reduces the rate of oocyte production without increasing the incidence of germline apoptosis.

In addition to *oma-1* and *mex-1*, mRNAs normally translated later, in the early embryo, were also disrupted by the lack of IFE-1. The translation of *pal-1* and *pos-1* mRNAs is under the control of several inhibitory proteins early in embryogenesis. POS-1 accumulation is limited to the posterior end of the 1- and 2-cell embryo by the expression of MEX-5 and MEX-6 in the anterior end and the binding of these proteins to the 3’UTR of *pos-1*(Schubert et al., 2000). The *pal-1* mRNA is repressed in certain blastomeres in a similar fashion (Hunter et al., 1996); (Huang et al., 2002). Therefore, the translational efficiency of these mRNAs is always low, even in wild type worms. In the absence of IFE-1 the translation of these mRNAs was even further decreased (nearly abolished). This supports a role for IFE-1 in even the inefficient translation of mRNAs that are controlled by other mechanisms of translational control.

The precocious accumulation of CED-4 that we observed in *ife-1* spermatocytes remains unexplained. In an attempt to address possible CED-4 overexpression by translation, we investigated the translation efficiency of *ced-4* in *ife-1* hermaphrodites. CED-4 is the *C.elegans* homolog to the mammalian apoptotic factor, Apaf-1. In mammalian systems the Apaf-1 mRNA is translated through the use of an internal ribosome entry site (IRES), independent of eIF4E and the methylated cap (Coldwell et al., 2000). It is not known if *ced-4* mRNA has a similar preference for cap-independent translation, but based on the decrease in translation efficiency in the absence of IFE-1, I suggest that *ced-4* mRNA can be efficiently translated by a mechanism that involves IFE-1; presumably a cap-dependent mechanism.

To understand the broader role of IFE-1 in preferentially recruiting mRNAs to the ribosome, more mRNAs will need to be examined. The lab is currently using Affymetrix microarrays to identify all mRNAs that are affected by the loss of IFE-1 in terms of translation efficiency. The use of microarrays will allow us to quantify and compare every mRNA in the non-translating and polysome portions of the sucrose gradients from wild type and *ife-1* worms. The results from this experiment may in turn identify new targets involved in oogenesis that contribute to oocyte growth, production, or maturation. In addition, specific mRNAs whose products function in cytokinesis in late spermatocytes may also be identified. Our current results verify that IFE-1-dependent mRNAs exist.

There is very little known about the translation of specific mRNAs during *C.elegans* spermatogenesis. The unique multinucleated phenotype displayed in *ife-1* spermatocytes demonstrates an important role for translational control in the final budding event in spermatocyte development. Using established methods to isolate populations enriched in male worms and performing the same isolation of mRNAs from sucrose gradients may allow for the detection of sperm-related mRNAs affected by the absence of IFE-1. This will not be trivial, as the propagation of a male population is not possible without hermaphrodites. Synchronization of sperm-producing L4 hermaphrodites is also unlikely to be sufficient. The switch to oogenesis in the distal gonad during larval stages is gradual, and may be difficult to pinpoint in large populations. However, one plausible approach is to use a temperature-sensitive mutant hermaphrodite strain that is unable to switch from spermatogenesis to oogenesis (e.g. *fem-3*) to determine sperm-specific translational control events by differences from the wild type.

Findings presented in this chapter indicate that IFE-1 has a unique role in the translation of stored mRNAs during oogenesis. In addition, IFE-1 appears to potentiate the translation of the apoptotic factor *ced-4*. The other germline isoforms of eIF4E, IFE-3 and IFE-5, are incapable of fully substituting for IFE-1. IFE-1 also appears to play a distinct role in the recruitment of several mRNAs from a repressed state in RNPs to ribosomes and eventually dense loading in polysomes for translation. Further experiments are needed to determine how many mRNAs actually utilize IFE-1 during gametogenesis and embryogenesis, and what other initiation pathways exist.

CHAPTER 6: EXPRESSION OF FLAG:IFE-1 TRANSGENE

Introduction

DNA transformation allows scientists to link the molecular characteristics of a protein to a specific phenotype (Mello et al., 1991; Mello et al., 1995). DNA transformation is also used to rescue mutant phenotypes and thereby identify compensating pathways. The wide use of genetics in *C.elegans* has produced a large proportion of genetic mutants which demonstrate unique phenotypes. DNA transformations in *C.elegans* have been performed for over twenty years. DNA is incorporated into the nuclei of developing oocytes as an extrachromosomal array by either microinjection or bombardment (Evans (ed.)). The most studied method is microinjection and will be discussed here. The expression plasmid containing the gene of interest was produced in bacteria and isolated. An additional plasmid encoding a selectable marker was also prepared. Various *C.elegans* marker genes are used to easily detect transformed progeny. The marker used in my study was *rol-6(su1006)*, a mutant form of a cuticle collagen gene which, when expressed in transformed animals, causes the worms to roll while swimming. The combined, linearized plasmids are injected into the syncytial gonad (Mello et al., 1991). The injected blunt-end DNA spontaneously ligates to produce long extrachromosomal arrays that are incorporated into nuclei and carried on through subsequent generations creating a transgenic line. Such arrays have been used to investigate the roles of promoter region, protein function, and 5'and 3' UTR regulatory sequences. In most cases such expression experiments include the use of reporter constructs. The role of promoter and UTRs can be studied using easily detectable markers *in situ* such as GFP, mCherry, or lacZ. Spatial and temporal expression of a given protein was addressed by fusing the gene or cDNA encoding a protein of interest in frame with a visible marker such as GFP. This method is widely exploited in *C.elegans* because of the transparency of the animal, which allows the protein product to be visualized in a live animal under fluorescence microscopy.

In addition to visualization in live animals, the expression of transgenes linked to markers or tags can be used for biochemical experiments. Commercial antibodies are used to detect common tags such as GST, Histidine-6, FLAG, and GFP. Antibodies to these tags make feasible molecular detection by western blots, immunoprecipitation, and immunohistochemistry. Affinity chromatography resins for some of these tags are also available to facilitate isolation of the fused protein. For example, Ni-agarose is used to isolate 6X-His tagged proteins.

In this dissertation, we have investigated the phenotype that results from deletion of the *ife-1* gene. This null mutation is the only lesion in the genome so we can assume that the defects in gametogenesis are a result of the absence of IFE-1. DNA transformation of wild type copies of the *ife-1* gene into *ife-1*(bn127) mutant worms may cause recovery from defective gametogenesis (phenotypic rescue). The experiments in this chapter represent our initial progress in accomplishing transgenesis, rescue and biochemical reisolation of tagged IFE-1 protein. These will be accomplished with the construction, injection, and creation of transgenic lines incorporating FLAG-tagged *ife-1* and *ife-5* transgenes and the selectable marker.

Results

To further investigate the role of IFE-1 and attempt to rescue the *ife-1* phenotype, we set out to create and transform a construct encoding a tagged IFE-1 protein. A plasmid containing the *ife-1* cDNA fused in frame with a region encoding an 11 amino acid FLAG tag was constructed in the pBlue Script SK vector under the control of 1.5 kb of the native endogenous *ife-1* promoter (Figure 6.1A). This was not a trivial problem as the *ife-1* gene is the third gene in a polycistron. The mRNAs for five genes in the operon are transcribed as one long transcript and processed into individual, mature mRNAs through trans-splicing events (Blumenthal, 1998). The *ife-1* promoter used in the transgene lies directly upstream of the first gene in the polycistron. The promoter was fused directly to the *ife-1* cDNA, followed by a 3' UTR sequence from the let-858 gene. The let-858 3' UTR sequence is commonly used in *C.elegans* transgenes to ensure efficient transcript processing and robust expression of transgenes. A second transgene was also designed where the flag and *ife-1* sequence are under the control of the *pie-1* promoter. PIE-1 is a transcription factor in early embryos and the *pie-1* mRNA is expressed in oocytes and associates with P granules (Schisa et al., 2001). The *pie-1* promoter is one of the few promoters known to be actively transcribed from a transgene in the germline and is therefore commonly implemented for germline expression, which can be very difficult to achieve. Constructs were also made replacing the *ife-5* cDNA for the *ife-1* cDNA to create tagged IFE-5 transgenes with the *ife-1* and *pie-1* promoters. The *pie-1* and *ife-1* promoters were used in order to examine the transgene under the endogenous *ife-1* promoter and to obtain the highest level of transgene germline expression associated with the *pie-1* promoter.

Figure 6.1 DNA transformations of IFEs into *C.elegans*. (A) Transgenic plasmids for DNA transformation with *ife-1* or *ife-5* cDNA and either the endogenous *ife-1* or *pie-1* promoter sequences. The *let-858* 3'UTR was added to facilitate mRNA processing in the worm. (B) Diagram of injection of DNA into the syncytial gonad in *C.elegans* for incorporation into oocytes.

Figure 6.1

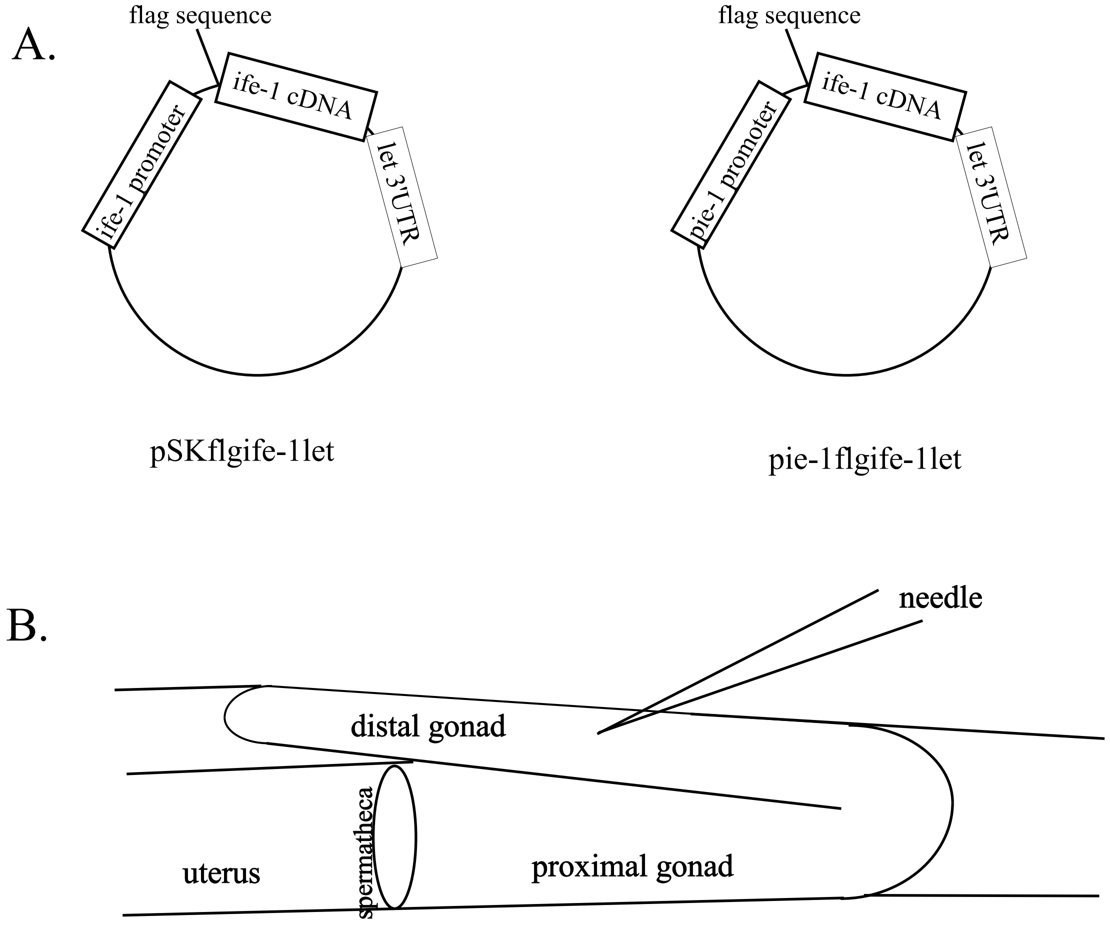
A.
flag sequence
ife-1 cDNA
ife-1 promoter
let 3'UTR
pSKflgife-1let
flag sequence
ife-1 cDNA
pie-1 promoter
let 3'UTR
pie-1flgife-1let
B.
needle
distal gonad
spermatheca
uterus
proximal gonad

Linearized Flag:IFE-1 constructs were co-injected with the pRF4 plasmid encoding the *rol-6* selectable marker into the syncytial gonad (Figure 6.1B). The shared cytoplasm of the early oocytes allow for the injected DNA to form long extrachromosomal arrays that are incorporated into all oocyte nuclei during the processes of meiosis and cell membrane closure. F1 progeny were screened for the expression of the *rol-6* phenotype. Since the co-injected DNAs unite to form randomly concatenated arrays, the expression of the *rol-6* phenotype essentially always coordinates with the expression of FLG:IFE-1. Rolling F1 worms (founders) were picked to individual plates to produce offspring. If F2 progeny of these founders demonstrated the rolling phenotype, then the array was incorporated into the germline cell lineage and a transgenic strain was obtained.

The extent of FLG:IFE-1 and FLG:IFE-5 expression was determined for each stable transgenic line. In order to determine if the rolling phenotype corresponds to a detectable level of FLG:IFE-1, western blots were performed on worm total protein lysates using the anti-FLAG or IFE-1 antibody. Figure 6.2 shows a western blot from lines transformed with the FLG:IFE-1 and the endogenous *ife-1* promoter. The transgene product is undetectable in all transformed strains by western blot, but is detected in the FLG:IFE-1 positive control produced in BL21 *E.coli* cells. This positive control utilizes the same DNA sequence as the transgene in a pET21b vector and is transformed and expressed in BL21 *E.coli* cells. Detection of actin (top blot) in the lysates showed equal loading of each protein extract. The lack of detection in the transgenic lines was likely the combination of two deleterious factors; a very low level of

Figure 6.2 Expression of FLG:IFE-1 from the endogenous promoter. These western blots attempt to detect FLG:IFE-1 from worm lysates of six stable transgenic lines derived from pSKflgife-1let injections. FLG:IFE-1 was only detected in extracts from the positive control BL21 pETflg:ife-1 *E.coli*. Levels of actin show equal loading of worm lysate. N2 is wild type, non-transformed worm lysate. In this western blot anti-FLAG antibody (Cell Signaling) was used. Subsequent western blots using the Sigma anti-Flag antibody showed greater sensitivity.

Figure 6.2

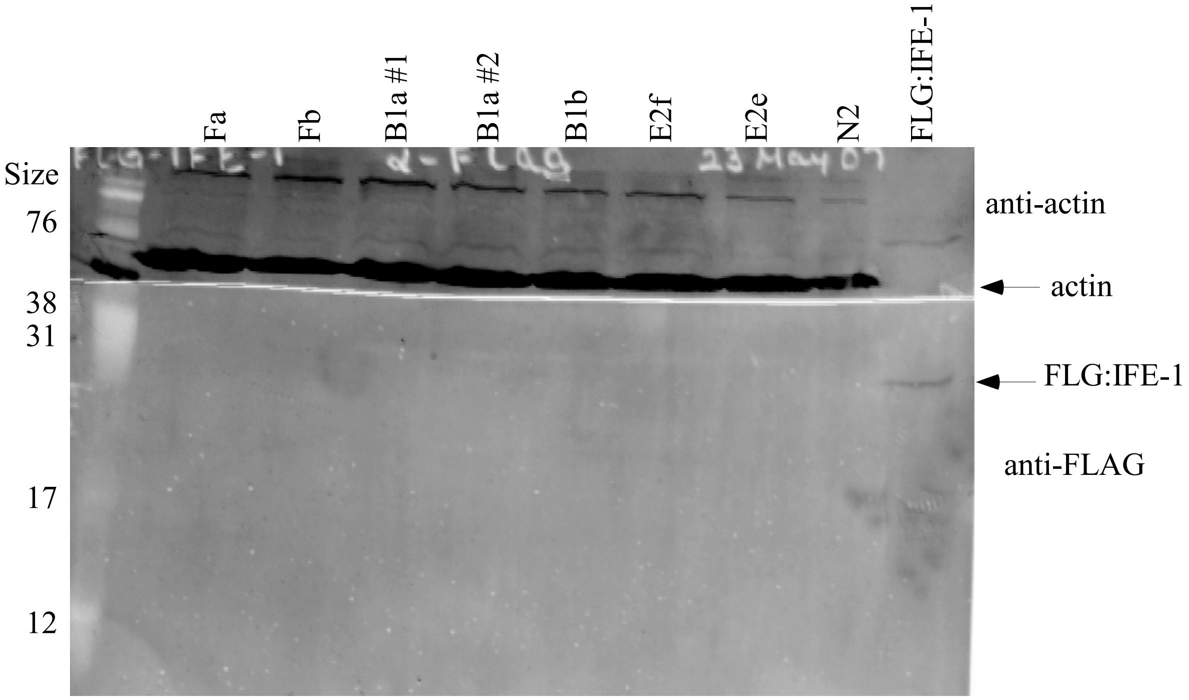
Fa
Fb
B1a #1
B1a #2
B1b
E2f
E2e
N2
FLG:IFE-1
FLG-IFE-1
α-FLAG
23 May 07
Size
76
38
31
17
12
anti-actin
actin
FLG:IFE-1
anti-FLAG

FLG:IFE-1 expression and a poor anti-FLAG antibody. Western blots using anti-IFE-1 antibody showed no better detection of FLAG tagged IFE-1 (data not shown). The anti-IFE-1 antibody is relatively insensitive and often requires affinity enrichment of endogenous IFE-1 for detection by western blots.

To induce better expression of the FLG:IFE-1 protein we attempted to stably integrate the transgene into the worm chromosomes. A transgenic line with a low percentage of rolling offspring was selected for transgene integration into the chromosomes. Radiation causes double stranded chromosome breaks and extrachromosomal arrays can enter these strand breaks. During the endogenous mechanisms of DNA repair, the transgene is occasionally incorporated into the chromosomes and a stable transformant can be produced. These are apparent by greater production of roller offspring (> 50%). Pools of worms displaying the rolling phenotype were selected at L4 larval stage, were exposed to three levels of radiation: 30, 40, and 50 mJoules. The highest level of radiation produced sterility or death of all exposed animals. Worm exposed to 40 mJ failed to produce any rolling offspring. From the lowest level of radiation (30 mJ), 19 roller offspring were isolated and placed on individual plates (data not shown). If successful integration occurred the worm would be heterozygous for the *flg:ife-1* sequence and should produce approximately 50% rolling offspring. Unfortunately, none of the 19 individuals produced more than the expected 20-30% rolling offspring, equivalent to segregation of the parental transgenic line. Further attempts to integrate a construct containing the native *ife-1* promoter have been done with similar results. Additional trials could be conducted in the future on a larger scale.

Since the detection of the FLG:IFE-1 transgene was unsuccessful using the endogenous promoter, I pursued expression of the transgene under the *pie-1* promoter. This promoter sequence is widely used to obtain detectable expression of transgenes in the *C.elegans* germline, but may not express the transgene in the same pattern as endogenous IFE-1 expression. The injection of the *flag:ife-1* plasmid with the *pie-1* promoter resulted in the acquisition of four transgenic lines (KX90-93). For improved western blot detection, FLG:IFE-1 was isolated from worm lysates by immunoprecipitation (IP) with an anti-FLAG affinity resin from Sigma. This agarose resin contains covalently linked anti-FLAG antibody. Detection of the FLG:IFE-1 by the anti-FLAG antibody (Sigma) from the IPs was hindered by the co-migration of FLG:IFE-1 (Mw 24kDa) with the IgG light chain from anti-Flag IP resin (Figure 6.3). However, whole worm lysate samples loaded in parallel showed light detection of a product at the expected 24 kDa size. The intensity of the putative Flg:IFE-1 bands in KX90, KX91, and KX92 extracts was stronger than the lysates of other transgenic strains, particularly the strain created using the endogenous *ife-1* promoter (lane "KX68"). This suggests that detectable FLG:IFE-1 is made from the *pie-1* promoter, but was not detectably expressed from the native *ife-1* promoter. In addition, an attempt at immunostaining was performed on the transgenic line using the Sigma anti-Flag antibody (data not shown), but no signal over background was found.

Conclusion

Although more work is needed to optimize expression, detection, and eventually isolation of the FLG:IFE protein complexes using these transgenic lines, progress has

Figure 6.3 Expression of FLG:IFE-1 from the *pie-1* promoter. Whole worm lysates from transgenic lines were incubated with anti-FLAG resin (Sigma) to immunoprecipitate FLG:IFE-1. KX68 is an older transgenic line with the endogenous *ife-1* promoter, KX90-93 are transgenic lines produced using the *pie-1* promoter. The western blot shows significant levels of detection of FLG:IFE-1 in the KX91 and KX92 total lysate lanes. The chimeric protein migrates at the same size as IgG light chain and is difficult to detect in IP lanes. The KX90, KX 91 and KX92 is detected with the anti-FLAG antibody (sigma) more intensely than the other samples. FLG:IFE-1 in the last lane is the BL21 *E.coli* positive control showing migration of the protein at approximately 24 kDa (*).

Figure 6.3

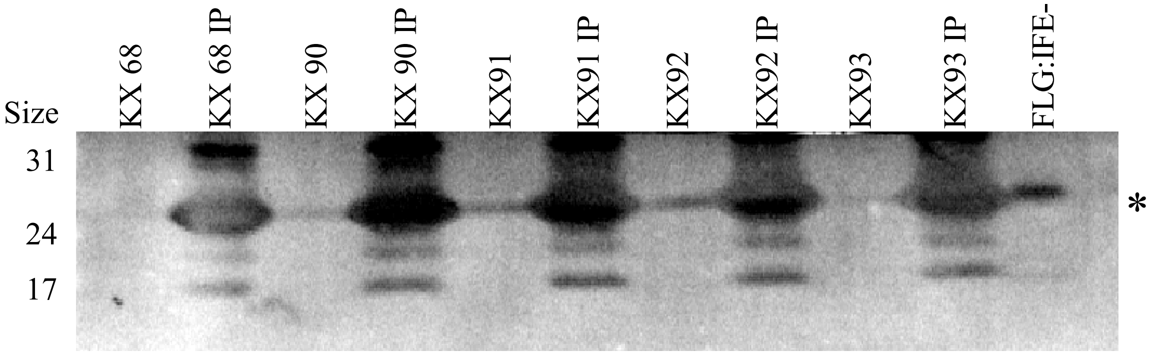
Size
KX 68
KX 68 IP
KX 90
KX 90 IP
KX91
KX91 IP
KX92
KX92 IP
KX93
KX93 IP
FLG:IFE-1
31
24
17
*

been made in the generation of several initial lines for both IFE-1 and IFE-5. Many other authors have noted that expression of transgenic proteins is especially difficult in germline tissue (Mello et al., 1995). Using the *pie-1* promoter elements I was able to successfully drive expression of detectable FLG:IFE-1 protein. Since the expression level is still lower than desired, these strains (KX90-93) may be subjected to integration of the transgene by UV radiation to potentially increase the level of expression. Larger scale worm cultures may also be beneficial to isolate more FLG:IFE-1. The commercial anti-FLAG resin could be used in a column and bound FLG:IFE-1 eluted by a change in pH or by competition with a 3X FLAG peptide. This method would be particularly useful to analyze other protein binding partners of IFE-1.

As described above, plasmids using the same promoters and 3' UTRs have been made incorporating the *ife-5* cDNA in place of *ife-1*. Little is known about the IFE-5 isoform of eIF4E. IFE-1 and IFE-5 share 80% identity in amino acid sequence. The expression of tagged transgenes for these two isoforms would help distinguish the role of IFE-5 in the worm and its difference with IFE-1. In Appendix B, more similarities between IFE-1 and IFE-5 are explored as they correspond to binding PGL-1 in P granules. The expression of those transgenes encoding mutant forms of IFE-1 and IFE-5 discussed in appendix B would facilitate studies on the necessity of P granule localization to IFE-1 function.

The initial expression of FLG:IFE-1 is a substantial accomplishment given the difficulty of expressing transgenes in germline tissue. The transgenic strains I produced will lead to further studies by the lab to understand the patterns of IFE-1 expression, its functional role in fertility, and its association with other proteins and mRNAs. The availability of these strains will lead to experiments performed by future graduate or undergraduate students in the lab as a training experience. Furthermore, my experiments have also provided some optimization of methods for obtaining such germline expression that will be useful to study various other proteins and their roles in translation in the germline.

CHAPTER 7: CONCLUSION

Throughout this dissertation I have elucidated several roles for the germline-specific eIF4E isoform, IFE-1 during gametogenesis in *C.elegans*. IFE-1 is necessary for efficient production of oocytes that maintain chromatin integrity as they grow to full size. Such growth and meiotic integrity allows these oocytes to mature upon fertilization producing viable offspring. A more specific role for IFE-1 in spermatogenesis also has been discovered. IFE-1 is required for secondary spermatocytes to complete cytokinesis during meiosis II. In spermatocytes lacking IFE-1, cytoplasmic contents are not sequestered to the residual body and spermatids do not bud off. In addition, I have demonstrated the requirement for IFE-1 for the efficient translation of stored maternal mRNAs, *pos-1, pal-1, oma-1, mex-1* and *glp-1,* but not for translation of the GAPDH mRNA, *gpd-3.* Interestingly, the relative contribution to the loading of each mRNA into heavy polysomes varies for each mRNA. In addition, some mRNAs are highly dependent on IFE-1 for heavy polysome loading, but are undiminished in their ability to form light polysomes, suggesting that IFE-3 and IFE-5 can initiate a population of these mRNAs, albeit poorly. IFE-1 is also required for efficient translation of the pro-apoptotic mRNA, *ced-4*. There are currently no data formally linking the translation defects to the cellular defects, but it is likely that the decrease in the translation of these and possibly other mRNAs lead to the unique phenotypes observed during gametogenesis.

Several of the mRNAs I chose for analysis reside in P granules. P granules store maternally supplied mRNAs and proteins during oogenesis and embryogenesis

(Kawasaki et al., 1998). IFE-1 is the only isoform of eIF4E that binds to the P granule protein PGL-1 (Amiri et al.). The association of IFE-1 with P granules is thought to facilitate the recruitment of stored mRNAs out of P granules and on ribosomes for translation. This idea is supported by the dependence of P granule associated mRNAs, *pos-1* and *mex-1,* on IFE-1 for efficient translation. In addition to the association with P granules, some fraction of IFE-1 localizes to the soluble portion of the cytoplasm. The IFE-1 molecules not bound to PGL-1 may associate with non-repressed (*oma-1, mex-1,* and *ced-4*) mRNAs as well as those repressed by other means (*pal-1, pos-1, and glp-1*) in the cytoplasm. Thus IFE-1 may have a role in the efficient translation of non-P granule associated mRNAs despite its concentration in these dynamic granules. The association of IFE-1 with P granules may therefore facilitate the stability and storage of the IFE-1 protein, supplying late oocytes with sufficient levels of this unique eIF4E isoform in preparation for the high demands of protein synthesis during oocyte maturation, fertilization, and embryogenesis.

There is precedent for regulated storage and release of eIF4E during late oogenesis. During *Xenopus* oogenesis mRNAs necessary for meiotic maturation are stored in RNPs with the proteins Maskin, eIF4E, and CPEB (Stebbins-Boaz et al., 1999). CPEB binds the CPE sequence in the 3’ UTR. Maskin binds CPEB in addition to the dorsal face of eIF4E. This association of proteins with both the 5’ and 3’ ends of mRNAs represses the recruitment of the pre-initiation complex, as Maskin inhibits the binding of eIF4G to eIF4E. Upon stimulation by the hormone progesterone, CPEB and Maskin become phosphorylated (Barnard et al., 2005). Maskin is released from the complex and CPEB stimulates poly(A) tail elongation through the recruitment of poly(A) polymerase. The dorsal face binding site on eIF4E becomes available for eIF4G binding, initiating the process of recruitment of the mRNA. Both Maskin and eIF4G share a similar amino acid sequence, YXXXXLΦ (X is variable, Φ is hydrophobic), which is responsible for binding eIF4E. This same sequence can be found in other 4E-BPs and is similar in numerous species from mammals to yeast. PGL-1 also contains this consensus sequence that is thought to mediate its binding to IFE-1. In addition, PGL-1 is an RNA binding protein with multiple RGG-box motifs in the C-terminus (Kawasaki et al., 1998). I have suggested that PGL-1 may act in a similar manner as Maskin, inhibiting the translation of mRNAs through its association with IFE-1 (Figure 7.1). However, additional experiments will be necessary to verify this mechanism. If a similar mechanism is used for PGL-1, a stimulus would be needed to release the association between IFE-1 and PGL-1. Evidence exists of similar means of translational repression in gametogenesis by 4E-BPs in various other organisms (Ptushkina et al., 1999; Gingras et al., 2001; Miron et al., 2001). Therefore it is likely that a homologous system exists in *C.elegans*.

This dissertation investigated IFE-1's role in translation of maternal mRNAs. These mRNAs are made and stored in RNPs until the germline isoforms of eIF4E, IFE-1, IFE-3 or IFE-5 recruit them to the ribosomes for translation. This recruitment out of the RNPs to the ribosome is the rate-limiting step in translation (Figure 7.2B, k_1). Furthermore, the rate of the recruitment of the first ribosome to a free mRNA (k_1) differs from the rate of initiation of additional ribosomes to form polysomes (k_2) (Nelson et al., 1987). Results from chapter 5 examining the translation of mRNAs by polysome isolation led us to determine the role of IFE-1 in the translation efficiency of these

Figure 7.1 Repression of mRNAs by PGL-1 and IFE-1. (A) mRNA is stored in P granules and repressed by PGL-1 inhibiting IFG-1 binding to IFE-1. (B) Removal or degradation of PGL-1 frees IFE-1 for recruitment of the mRNA to the pre-initiation complex.

Figure 7.1

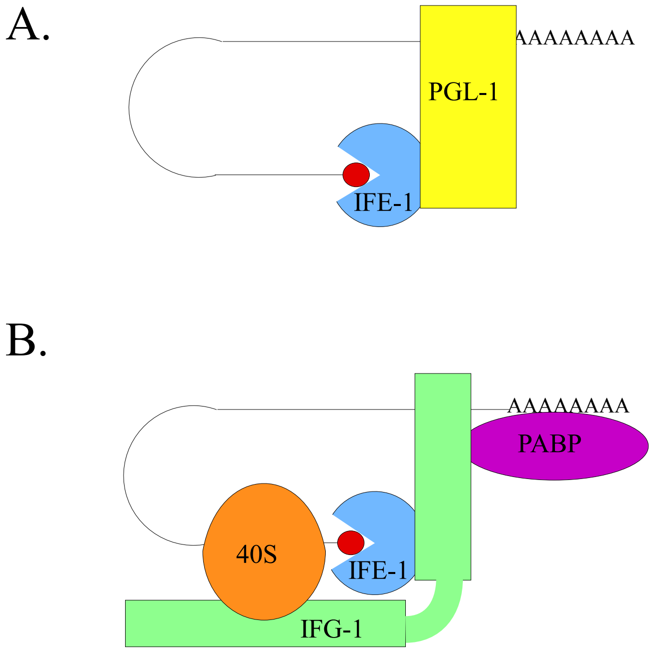
A.
AAAAAAAA
PGL-1
IFE-1
B.
AAAAAAAA
PABP
40S
IFE-1
IFG-1

Figure 7.2 Interpreting the rate of ribosome initiation on mRNAs. (A) This schematic of a 254 nm absorbance profile from a sucrose gradient shows regions of non-translating mRNAs, monosomes (80S), and polysomes. Depicted directly below the profile are mRNAs with the corresponding ribosomes bound for those fractions of the gradient. (B) The rate of initiation of the first ribosome (k1) is generally slower than the rate of reinitiation of ribosome to form polysomes (k2). The mRNA depicted represents a mRNA that utilizes IFE-1 for efficient formation of polysomes, higher rate of initiation indicated by larger, thicker arrow. When IFE-1 is absent, IFE-3 and IFE-5 cannot facilitate the high rate of reinitiation, indicated by smaller, thinner arrow. The primary rate of initiation (k1) does not differ as dramatically in the absence of IFE-1.

Figure 7.2

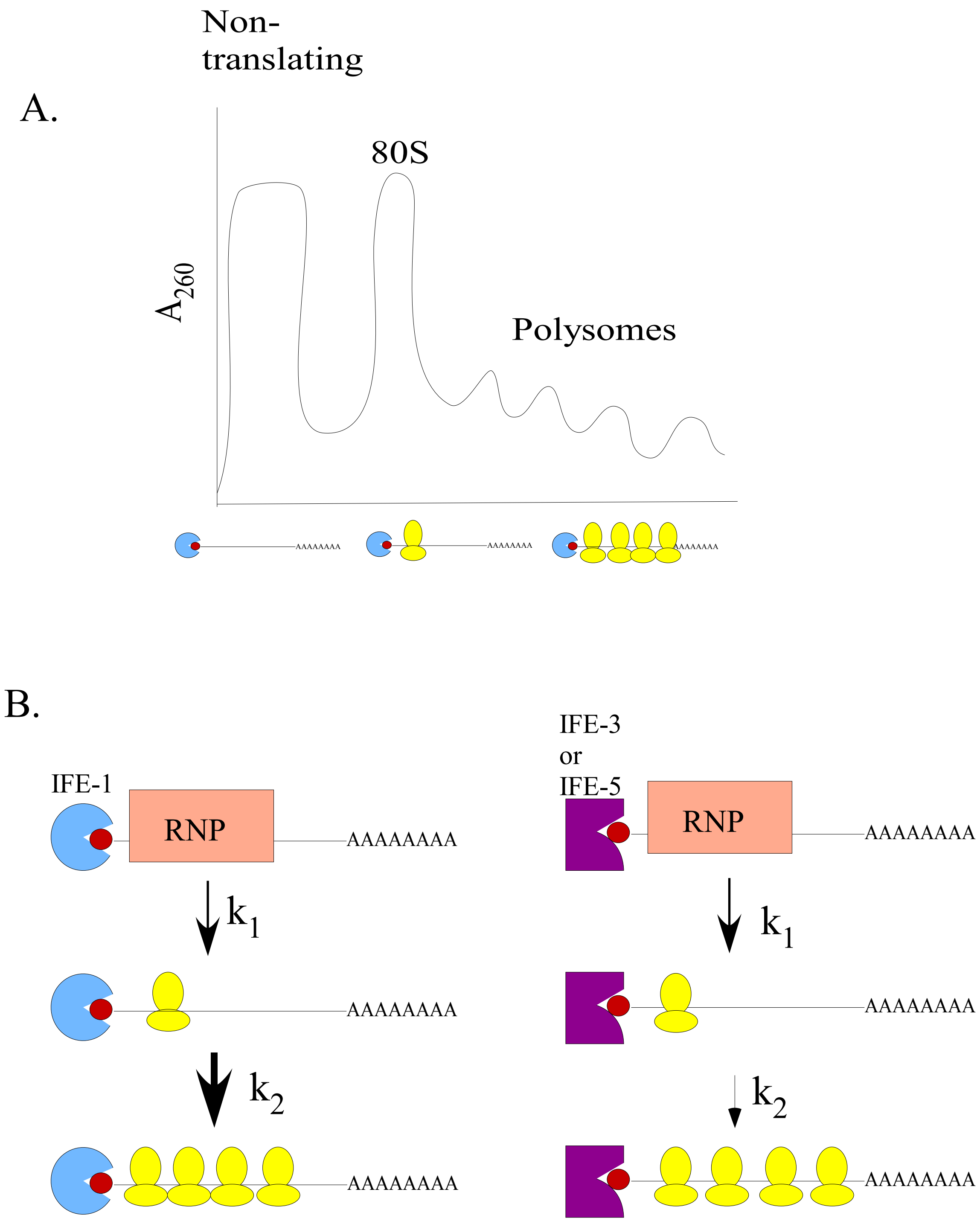
Non-
translating
A.
80S
A_{260}
Polysomes
AAAAAAAA
AAAAAAAA
AAAAAAAA
B.
IFE-1
RNP
AAAAAAAA
k_1
AAAAAAAA
k_2
AAAAAAAA
IFE-3
or
IFE-5
RNP
AAAAAAAA
k_1
AAAAAAAA
k_2
AAAAAAAA

mRNAs. The distribution of *mex-1, oma-1* and *ced-4* mRNA in the sucrose gradients prepared from wild type and *ife-1* worms showed that the absence of IFE-1 removes these mRNAs from polysome fractions, but there is very little change in the fractions from the 80S monosome region. This indicates that IFE-3 and IFE-5 may be able to facilitate inefficient loading of these mRNA to the first ribosome. The reduction in the mRNA distributed in the polysome fractions led us to believe that the efficient loading of these specific mRNAs onto polysomes requires IFE-1. After an initial ribosome has translated the circularized message it dissociates from the complex. It is the rapid re-initiation of these ribosomes that result in polysome formation, and it is the rate of this re-initiation (Figure 7.2B, k_2) that appears to specifically require IFE-1.

The release of the stored mRNAs from RNPs is equally important to the translation of the mRNAs. This was noticed in the evaluation of the translation efficiency of *pos-1, pal-1,* and *glp-1* in the lack of IFE-1. These stored maternal mRNAs are spatially repressed in the embryo by inhibitory proteins binding their 3' UTR. In addition, *glp-1* mRNA is also repressed by GLD-1 in the meiotic region of the gonad. The repression by these elements inhibits the recruitment of these mRNAs to the ribosome through mechanisms not yet fully understood. *pos-1* mRNA is associated with P granules. Since IFE-1 is also found in these dynamic RNPs, IFE-1 may play a role in the recruitment of *pos-1* out of the repression of the mRNA. The unknown mechanism of releasing these mRNAs from RNPs for translation may be facilitated by IFE-1. In the case of these inefficiently translating mRNAs it is apparent that initial recruitment (the rate of initiating the first ribosome) is strongly dependent on IFE-1.

P granules are also found in early spermatocytes and have a similar role for paternal mRNA. PGL-1 is expressed during spermatogenesis and degrades prior to the production of secondary spermatocytes (Amiri et al., 2001). It is possible that IFE-1 also associates with spermatocyte P granules by binding PGL-1 during spermatogenesis. As suggested for oogenesis, PGL-1 may be responsible for repressing the translation of mRNAs bound to IFE-1 during spermatogenesis. PGL-1 degrades after the chromosomes are condensed and transcription is silenced. This degradation may free IFE-1 and associated mRNAs for translation. Our phenotypic data suggest that the mRNAs repressed by IFE-1 and PGL-1 are involved in the transition to mature spermatids. The lack of IFE-1 results in a temperature-sensitive phenotype in which spermatocytes fail to complete cytokinesis. A mutation in the CPEB homolog gene, *cbp-1* results in a similar phenotype. Loss of CPB-1 in *C.elegans* prevents cytokinetic events in primary spermatocytes (Luitjens et al., 2000). Since CBEPs are also involved in translational control of stored mRNAs during oogenesis in various species (i.e. *Xenopus*), it is very likely that CPB-1 is involved in regulating the translation of paternally stored mRNAs during spermatogenesis. In the absence of either of these two proteins, which may have roles in mRNA recruitment during spermatogenesis, spermatocytes fail to complete cytokinesis and prevent the production of mature spermatids. This suggests that cytokinetic events during spermatogenesis are controlled by proteins whose mRNAs are under translational control.

In many organisms the programmed cell death of germ cells regulates the number and quality of gametes produced. In this dissertation I have demonstrated the novel expression of the pro-apoptotic protein, CED-4, in *C.elegans* spermatocytes by immunohistochemistry. To our knowledge, the expression of CED-4 in *C.elegans* spermatocytes has not been addressed prior to my analysis. CED-4 expression is first normally detected prior to meiosis II in wild type primary spermatocytes. Small apoptosome-like structures are localized to the cytoplasm and limited to the primary and secondary spermatocytes in wild type male gonads. The discovery of CED-4 expression in spermatocytes suggests that like other organisms, *C.elegans* may utilize pro-apoptotic proteins for a positive role in spermatogenesis. With the loss of IFE-1, CED-4 was detected earlier in the spermatogenic process. In the previous paragraph I addressed the concept that IFE-1 may be involved in the repression of mRNAs with PGL-1. The *ced-4* mRNA may be among these regulated mRNAs. Our immunostaining results indicate that loss of IFE-1 results in the premature expression or early stabilization of CED-4 protein. The normal onset of CED-4 expression appears to correspond temporally with the degradation of PGL-1 from P-granules. One interpretation of our results is that IFE-1 may bind the methylated cap of *ced-4* and localize the mRNA to an inhibitory complex with PGL-1 (Figure 7.3). When PGL-1 is degraded during pachytene stage, IFE-1 is capable of binding eIF4G (IFG-1) and the pre-initiation complex to promote CED-4 synthesis.

Curiously, our observations demonstrate a positive role for IFE-1 in the translation efficiency of *ced-4* mRNA that appears to contradict the role of IFE-1 in repressing *ced-4* translation. The results from sucrose gradients (Figure 5.7) demonstrated that IFE-1 was required for the efficient loading of *ced-4* mRNA to polysomes. These results suggest that IFE-1 is involved in the activation of *ced-4* translation, not in its repression. To add to the confusion, the mammalian homolog of

Figure 7.3 Proposed mechanism for repression of *ced-4* mRNA in spermatocytes. The *ced-4* mRNA may be repressed early in spermatogenesis through association with IFE-1 and P granules. The binding of IFE-1 to PGL-1 would facilitate repression of translation for the IFE-1 bound *ced-4* mRNA. During late meiotic stages, P granules dissolve and IFE-1 and *ced-4* are released for association with the pre-initiation complex and translation. In the absence of IFE-1 *ced-4* is not as efficiently translated on polysomes.

Figure 7.3

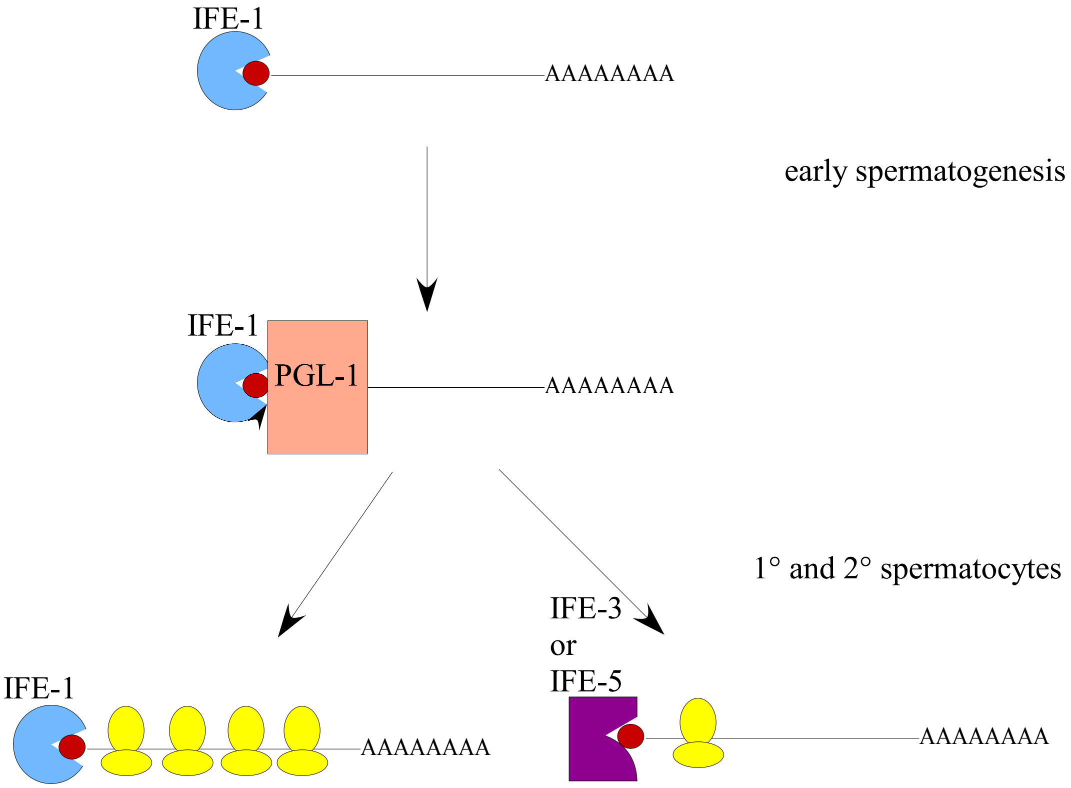
IFE-1
AAAAAAAA
early spermatogenesis
IFE-1
PGL-1
AAAAAAAA
1° and 2° spermatocytes
IFE-3
or
IFE-5
IFE-1
AAAAAAAA
AAAAAAAA

CED-4, Apaf-1 is only translated through the use of an IRES and cap-independent translation(Coldwell et al., 2000; Mitchell et al., 2003). Our data suggest *C.elegans* *ced-4* mRNA is translated largely by cap-dependent mechanism, with IFE-1 facilitating the recruitment to the ribosome. There are two plausible explanations for the inconsistent results. First, samples applied to the sucrose gradients consisted mainly of adult hermaphrodite worms undergoing primarily oogenesis. Since CED-4 is expressed in the female germline and somatic tissue, very little of the mRNA isolated on the sucrose gradients was from spermatocytes. It is noteworthy that IFE-1-deficient oocytes do not undergo more germ cell apoptosis (Figure 3.6), and no increased CED-4 level was observed in the hermaphrodite gonad (Figure 3.7). In order to further analyze the translation of *ced-4* during spermatogenesis, polysomes would need to be isolated from a male population, which is not sustainable in culture nor easily isolated. The second explanation is that *ced-4* mRNA translation can occur by both cap-dependent and cap-independent mechanisms. In Contreras, et al. depletion of the p170 isoform of IFG-1 to impair cap-dependent translation unexpectedly induced CED-4 accumulation in oocytes, demonstrating that *ced-4* mRNA, like Apaf-1 mRNA can be translated via cap-independent mechanisms (Contreras et al., 2008). The partitioning of cap-dependent and cap-independent synthesis of CED-4 may be cell-type specific.

The expression of the pro-apoptotic CED-4 in *C.elegans* spermatogenesis was surprising. Unlike the apoptotic events of *C.elegans* oogenesis, there are no reported accounts of apoptosis during spermatogenesis in nematodes. However, apoptosis does occur during spermatogenesis in mammalian systems (Cagan, 2003; Sutovsky, 2006). Recently it has also been documented that pro-apoptotic proteins, caspase-3 and Apaf-1 are required for the removal of cytoplasmic contents during spermatogenesis in mice and flies (Cagan, 2003). I believe that expression of CED-4 in *C.elegans* spermatocytes is involved in sperm maturation in a similar mechanism. In wild type worms, CED-4 expression and the appearance of apoptosomes commence with the onset of cellular divisions in meiosis I. During meiosis II, the cytoplasmic contents remain in the residual body as the spermatid buds off. CED-4 accumulation and the formation of the apoptosome activate the caspase-3 homolog CED-3. CED-3 is responsible for cleaving various cellular components during apoptosis. The proteolytic activity of CED-3 may be utilized in sequestering cytoplasmic contents to the residual body. CED-3 may also aid in the rapid degradation and engulfment of the residual bodies. Additional experiments involving determination of CED-3 activity in spermatocytes and residual bodies would determine if CED-3 fulfills the same roles as caspase-3 in *Drosophila*.

Currently experiments are underway in the lab to further investigate the role of IFE-1 during gametogenesis. The expression of a transgene linking the *ife-1* cDNA to a sequence encoding a FLAG tag will allow the execution of experiments that were previously not feasible. Due to the high homology between the five eIF4E isoforms, and the low affinity of rabbit anti-IFE-1 isotype-specific antibodies, IFE-1 immunohistochemistry and immunoprecepitations have not been successful. The expression of the FLAG-tagged *ife-1* fusion transgene now permits the use of a highly specific commercial antibody for these experiments. Immunoprecipitation would lead to discovery of additional binding partners for IFE-1 and even potentially resolve new mechanisms in translational control. Even more exciting, the isolation of mRNAs from immunoprecipitated IFE-1 complexes (inhibited and translating) could be subjected to microarray analysis for direct identification of IFE-1 regulated mRNAs. Supporting the results by polysome isolation by sucrose gradients, the specific mRNAs which utilize IFE-1 for recruitment to the ribosome can be determined. These future experiments will lead to understanding the role of tissue-specific eIF4E isoforms in translational control of mRNAs.

The work described in this dissertation supports a unique and unforeseen role for a tissue-specific isoform of eIF4E in the regulation of gene expression. In the scientific community there are many precedents for regulating individual genes at the level of transcription, but little is known mechanistically about regulation at the level of translation initiation. In the development of gametes and early embryogenesis this mode of gene regulation necessarily predominates, and examples of translational control influencing the spatial and temporal expression of protein are being continually discovered. Here I have demonstrated the use of a germline-specific isoform of eIF4E in the translational regulation of several specific mRNAs whose products play vital roles in subsequent development. These results support a role for regulated translation initiation as a controlling mechanism for individual gene expression during cell fate decisions, instead of the previously thought notion of simply globally controlling the synthetic process.

References

Alberts, B. j., Alexander; Lewis, Julian; Raff, Martin; Roberts, Keith; Walter, Peter. (2002). Molecular Biology of the Cell. New York: Garland Science, Taylor and Francis Group.

Ambros, V. (2004). The functions of animal microRNAs. *Nature* **431**, 350-355.

Amiri, A., Keiper, B. D., Kawasaki, I., Fan, Y., Kohara, Y., Rhoads, R. E. and Strome, S. (2001). An isoform of eIF4E is a component of germ granules and is required for spermatogenesis in *C. elegans*. *Development* **128**, 3899-3912.

Arama, E., Agapite, J. and Steller, H. (2003). Caspase activity and a specific cytochrome C are required for sperm differentiation in Drosophila. *Dev Cell* **4**, 687-697.

Barnard, D. C., Cao, Q. and Richter, J. D. (2005). Differential phosphorylation controls Maskin association with eukaryotic translation initiation factor 4E and localization on the mitotic apparatus. *Mol Cell Biol* **25**, 7605-7615.

Bettegowda, A. and Smith, G. W. (2007). Mechanisms of maternal mRNA regulation: implications for mammalian early embryonic development. *Front Biosci* **12**, 3713-3726.

Blumenthal, T. (1998). Gene clusters and polycistronic transcription in eukaryotes. *BioEssays* **20**, 480-487.

Bowerman, B. (1998). Maternal control of pattern formation in early Caenorhabditis elegans embryos. *Curr Top Dev Biol* **39**, 73-117.

Brenner, S. (1974). The genetics of Caenorhabditis elegans. *Genetics* **77**, 71-94.

Cagan, R. L. (2003). Spermatogenesis: borrowing the apoptotic machinery. *Curr Biol* **13**, R600-602.

Chen, J. J. (2007). Regulation of protein synthesis by the heme-regulated eIF2alpha kinase: relevance to anemias. *Blood* **109**, 2693-2699.

Chen, J. J. and London, I. M. (1995). Regulation of protein synthesis by heme-regulated eIF-2 alpha kinase. *Trends Biochem Sci* **20**, 105-108.

Coldwell, M. J., Mitchell, S. A., Stoneley, M., MacFarlane, M. and Willis, A. E. (2000). Initiation of Apaf-1 translation by internal ribosome entry. *Oncogene* **19**, 899-905.

Coldwell, M. J., Hashemzadeh-Bonehi, L., Hinton, T. M., Morley, S. J. and Pain, V. M. (2004). Expression of fragments of translation initiation factor eIF4GI reveals a nuclear localisation signal within the N-terminal apoptotic cleavage fragment N-FAG. *J Cell Sci* **117**, 2545-2555.

Contreras, V., Richardson, M. A., Hao, E. and Keiper, B. D. (2008). Depletion of the cap-associated isoform of translation factor eIF4G induces germline apoptosis in C. elegans. *Cell Death Differ* **15**, 1232-1242.

Crittenden, S. L., Troemel, E. R., Evans, T. C. and Kimble, J. (1994). GLP-1 is localized to the mitotic region of the *C. elegan*s germ line. *Development* **120**, 2901-2911.

Dinkova, T. D., Keiper, B. D., Korneeva, N. L., Aamodt, E. J. and Rhoads, R. E. (2005). Translation of a small subset of Caenorhabditis elegans mRNAs is dependent on a specific eukaryotic translation initiation factor 4E isoform. *Mol Cell Biol* **25**, 100-113.

Edgar, L. G., Wolf, N. and Wood, W. B. (1994). Early transcription in *Caenorhabditis elegans* embryos. *Development* **120**, 443-451.

Erson, A. E. and Petty, E. M. (2008). MicroRNAs in development and disease. *Clin Genet* **74**, 296-306.

Evans (ed.), T. C. (2006). Transformation and microinjection. In *WormBook*, (ed. T. C. e. R. Community): WormBook.

Evans, T. C. and Hunter, C. P. (2005). Translational control of maternal RNAs. In *WormBook*, (ed. T. C. e. R. Community): WormBook.

Fire, A., Xu, S., Montgomery, M. K., Kostas, S. A., Driver, S. E. and Mello, C. C. (1998). Potent and specific genetic interference by double-stranded RNA in *Caenorhabditis elegans*. *Nature* **391**, 806-811.

Garcia, M. A., Meurs, E. F. and Esteban, M. (2007). The dsRNA protein kinase PKR: virus and cell control. *Biochimie* **89**, 799-811.

Gebauer, F. and Hentze, M. W. (2004). Molecular mechanisms of translational control. *Nat Rev Mol Cell Biol* **5**, 827-835.

Gingras, A. C., Raught, B., Gygi, S. P., Niedzwiecka, A., Miron, M., Burley, S. K., Polakiewicz, R. D., Wyslouch-Cieszynska, A., Aebersold, R. and Sonenberg, N. (2001). Hierarchical phosphorylation of the translation inhibitor 4E-BP1. *Genes & Development* **15**, 2852-2864.

Gingras, A.-C., Raught, B. and Sonenberg, N. (1999). eIF4 initiation factors: Effectors of mRNA recruitment to ribosomes and regulators of translation. *Annu. Rev. Biochem.* **68**, 913-963.

Giorgini, F., Davies, H. G. and Braun, R. E. (2002). Translational repression by MSY4 inhibits spermatid differentiation in mice. *Development* **129**, 3669-3679.

Gonczy, P. and Rose, L. S. (2005). Asymmetric cell division and axis formation in the embryo. *WormBook*, 1-20.

Govindan, J. A. and Greenstein, D. (2007). Embryogenesis: anchors away! *Curr Biol* **17**, R890-892.

Greenstein, D. (2005). Control of oocyte meiotic maturation and fertilization. In *WormBook*, (ed. T. C. e. R. Community): WormBook.

Gumienny, T. L., Lambie, E., Hartwieg, E., Horvitz, H. R. and Hengartner, M. O. (1999). Genetic control of programmed cell death in the Caenorhabditis elegans hermaphrodite germline. *Development* **126**, 1011-1022.

Gupta, G. S. (2005). Proteomics of Spermatogenesis. New York: Spinger.

Gur, Y. and Breitbart, H. (2008). Protein synthesis in sperm: dialog between mitochondria and cytoplasm. *Mol Cell Endocrinol* **282**, 45-55.

Hang, J. S., Grant, B. D. and Singson, A. (2008). Meiotic maturation: receptor trafficking is the key. *Curr Biol* **18**, R416-418.

He, L. and Hannon, G. J. (2004). MicroRNAs: small RNAs with a big role in gene regulation. *Nat Rev Genet* **5**, 522-531.

Henderson, M. A., Cronland, E., Dunkelbarger, S., Contreras, V., Strome, S. and Keiper, B. D. (2009). A germline-specific isoform of eIF4E (IFE-1) is required for efficient translation of stored mRNAs and maturation of both oocytes and sperm. *J Cell Sci* **122**, 1529-1539.

Hengartner, M. O. (2000). The biochemistry of apoptosis. *Nature* **407**, 770-776.

Holcik, M. and Sonenberg, N. (2005). Translational control in stress and apoptosis. *Nat Rev Mol Cell Biol* **6**, 318-327.

Honarpour, N., Du, C., Richardson, J. A., Hammer, R. E., Wang, X. and Herz, J. (2000). Adult Apaf-1-deficient mice exhibit male infertility. *Dev Biol* **218**, 248-258.

Huang, N. N., Mootz, D. E., Walhout, A. J., Vidal, M. and Hunter, C. P. (2002). MEX-3 interacting proteins link cell polarity to asymmetric gene expression in Caenorhabditis elegans. *Development* **129**, 747-759.

Hubbard, E. J. A. and Greenstein, D. (2005). Introduction to the germ line. In *WormBook*, (ed. T. C. e. R. Community): WormBook.

Hunter, C. P. and Kenyon, C. (1996). Spatial and temporal controls target pal-1 blastomere-specification activity to a single blastomere lineage in C. elegans embryos. *Cell* **87**, 217-226.

Johnstone, O. and Lasko, P. (2001). Translational regulation and RNA localization in Drosophila oocytes and embryos. *Annu Rev Genet* **35**, 365-406.

Jud, M. C., Czerwinski, M. J., Wood, M. P., Young, R. A., Gallo, C. M., Bickel, J. S., Petty, E. L., Mason, J. M., Little, B. A., Padilla, P. A. and Schisa, J. A. (2008). Large P body-like RNPs form in C. elegans oocytes in response to arrested ovulation, heat shock, osmotic stress, and anoxia and are regulated by the major sperm protein pathway. *Dev Biol* **318**, 38-51.

Kawasaki, I., Shim, Y. H., Kirchner, J., Kaminker, J., Wood, W. B. and Strome, S. (1998). PGL-1, a predicted RNA-binding component of germ granules, is essential for fertility in *C. elegans*. *Cell* **94**, 635-645.

Keiper, B. D., Lamphear, B. J., Deshpande, A. M., Jankowska-Anyszka, M., Aamodt, E. J., Blumenthal, T. and Rhoads, R. E. (2000). Functional characterization of five eIF4E isoforms in Caenorhabditis elegans. *Journal of Biological Chemistry* **275**, 10590-10596.

Kimble, J. and Crittenden, S. L. (2007). Controls of germline stem cells, entry into meiosis, and the sperm/oocyte decision in Caenorhabditis elegans. *Annu Rev Cell Dev Biol* **23**, 405-433.

Kimble, J., Edgar, L. and Hirsh, D. (1984). Specification of male development in Caenorhabditis elegans: the fem genes. *Dev. Biol.* **105**, 234-239.

Kleene, K. C. (2003). Patterns, mechanisms, and functions of translation regulation in mammalian spermatogenic cells. *Cytogenet. Genome Res.* **103**, 217-224.

L'Hernault, S. W. (2006). Spermatogenesis. In *WormBook*, (ed. T. C. e. R. Community): WormBook.

L'Hernault, S. W. (2009). The genetics and cell biology of spermatogenesis in the nematode C. elegans. *Mol Cell Endocrinol* **306**, 59-65.

Luitjens, C., Gallegos, M., Kraemer, B., Kimble, J. and Wickens, M. (2000). CPEB proteins control two key steps in spermatogenesis in C. elegans. *Genes Dev* **14**, 2596-2609.

Mamane, Y., Petroulakis, E., Rong, L., Yoshida, K., Ler, L. W. and Sonenberg, N. (2004). eIF4E--from translation to transformation. *Oncogene* **23**, 3172-3179.

Mello, C. and Fire, A. (1995). DNA transformation. *Methods Cell Biol* **48**, 451-482.

Mello, C. C., Kramer, J. M., Stinchcomb, D. and Ambros, V. (1991). Efficient gene transfer in C.elegans: extrachromosomal maintenance and integration of transforming sequences. *Embo J* **10**, 3959-3970.

Merrick, W. C. (1992). Mechanism and regulation of eukaryotic protein synthesis. *Microbiol. Reviews* **56**, 291-315.

Miller, M. A., Nguyen, V. Q., Lee, M. H., Kosinski, M., Schedl, T., Caprioli, R. M. and Greenstein, D. (2001). A sperm cytoskeletal protein that signals oocyte meiotic maturation and ovulation. *Science* **291**, 2144-2147.

Miron, M., Verdu, J., Lachance, P. E., Birnbaum, M. J., Lasko, P. F. and Sonenberg, N. (2001). The translational inhibitor 4E-BP is an effector of PI(3)K/Akt signalling and cell growth in Drosophila. *Nat Cell Biol* **3**, 596-601.

Mitchell, S. A., Spriggs, K. A., Coldwell, M. J., Jackson, R. J. and Willis, A. E. (2003). The Apaf-1 internal ribosome entry segment attains the correct structural conformation for function via interactions with PTB and unr. *Mol Cell* **11**, 757-771.

Miyoshi, H., Dwyer, D. S., Keiper, B. D., Jankowska-Anyszka, M., Darzynkiewicz, E. and Rhoads, R. E. (2002). Discrimination between mono- and trimethylated cap structures by two isoforms of *Caenorhabditis elegans* eIF4E. *EMBO J.* **21**, 4680-4690.

Murray, A. W. (2004). Recycling the cell cycle: cyclins revisited. *Cell* **116**, 221-234.

Napoli, I., Mercaldo, V., Boyl, P. P., Eleuteri, B., Zalfa, F., De Rubeis, S., Di Marino, D., Mohr, E., Massimi, M., Falconi, M., Witke, W., Costa-Mattioli, M., Sonenberg, N., Achsel, T. and Bagni, C. (2008). The fragile X syndrome protein represses activity-dependent translation through CYFIP1, a new 4E-BP. *Cell* **134**, 1042-1054.

Nelson, E. M. and Winkler, M. M. (1987). Regulation of mRNA entry into polysomes. *J Biol Chem* **262**, 11501-11506.

Nelson, M. R., Leidal, A. M. and Smibert, C. A. (2004). Drosophila Cup is an eIF4E-binding protein that functions in Smaug-mediated translational repression. *Embo J* **23**, 150-159.

Ogura, K., Kishimoto, N., Mitani, S., Gengyo-Ando, K. and Kohara, Y. (2003). Translational control of maternal glp-1 mRNA by POS-1 and its interacting protein SPN-4 in Caenorhabditis elegans. *Development* **130**, 2495-2503.

Portman, D. S. (2006). Profiling C. elegans gene expression with DNA microarrays. *WormBook*, 1-11.

Prevot, D., Darlix, J. L. and Ohlmann, T. (2003). Conducting the initiation of protein synthesis: the role of eIF4G. *Biol Cell* **95**, 141-156.

Proud, C. G. (2006). Regulation of protein synthesis by insulin. *Biochem Soc Trans* **34**, 213-216.

Ptushkina, M., von der Haar, T., Karim, M. M., Hughes, J. M. and McCarthy, J. E. (1999). Repressor binding to a dorsal regulatory site traps human eIF4E in a high cap-affinity state. *Embo J* **18**, 4068-4075.

Puri, P. L. M., T.K.; Levrero, M.; Giordano, M. (1999). The Intrinsic Cell Cycle: from Yeast to Mammals. In *The Molecular Basis of Cell Cycle and Growth Control* (ed. G. S. B. Stein, R.; Giordano, A.; Denhardt, D.T.), pp. 15-79. New York: Wiley-Liss.

Richter, J. D. (2007). CPEB: a life in translation. *Trends Biochem Sci* **32**, 279-285.

Riddle, D. L., Blumenthal, T., Meyer, B. J. and Priess, J. R. (1997). Chapter 1: Introduction to *C. elegans*. In *C. ELEGANS II* (eds D. L. Riddle T. Blumenthal B. J. Meyer and J. R. Priess), 1-22pp. Cold Spring Harbor, NY: Cold Spring Harbor Laboratory Press.

Rosenwald, I. B., Lazaris-Karatzas, A., Sonenberg, N. and Schmidt, E. V. (1993). Elevated levels of cyclin D1 protein in response to increased expression of eukaryotic initiation factor 4E. *Mol. Cell. Biol.* **13**, 7358-7363.

Sarnow, P., Cevallos, R. C. and Jan, E. (2005). Takeover of host ribosomes by divergent IRES elements. *Biochem Soc Trans* **33**, 1479-1482.

Schafer, W. R. (2006). Neurophysiological methods in C. elegans: an introduction. In *WormBook*, (ed. T. C. e. R. Community): WormBook.

Schisa, J. A., Pitt, J. N. and Priess, J. R. (2001). Analysis of RNA associated with P granules in germ cells of C. elegans adults. *Development* **128**, 1287-1298.

Schmelzle, T. and Hall, M. N. (2000). TOR, a central controller of cell growth. *Cell* **103**, 253-262.

Schubert, C. M., Lin, R., de Vries, C. J., Plasterk, R. H. and Priess, J. R. (2000). MEX-5 and MEX-6 function to establish soma/germline asymmetry in early C. elegans embryos. *Mol Cell* **5**, 671-682.

Seydoux, G. and Strome, S. (1999). Launching the germline in *Caenorhabditis elegans*: regulation of gene expression in early germ cells. *Development* **126**, 3275-3283.

Sonenberg, N. and Hinnebusch, A. G. (2009). Regulation of translation initiation in eukaryotes: mechanisms and biological targets. *Cell* **136**, 731-745.

Spriggs, K. A., Bushell, M., Mitchell, S. A. and Willis, A. E. (2005). Internal ribosome entry segment-mediated translation during apoptosis: the role of IRES-trans-acting factors. *Cell Death Differ* **12**, 585-591.

Stebbins-Boaz, B., Cao, Q., de Moor, C. H., Mendez, R. and Richter, J. D. (1999). Maskin is a CPEB-associated factor that transiently interacts with elF-4E. *Mol. Cell* **4**, 1017-1027.

Strome, S. (2005). Specification of the germ line. In *WormBook*, (ed. T. C. e. R. Community): WormBook.

Sutovsky, P. M., Gaurishankar. (2006). Mammalian spermatogenesis and sperm structure: anantomical and compartmental analysis. In *The Sperm Cell* (ed. C. B. De Jonge, Christopher). Cambridge: Cambridge University Press.

Syntichaki, P., Troulinaki, K. and Tavernarakis, N. (2007). eIF4E function in somatic cells modulates ageing in Caenorhabditis elegans. *Nature* **445**, 922-926.

Tabara, H., Hill, R. J., Mello, C. C., Priess, J. R. and Kohara, Y. (1999). pos-1 encodes a cytoplasmic zinc-finger protein essential for germline specification in C. elegans. *Development* **126**, 1-11.

Wek, R. C. and Cavener, D. R. (2007). Translational control and the unfolded protein response. *Antioxid Redox Signal* **9**, 2357-2371.

Wek, R. C., Jiang, H. Y. and Anthony, T. G. (2006). Coping with stress: eIF2 kinases and translational control. *Biochem Soc Trans* **34**, 7-11.

Wolgemuth, D. J., Laurion, E. and Lele, K. M. (2002). Regulation of the mitotic and meiotic cell cycles in the male germ line. *Recent Prog Horm Res* **57**, 75-101.

Wolke, U., Jezuit, E. A. and Priess, J. R. (2007). Actin-dependent cytoplasmic streaming in C. elegans oogenesis. *Development* **134**, 2227-2236.

Yamamoto, I., Kosinski, M. E. and Greenstein, D. (2006). Start me up: cell signaling and the journey from oocyte to embryo in C. elegans. *Dev Dyn* **235**, 571-585.

Zannoni, S., L'Hernault, S. W. and Singson, A. W. (2003). Dynamic localization of SPE-9 in sperm: a protein required for sperm-oocyte interactions in Caenorhabditis elegans. *BMC Dev Biol* **3**, 10.

Zhou, Z., Hartwieg, E. and Horvitz, H. R. (2001). CED-1 is a transmembrane receptor that mediates cell corpse engulfment in C. elegans. *Cell* **104**, 43-56.

APPENDIX A: ATTEMPTS TO ASSAY PGL-1 AND IFE-1 BINDING *IN VITRO*

Introduction

IFE-1 and IFE-5 are both expressed in the germline and are 80% identical at the amino acid level. Both isoforms are able to bind mono- and tri-methylated cap structures, while the third germline isoform, IFE-3, cannot (Keiper et al., 2000). Despite the similarities, IFE-1 associates with P granules by binding to PGL-1, but IFE-5 does not bind PGL-1 (Amiri et al., 2001). I have hypothesized that it is this association with PGL-1 that contributes to the role of IFE-1 in translational control of stored maternal mRNAs both in and out of P granules. To further investigate the role of PGL-1 binding, site-directed mutations have been made in IFE-1. The targeted region was the dorsal face of the putative IFE-1 structure that has been proposed in all eIF4Es to bind eIF4G and 4E-BPs (Ptushkina et al., 1999; Miyoshi et al., 2002). To assess whether this surface also mediates PGL-1 binding, as well as determine the specificity for IFE-1 (and not IFE-5), three residues were switched to their IFE-5 counterparts, and entire helices swapped between isoforms. Pull down assays using tagged, recombinant IFEs or PGL-1, as well as co-immunoprecipitations (co-IPs) were attempted to establish a specific protein-protein binding assay. Unfortunately, substantial non-specific interactions and/or inefficient association of the recombinant proteins called into question the methods implemented.

Results

The amino acid sequences of IFE-1 and IFE-5 are very homologous, particularly in the dorsal face of the protein. Figure A.1A shows the sequence for amino acid residues 40-59 in both IFE-1 and IFE-5. This region forms one of the three alpha helices on the dorsal face of this eIF4E isoform (Figure A.1B). This portion of the protein is proposed to be responsible for the binding of eIF4G and 4E-BPs in other organisms (Ptushkina et al., 1999). I proposed that PGL-1 may also utilize this dorsal helix for binding IFE-1. In this region of the proteins there are only 3 residues that differ between the IFE-1 and IFE-3 (Figure A.1A). Since it has been shown that IFE-1 can bind PGL-1, while IFE-5 cannot, I have made site-directed mutations that swapped the two sequences. Therefore, it was hypothesized that if the new IFE-1 mutant could not bind PGL-1 and the IFE-5 mutant could, then these IFE-1 residues are essential and discriminatory for association of this unique eIF4E isoform with P granules through binding PGL-1.

In order to evaluate the binding of the mutants, a method was required with which I could easily show the association with PGL-1 with IFE-1. In addition, I included binding IFE-1 to IFG-1 to investigate the potential use of these residues in binding the pre-initiation complex. In figure A.2, IFE-1, PGL-1, and IFG-1 were synthesized in rabbit reticulysate in the presence of ^{35}S-Methionine (indicated by “total” sample). The IFE-1 protein was fused to a 6X-Histidine tag. Using Ni-agarose resin to bind the histidine tag, the IFE-1 sample was successfully retained. Unfortunately, PGL-1 was not bound by the resin through binding the IFE-1 protein. When IFE-1 and IFG-1 were co-incubated with Ni-agarose, IFG-1 was found with IFE-1 in the bound fraction. However, IFG-1 also bound non-specifically to the resin in the absence of IFE-1.

Figure A.1 Site-directed mutations introduced into the dorsal face helix of IFE-1. (A) Amino acid sequence of residues 40-59 of IFE-1 and IFE-5. Boxes show the few differences in these very homologous iosforms. (B) Ribbon structure of IFE-1 with residues targeted for mutation marked. All three amino acids are on the same alpha helix of the dorsal face with side chains protruding out of the protein. The structure was synthesized from the coordinates of the IFE-5 structure presented in Miyoshi et al. (Miyoshi et al., 2002). The IFE-1 structure was fit to the same structure using Molecular Dynamics Software by Dr. Brett Keiper.

Figure A.1

A.

45 50 55

IFE-1 TFNTVSEFWALYDAIRPPSG
IFE-5 TFNTVPEFWAFYDAILPPSG

B.

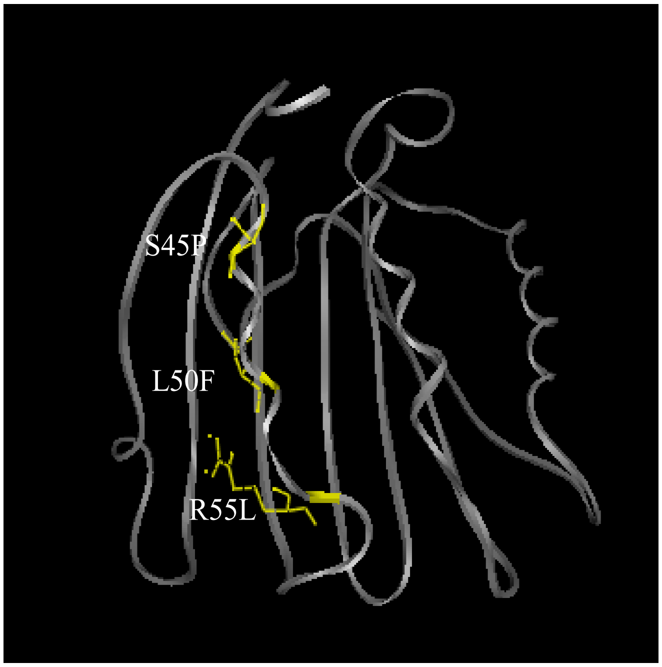
S45P
L50F
R55L

Figure A.2 Binding of PGL-1 to His-IFE-1. ^{35}S-Methionine-labeled recombinant PGL-1, His$_6$-IFE-1 and IFG-1 are shown in the first three lanes. Ni-agarose was used to isolate the His$_6$-IFE-1 and its bound proteins. PGL-1 failed to associate with the His$_6$-IFE-1. IFG-1 was found associated with His$_6$-IFE-1 isolated by Ni-agarose, but was also bound by the resin alone. This indicates non-specific binding of IFG-1 to Ni-agarose and a lack of PGL-1 association of the recombinant proteins under these conditions.

Figure A.2

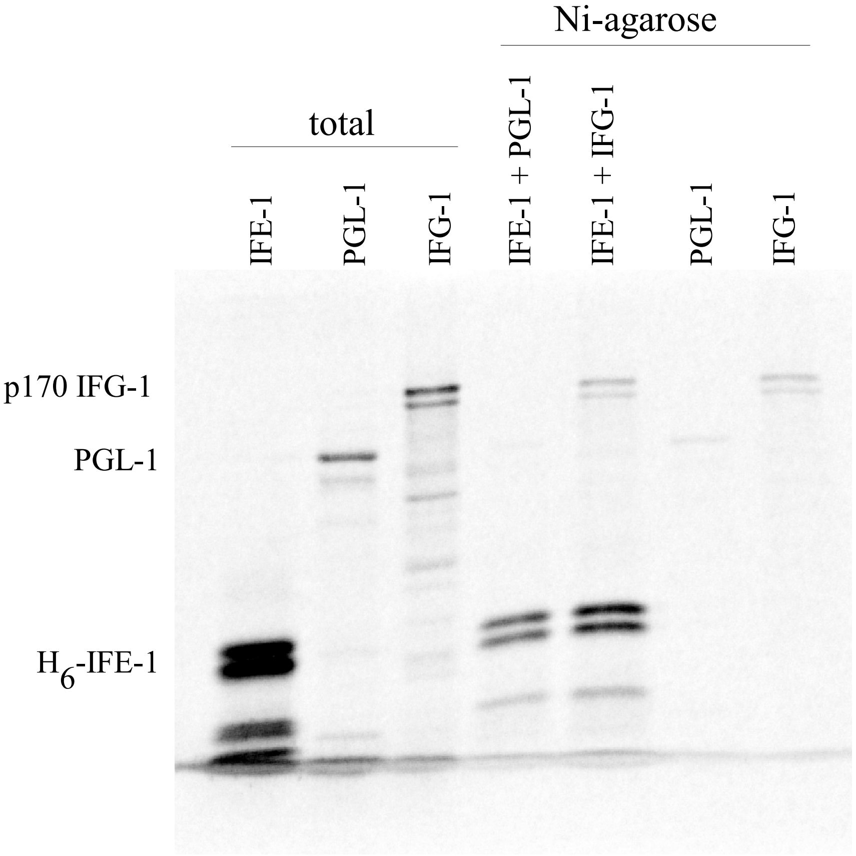
Ni-agarose
total
IFE-1
PGL-1
IFG-1
IFE-1 + PGL-1
IFE-1 + IFG-1
PGL-1
IFG-1
p170 IFG-1
PGL-1
H6-IFE-1

Since work presented in Amiri et al. successfully showed that only the IFE-1 isoform bound PGL-1, I decided to follow the experimental procedure in this publication (Amiri et al., 2001). GST-PGL-1 and GST were made in BL21 *E.coli* cells and bound to glutathione-agarose beads. ^{35}S-IFE-1 was incubated with the GST-PGL-1 and GST beads. After the beads where washed with various salt and detergent-containing buffers, the samples were eluted with SDS and resolved on a SDS-PAGE gel. Phosphorimage exposure of radiolabeled proteins showed non-specific binding of ^{35}S-IFE-1 to GST, regardless of the salt condition (Figure A.3 and Table A.1). A substantial enrichment of labeled IFE-1 was observed under wash conditions A, B, and C. However, significant non-specific binding of IFE-1 to GST was observed in most cases. The binding of IFE-1 was lost in 0.05% SDS washes from GST and GST-PGL-1. These and numerous other sets of binding and wash conditions were implemented, and found to be unsatisfactory to clearly demonstrate specific IFE-1-PGL-1 binding using affinity resins.

In an attempt to avoid non-specific binding, another approach with a potentially more specific binding strategy was tried, that of co-IPs. PGL-1, IFG-1 where made in rabbit reticulysate with ^{35}S-Methionine and incubated with recombinant, FLG:IFEs made in BL21 *E.coli* cells. The anti-FLAG antibody (Cell Signaling) was pre-bound to Sepharose A beads and exposed to the protein solution for precipitation of the complex. Figure A.4A shows that no detectable precipitation of the radiolabeled proteins with FLG:IFE-1 was observed. Unlike previous attempts, non-specific binding was not observed. Western blots of additional IP experiments using this anti-FLAG antibody (Cell Signaling) suggested that the recombinant FLG:IFE-1 was not precipitated by this antibody and resin for reasons that are unclear (data not shown).

Figure A.3 Binding of ^{35}S-IFE-1 to GST-PGL-1. This gel show the isolation of ^{35}S-IFE-1 isolated from glutathione-agarose resin bound to GST-PGL-1 or GST at various wash conditions. In low salt wash conditions ^{35}S-IFE-1 binds non-specifically to GST (A). Various wash conditions are shown on Table B.1. The addition of 0.05% SDS removed all ^{35}S-IFE-1 binding, including to GST-PGL-1 (buffers D and E). The remaining low and high salt conditions failed to fully prevent non-specific association between ^{35}S-IFE-1 and the GST resin.

Figure A.3

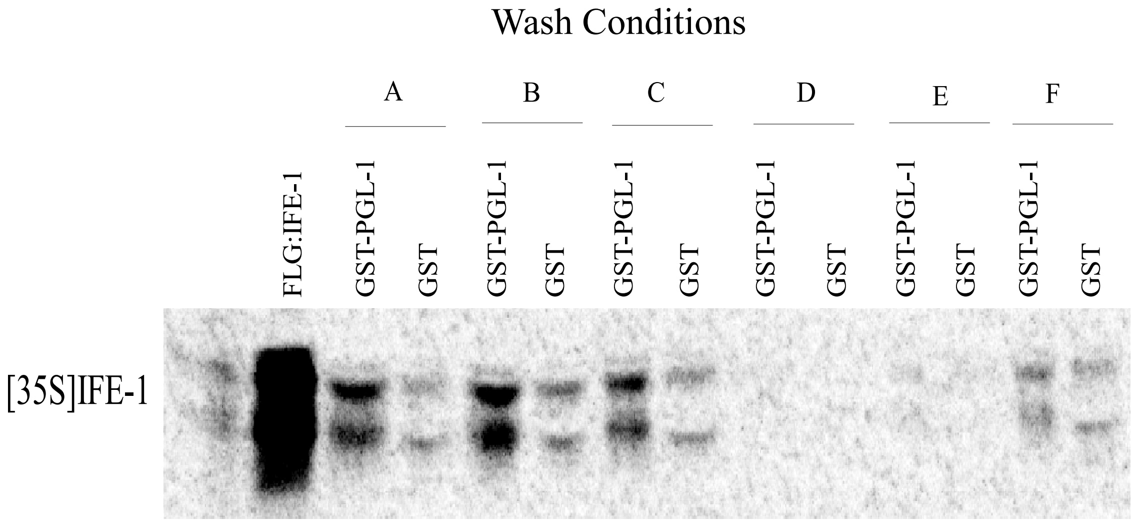
Wash Conditions
A
B
C
D
E
F
FLG:IFE-1
GST-PGL-1
GST
GST-PGL-1
GST
GST-PGL-1
GST
GST-PGL-1
GST
GST-PGL-1
GST
GST-PGL-1
GST
[35S]IFE-1

Table A.1 Buffers for washes of GST-PGL-1 and GST resins. This table shows the conditions of the wash buffers for experiments in Figure B.2.

Table A.1

Buffer	Contents:	
A	100 mM NaCl 400 mM KCl 20 mM Hepes pH 7.4	0.5% non-fat dry milk 5 mM DTT
B	100 mM NaCl 900 mM KCl 20 mM Hepes pH 7.4	0.5% non-fat dry milk 5 mM DTT
C	100 mM NaCl 400 mM KCl 20 mM Hepes pH 7.4	0.5% non-fat dry milk 5 mM DTT 0.5% Tween
D	100 mM NaCl 20 mM Hepes pH 7.4 0.5% non-fat dry milk	5 mM DTT 0.05% SDS
E	100 mM NaCl 400 mM KCl 20 mM Hepes pH 7.4	0.5% non-fat dry milk 5 mM DTT 0.05% SDS
F (BSA was used to block non-specific binding of resin)	100 mM NaCl 400 mM KCl 20 mM Hepes pH 7.4	0.5% non-fat dry milk 5 mM DTT

Additional anti-FLAG antibodies are commercially available and another supplier was tested. With a review of current literature I decided that the Sigma anti-FLAG resin would be most appropriate. In this resin, the anti-FLAG antibody is covalently bound to agarose beads reducing the number of steps of the experiment. Figure A.4B shows successful isolation of FLG:IFE-1 and FLG-IFE-5 using the anti-FLAG resin. PGL-1 was not bound to this resin non-specifically. However, PGL-1 also failed to precipitate with the FLG:IFE-1. Use of more mild washes and various salt and detergent concentrations eventually allowed co-precipitation with FLG:IFE-1, but those conditions were accompanied by non-specific PGL-1 binding to the resin. Clearly additional optimization will be needed to efficiently assay recombinant IFE-1 and PGL-1 binding to one another under controlled *in vitro* conditions.

Conclusion

The unique differences that allow IFE-1 to associate with P granules, while IFE-5 does not, must exist in the primary amino acid sequence of each eIF4E isoform. By evaluating the role of just three residues of alpha helix it is conceivable that the differences between these proteins can be discovered. The importance of sequence homology of the dorsal face has been determined through the binding of 4E-BPs and eIF4G to eIF4E isoforms in other organisms (Ptushkina et al., 1999). Binding of these proteins to eIF4E controls protein synthesis mediated by the cap-dependent mechanism. The identification of unique residues in IFE-1 that mediate translational control of stored maternal mRNAs would support the role of germline specific eIF4E isoforms. The creation of site-directed mutants may distinguish between protein binding partners for

Figure A.4 Co-immunoprecepitations using anti-FLAG antibodies. (A) Co-IPs of bacterial-made recombinant FLG:IFE-1 and FLG:IFE-5 with 35S-PGL-1 or 35S-IFG-1. Anti-FLAG antibody (Cell Signaling). (B) Co-IPs of 35S-PGL-1 with 35S-IFE-1 and 35S-IFE-5. The first 3 lanes are samples of total protein. Subsequent lanes indicate products sequestered by anti-FLAG resin (Sigma). Resin from Sigma was able to precipitate FLG:IFEs but did not co-precipitate detectable PGL-1.

Figure A.4

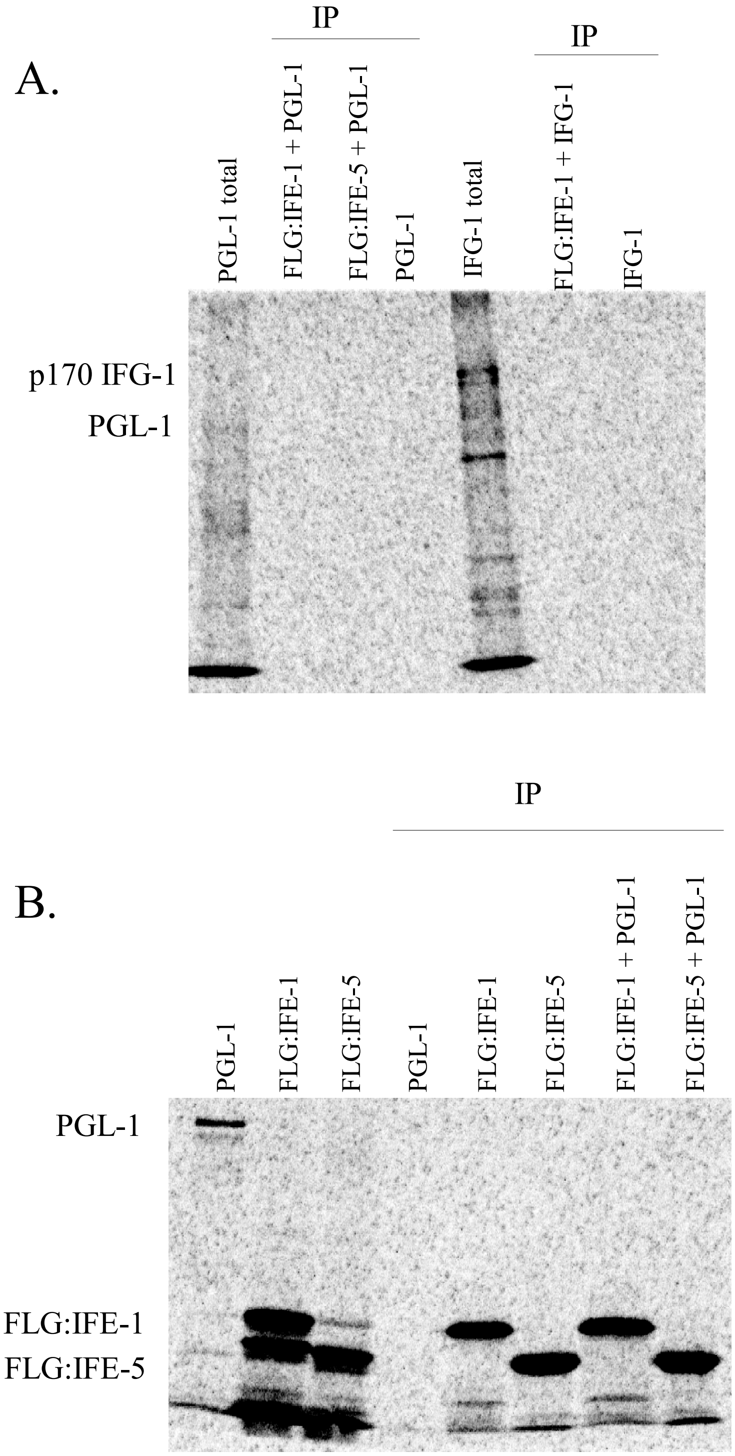
A.
IP
IP
PGL-1 total
FLG:IFE-1 + PGL-1
FLG:IFE-5 + PGL-1
PGL-1
IFG-1 total
FLG:IFE-1 + IFG-1
IFG-1
p170 IFG-1
PGL-1
B.
IP
PGL-1
FLG:IFE-1
FLG:IFE-5
PGL-1
FLG:IFE-1
FLG:IFE-5
FLG:IFE-1 + PGL-1
FLG:IFE-5 + PGL-1
PGL-1
FLG:IFE-1
FLG:IFE-5

individual IFEs and are potentially quite useful to determine isoform-specific translation complexes. Preventing progress in this study, however, is the lack of a simple *in vitro* method to efficiently determine PGL-1-IFE-1 binding. Work in the lab will continue to pursue this study using further optimization of the binding assay, perhaps by addition of native worm extracts or column elution instead of the batch binding. As I have now successfully expressed the Flag-tagged IFEs in transgenic worms, it may ultimately be easier to carry out such binding experiments *in vivo* (see chapter 6).

APPENDIX B: DISRUPTION OF IFG-1 GENE EXPRESSION USING A TRANSPOSABLE ELEMENT INSERTION

Introduction

The formation of the pre-initiation complex is essential for the recruitment of mRNA to the ribosome. In addition to eIF4E and its influence on translational control, as described in the previous chapters, other translation factors are required for the formation of the pre-initiation complex. The translation initiation factor 4G (eIF4G) is the scaffolding protein that connects eIF4E and the methylated cap of mRNA to the ribosomal subunit. In *C.elegans* eIF4G exists as two isoforms derived from the same gene, termed IFG-1 p170 and p130 (Contreras et al., 2008). Recent studies from our lab showed that these isoform differ in the N-terminus and the ability to bind the eIF4E isoforms. The p170 eIF4G isoform has the complete N-terminal sequence and has been shown to associated with m^7G-cap affinity column, indicating that p170 binds one or more IFE proteins. The shorter p130 isoform lacks the N-terminal region and does not bind the IFEs. Further data from this published study by Mr. Vince Contreras allowed us to suggest that p170 is utilized in cap-dependent translation, while p130 is utilized in cap-independent translation.

The published study utilized RNA interference (RNAi) to knock down levels of p170 in *C.elegans*. Interestingly, the prominent phenotype observed affected fertility almost exclusively, which was impaired due to the lack of late stage oocytes. Depletion of cap-dependent p170 stimulated germline apoptotic events in the hermaphrodite gonad approximately eight-fold, resulting in extremely low oocyte production (Contreras et al., 2008). In mammalian systems cap-independent translation is utilized during apoptosis to promote the synthesis of proapoptotic factors like Apaf-1. In the *C.elegans* gonad the reduction of p170 resulted in increased Apaf-1 (CED-4) expression, presumably via cap-independent translation. Since both isoforms of IFG-1 are derived from the same gene it is not possible to knock down p130 without also reducing levels of p170. Thus, to learn more about the roles of these two isoforms, more sophisticated genetic means are being developed to enhance or suppress the expression of p170 and p130 IFG-1 independently.

Recently transposons have been utilized as a method to direct insertional mutations into genes. The transposon sequence can interrupt the production of a viable protein resulting in a new phenotype. The insertion of a known transposon sequence facilitates the tracking of the insertion and simplifies the screening of mutants. We were fortunate to obtain a *C.elegans* mutant isolate that bears the *Drosophila* Mos transposon in the middle of the *ifg-1* gene. The insertion dramatically reduces, but does not abolish, expression of IFG-1 isoforms. Using this strain I show preliminary evidence that this disruption in the *ifg-1* results in a form of temperature-sensitive sterility and increases germ cell death.

Results

As presented in Granger et al., over 600 lines were created containing the Mos transposon. Plate 9.75 (from Laurent Segalat, CNRS) contained the Mos transposon inserted in the *ifg-1* gene between exons 5 and 6 (Figure B.1A). The strain was

Figure B.1 The insertion of the Mos transposon in *ifg-1* (A) The *ifg-1* gene showing the position of the *Drosophilia*-derived Mos transposon insertion in intron 5. The positions of primers used for allele-specific genomic PCR are shown. (B) Punnet square of self-fertilization genotypes from the F1 offspring of heterozygous hermaphrodites. The homozygous KX34 strain used in all subsequent experiments, was derived from this cross (lower, right quadrant).

Figure B.1

A.

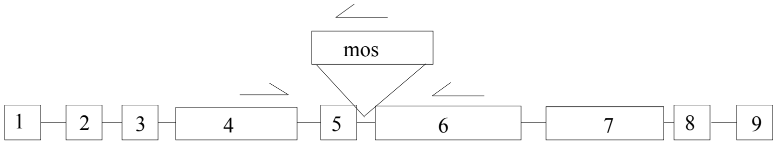
mos
1
2
3
4
5
6
7
8
9

B.

Oocytes

Spermatocytes	+	ifg-1:mos
+	+ / +	ifg-1:mos / +
ifg-1:mos	+ / ifg-1:mos	ifg-1:mos / ifg-1:mos

KX 34 strain

outcrossed against wild type males to ensure the absence of additional mutations, and the *ifg-1:mos* allele tracked with genomic PCR. Self-fertilization of the heterozygous *ifg-1:mos* hermaphrodite produced a viable homozygous offspring (Figure A.1B). The genotype of this new strain was determined by genomic PCR, which verified that the worms lacked the wild type *ifg-1* gene (Figure A.2 plate B6). Further molecular analysis of the KX34 strain (*ifg-1:mos* homozygous) by others in the lab detected various alterations in splicing of the *ifg-1* mRNA. Northern blot and RT-PCR experiments showed a small amount of properly spliced *ifg-1* mRNA, in addition to unspliced and incorrectly spliced forms (Dr. Brett Keiper and Dr. Enhui Hao, personal communication). The genotype and molecular expression data for KX34 suggest that this strain would be useful to further study the splicing of the *ifg-1* mRNA and suppressed expression of the IFG-1 proteins.

To evaluate the phenotype elicited by a splicing defect in the *ifg-1* gene using this new homozygous *ifg-1:mos* strain, the brood size and growth of KX34 and wild type hermaphrodites was recorded as development was observed over 96 hours at various temperatures (Figure B.3). The *ifg-1:mos* strain produced a substantial number of arrested embryos at all three temperatures examined, 15°, 20°, and 25°C (Figure B.3A). Overall, the *ifg-1:mos* strain produced 14% the viable offspring as compared to wild type. These data suggest that the disruption of the *ifg-1* gene dramatically reduces fertility. Interestingly, this strain produced more viable offspring at 20°C than at either 15° or 25°C, indicating both a heat-sensitive and cold-sensitive disruption of *ifg-1* expression by the Mos insertion. This is not uncommon for mutations that disrupt splicing efficiency.

Figure B.2 Isolation of homozygous *ifg-1:mos* strain. Whole worm genomic PCR products from individual "mother" hermaphrodites from clone plates B1-6. Plate B6 was the only clone homozygous for the Mos insertion in the *ifg-1* gene (KX34).

Figure B.2

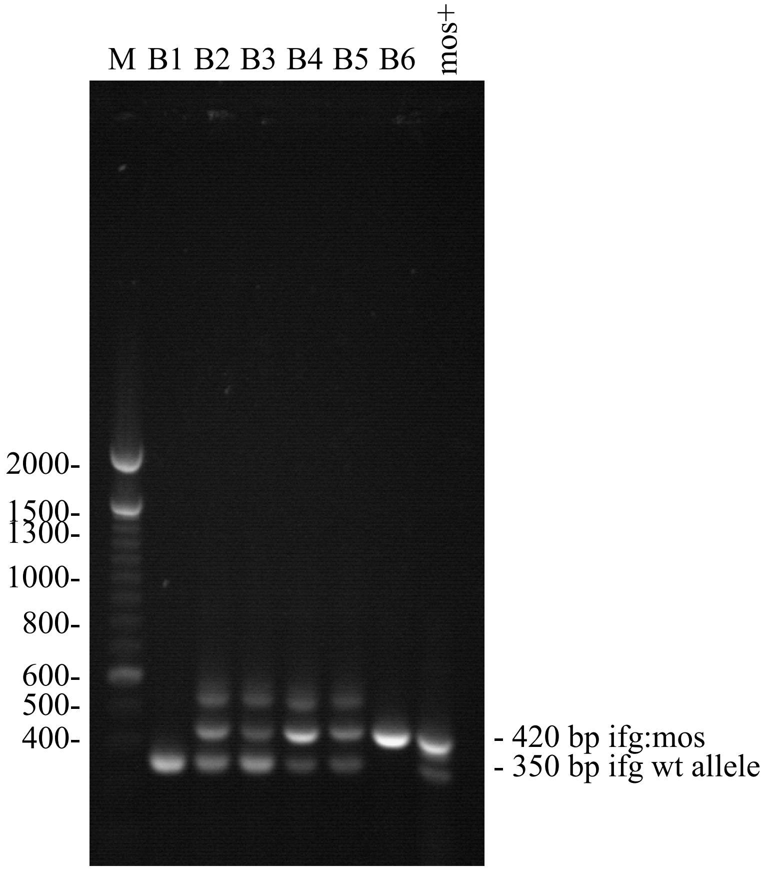
M
B1
B2
B3
B4
B5
B6
mos+
2000-
1500-
1300-
1000-
800-
600-
500-
400-
- 420 bp ifg:mos
- 350 bp ifg wt allele

Figure B.3 Brood size and developmental progression of *ifg-1:mos* worms at various temperatures. (A) Brood sizes produced from three *ifg-1:mos* homozygous hermaphrodites at 15°, 20°, and 25°C. Extent of embryonic, larval, and adult development was assessed by visual morphology at 24 hour intervals. (B) Brood size of three wild type hermaphrodites.

Figure B.3

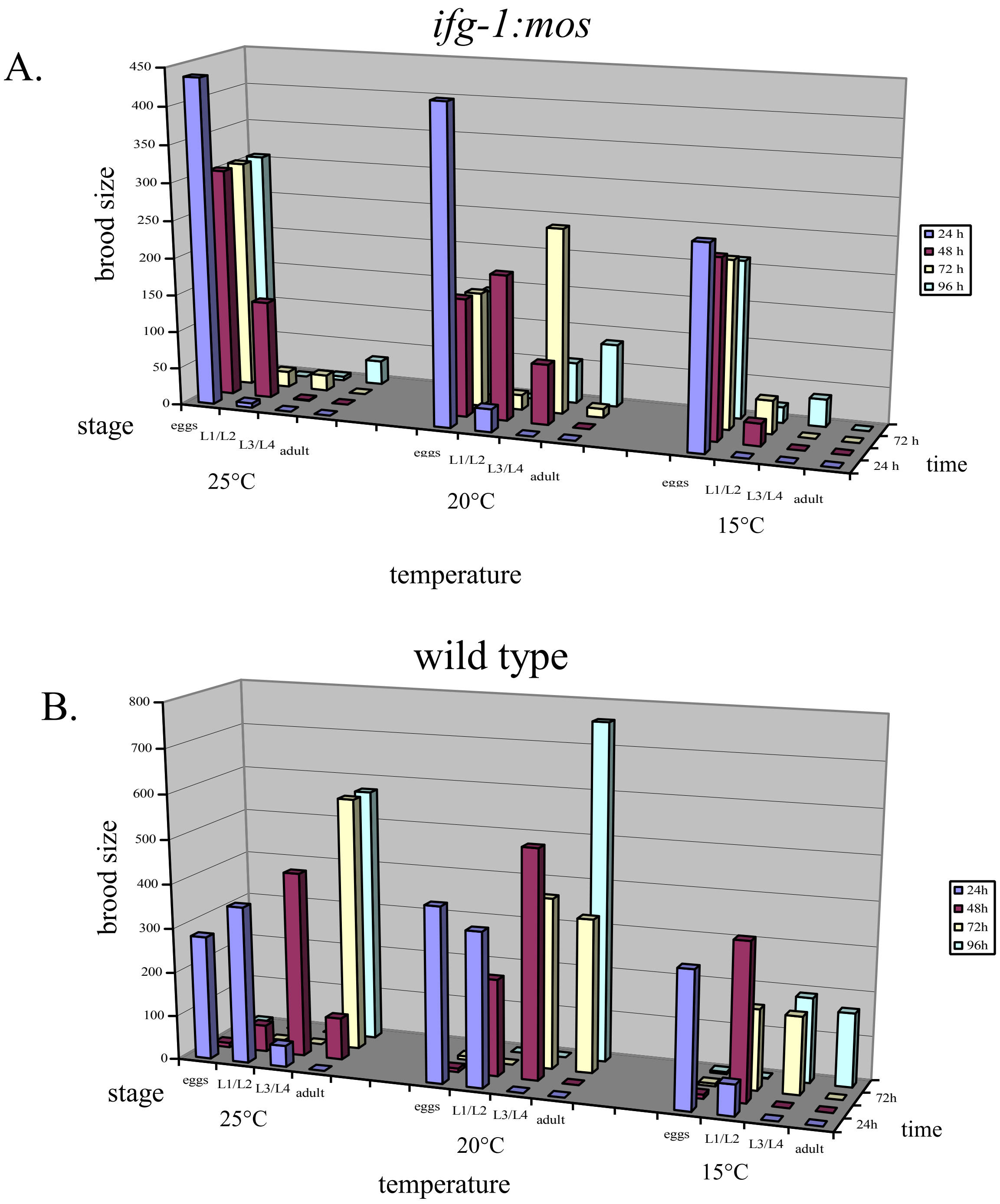
ifg-1:mos
A.
450
400
350
300
250
200
150
100
50
0
brood size
stage
eggs
L1/L2
L3/L4
adult
25°C
20°C
15°C
temperature
24 h
48 h
72 h
96 h
72 h
24 h
time
wild type
B.
800
700
600
500
400
300
200
100
0
brood size
stage
eggs
L1/L2
L3/L4
adult
25°C
20°C
15°C
temperature
24h
48h
72h
96h
72h
24h
time

Progeny produced at 25°C grew to sterile adults with extensive cell degradation in the germline. This represents a temperature-sterility that affects the F1 population. This form of sterility is termed "maternal-effect sterility." DIC microscopy of these sterile F1 progeny showed degenerated gonad tissue with large empty vacuoles (Figure B.4). Progeny produced at 15°C were not sterile and did not show loss of oocyte viability in the gonad. Therefore disruption of *ifg-1* splicing results in a maternal-effect sterility at 25°C, but shows decreased fertility at all three temperatures evaluated.

As described above, the splicing defect introduced by the Mos insertion did not fully block normal *ifg-1* mRNA splicing. To determine how much wild type IFG-1 p170 is still capable of being synthesized in *ifg-1:mos* worms, western blot analysis was performed. Figure B.5 shows the levels of p170 isoform using the N-terminal antibody in wild type and *ifg-1:mos* worms grown at 20° and 25°C. The detection of actin shows there was less total protein loaded from the KX34 samples than wild type lysates. Nevertheless, The *ifg-1:mos* strain appeared to produce substantially less p170 than wild type at both temperatures, though a more thorough quantification is warranted. These results allow us to conclude that the insertion of the mos transposon in intron 5 leads to a substantial decrease in p170 protein levels in adult worms. Interestingly, when Mr. Contreras later conducted similar western blotting experiments using a more sensitive central domain antibody that also detects p130 IFG-1, more residual p170 was observed (but still depleted) and a more substantial residual amount of p130 was noted. The reason for the greater persistence of the p130 isoform is not yet known. Creation of the *ifg-1:mos* homozygous strain demonstrated many potential benefits to studying the function of the IFG-1 isoforms *in vivo* in *C.elegans.*

Figure B.4 Gonad morphology of F1 offspring. DIC microscopy of wild type and KX34, *ifg-1:mos,* F1 progeny at adulthood at both 15° and 25°C. (A,B,C) Both strains grown at 15°C show normal development of oocytes with linear progression of maturing oocytes in the proximal gonad (top). The wild type hermaphrodites grown at 25°C also appears to have normal progression of oocytes. (D) KX34 F1 hermaphrodites from mothers exposed to elevated temperatures (25°C) show server necrosis and large vacuoles in the gonad (arrows).

Figure B.4

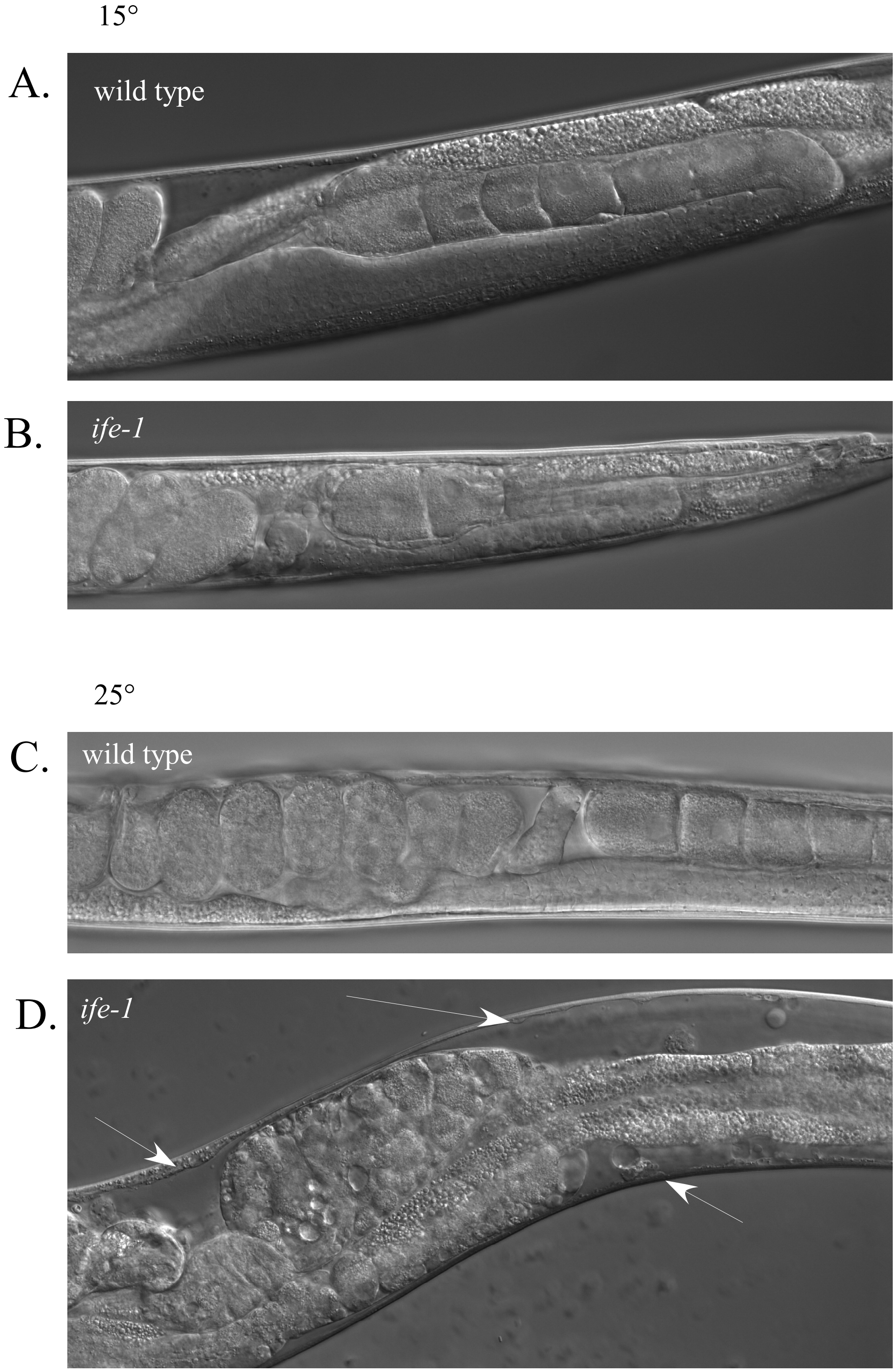
15°
A.
wild type
B.
ife-1
25°
C.
wild type
D.
ife-1

Figure B.5 Reduction of IFG-1 p170 levels in KX34 worms. Western blot of IFG-1 p170 and actin from wild type and *ifg-1:mos* hermaphrodites grown at 20° and 25°C. The anti-N-terminal antibody was used to detect IFG-1, which recognizes an epitope lacking in p130 IFG-1 (Contreras et al., 2008). Despite unequal protein loading, a substantial loss of p170 IFG-1 was apparent in the *ifg-1:mos* strain.

Figure B.5

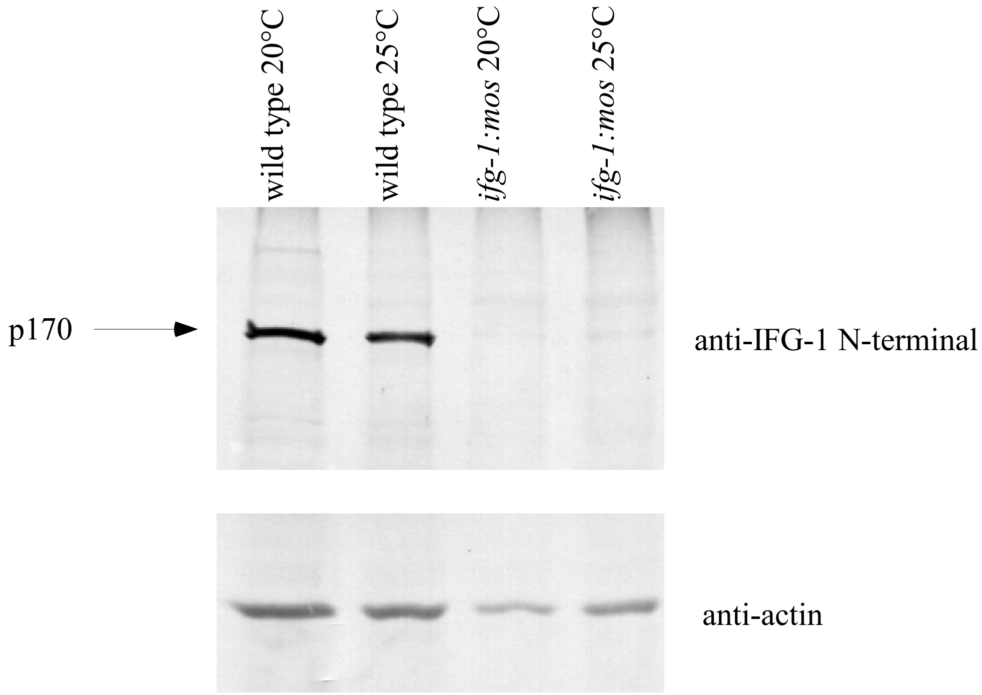
wild type 20°C
wild type 25°C
ifg-1:mos 20°C
ifg-1:mos 25°C
p170
anti-IFG-1 N-terminal
anti-actin

Further characteristics of the *ifg-1:mos* strain have been analyzed by others in our lab and included examining the effects of alternative splicing of intron 5, which occurs due to the presence of the mos insertion. In addition, northern blot analysis, RT-PCR, and sequencing have demonstrated the production of longer aberrantly spliced *ifg-1* mRNAs containing some Mos sequences that contain nonsense mutations.

Conclusion

The results presented here show that disruption of the *ifg-1* gene by Mos transposon insertion leads to dramatically decreased fertility and decreased production of IFG-1 protein. Also observed was an increase in embryonic arrests and a unique temperature-sensitive sterility in the F1 generation. Inconsistencies in the phenotype of the *ifg-1:mos* strain in germline morphology suggest that the gene disruption effects of Mos insertion are “leaky.” This leaky (and temperature-sensitive) phenotype, however, may be beneficial in producing viable progeny to study moderate IFG-1 depletion with less severe phenotypes than found by RNAi or the *ifg-1* null mutation. In addition, the effect of temperature on splicing can be used to temporally induce IFG-1 depletion at specific times during development, and potentially even select for specific IFG-1 isoforms. Additional experiments are needed to evaluate the onset of temperature-sensitive sterility, the effect of the *ifg-1* disruption on the induction of germline apoptosis, and the control of cap-dependent and independent translation. These attributes will make the *ifg-1:mos* strain a very valuable tool for developmental studies of eIF4G translational function, once the complex expression of this allele has been characterized.